

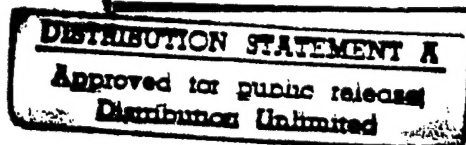


METABOLIC INHIBITION OF A TOLUENE-ENRICHED
MICROBIAL POPULATION DUE TO LEAD (Pb^{2+}):
VERIFICATION OF A FREE METAL ION TOXICITY MOD

THESIS

Patrick J. S. Marbas, Captain, USAF

AFIT/GEE/ENV/97D-18



DTIC QUALITY INSPECTED 3

DEPARTMENT OF THE AIR FORCE
AIR UNIVERSITY
AIR FORCE INSTITUTE OF TECHNOLOGY

Wright-Patterson Air Force Base, Ohio

19980114 130

AFIT/GEE/ENV/97D-18

METABOLIC INHIBITION OF A TOLUENE-ENRICHED
MICROBIAL POPULATION DUE TO LEAD (Pb^{2+}):
VERIFICATION OF A FREE METAL ION TOXICITY MODEL

THESIS

Patrick J. S. Marbas, Captain, USAF

AFIT/GEE/ENV/97D-18

DTIC QUALITY INSPECTED 3

Approved for public release; distribution unlimited

AFIT/GEE/ENV/97D-18

METABOLIC INHIBITION OF A TOLUENE-ENRICHED MICROBIAL
POPULATION DUE TO LEAD (Pb^{2+}):
VERIFICATION OF A FREE METAL ION TOXICITY MODEL

THESIS

Presented to the Faculty of the Graduate School of Engineering
Air Education and Training Command
In Partial Fulfillment of the
Requirements for the Degree of
Master of Science in Environmental and Engineering Management

Patrick J. S. Marbas, Captain, USAF

AFIT/GEE/ENV/97D-18

December 1997

Approved for public release; distribution unlimited

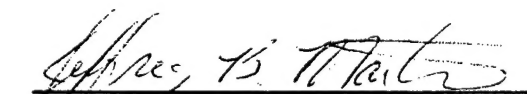
AFIT/GEE/ENV/97D-18

METABOLIC INHIBITION OF A TOLUENE-ENRICHED MICROBIAL
POPULATION DUE TO LEAD (Pb^{2+}):
VERIFICATION OF A FREE METAL ION TOXICITY MODEL


THESIS

Patrick J. S. Marbas, B.S.,
Captain, USAF

Presented to the Faculty of the Graduate School of Engineering
of the Air Force Institute of Technology
In Partial Fulfillment of the
Requirements for the Degree of
Master of Science in Engineering and Environmental Management


Maj. Jeffrey Martin, Member


Dr. Larry Burggraf, Co-Chairman


Charles Beckmann, Co-Chairman

Acknowledgments

I am indebted to my thesis advisors, Charles Bleckmann, Larry Burggraf, and Major Jeffrey Martin. Their insight and guidance during the research effort were invaluable. I would like to extend special thanks to Larry Burggraf for the tremendous support given throughout the entire project, especially during the data analysis portion of the thesis.

This project would not have been possible without the generous financial support from Major Mike Chipley and from the Air Force Office of Scientific Research, the projects sponsoring agency.

I would like to express my gratitude to Leroy Cannon and Belinda Johnson; both helped me gather the many materials required for my experiments. I must thank Steve Maxwell for all the precise work he performed while working in the laboratory as a technician. Steve's work was significant in the development and perfection of the experimental methodology. I appreciate Dan Levitt and the management staff at the Fairborn Water Reclamation Center for their continued support of environmental thesis projects requiring activated sludge.

Finally, I would like to thank my wife, Laurie, for her tremendous patience, support, and understanding throughout the graduate program and especially through the thesis process. I thank my wife's grandmother, Maxine Turner, for all the help she has provided our family during the many times I was away in the laboratory. And I thank my children, Emily and Jonathan, for helping me keep perspective on the truly important things in life.

Table of Contents

	Page
Acknowledgements.....	ii
List of Figures.....	vi
List of Tables	ix
Abstract.....	xii
I. Introduction	1-1
Background	1-1
Importance of Research.....	1-3
Problem Statement	1-3
Research Objectives	1-4
Thesis Overview.....	1-4
II. Literature Review	2-1
Introduction	2-1
Bacteria Morphology	2-1
Gram-Negative Morphology.....	2-2
Gram-Positive Morphology	2-2
Aerobic Degradation of Toluene.....	2-3
Toluene Transport into Cytoplasm	2-4
Metal Adsorption to Cellular Components	2-6
Mechanisms Resulting in Metabolic Inhibition	2-7
Disruption of the Toluene Transport.....	2-7
Cell Lysis	2-8
Viability and Metabolic Inhibition.....	2-9
Development of the Toxicity Model (TM)	2-10
Model Assumptions	2-10
Equilibrium Equations	2-11
III. Methodology.....	3-1
Overview	3-1
Materials.....	3-1
Microcosm	3-1
Innoculum	3-1
Dilution Water	3-2

Metal Treatment.....	3-3
Filtering Apparatus	3-3
Dissolved Oxygen Meter and BOD Probe.....	3-4
Lead Selective Electrode and Meter	3-4
Standard Techniques	3-4
Standard Preparation of Microcosms.....	3-4
Special Preparation of Microcosm.....	3-5
Blanks	3-5
Filtering and Weighing Technique	3-5
DO Measurement Technique	3-6
Lead Activity Measurement Technique.....	3-6
Lead Activity Calibration Procedure	3-6
Experimental Procedures	3-7
DO Consumption Rate Linearity Experiment.....	3-7
DO Consumption Rate Reproducibility Experiments.....	3-7
Various Inoculum Volume Experiments	3-8
Activity Measurement Reproducibility Experiment.....	3-9
Metabolic Inhibition Experiments	3-9
Lead Adsorption Experiment.....	3-10
IV. Findings and Analysis	4-1
Overview/Introduction	4-1
Experimental Measurements	4-1
DO Consumption Rate Linearity Experiment.....	4-2
DO Consumption Rate Reproducibility Experiments.....	4-2
Various Inoculum Volume Experiments	4-5
Activity Measurement Reproducibility Experiment.....	4-11
Metabolic Inhibition Experiments	4-14
Metal Complexation Experiments	4-25
Langmuirian Adsorption Behavior	4-31
Predicted Toxicity Response.....	4-33
V. Conclusions	5-1
Conclusions.....	5-1
Future Research.....	5-3
Appendix A: Bioreactor	A-1
Bioreactor.....	A-1
Toluene Source.....	A-1
Growth Solution.....	A-2
Appendix B: Atomic Adsorption Spectroscopy	B-1

Sample Preparation	B-1
Results	B-2
Appendix C: Cu ²⁺ and Cd ²⁺ Metabolic Inhibition Experiments	C-1
Cu ²⁺ Metabolic Inhibition Experiments	C-1
31 Jul Experiment	C-1
13 Aug Experiment	C-3
28 Aug Experiment	C-5
Cd ²⁺ Metabolic Inhibition Experiments	C-7
31 Jul Experiment	C-7
14 Aug Experiment	C-10
20 Aug Experiment	C-12
12 Sept Experiment	C-14
Bibliography	Bib-1
Vita	Vita-1

List of Figures

	Page
Figure 2.1. A model of facilitated diffusion	2-4
Figure 4.1. Time Versus Dissolved Oxygen (DO) Reading	4-2
Figure 4.2. Innoculum Volume Versus Dissolved Oxygen (DO) Consumption Rate, Experiment performed 2 Sept 97	4-7
Figure 4.3. Innoculum Volume Versus Dissolved Oxygen (DO) Consumption Rate, Experiment Performed 5 Oct 97	4-9
Figure 4.4. Microbial Mass Versus Dissolved Oxygen (DO) Consumption Rate, Experiment Performed 5 Oct 97.....	4-10
Figure 4.5. Innoculum Volume Versus Microbial Mass, Experiment Performed 5 Oct 97.....	4-11
Figure 4.6. Total Lead Concentration Versus Electrode Potential, Uncorrected Data, Experiment Performed 8 Aug 97	4-12
Figure 4.7. Total Lead Concentration Versus Electrode Potential, Corrected Data, Experiment Performed 8 Aug 97	4-13
Figure 4.8. Total Lead Concentration Versus Average Lead Activity, Experiment Performed 8 Aug 97.....	4-15
Figure 4.9. Total Lead Concentration Versus Average Lead Activity, Experiment Performed 30 Aug 97.....	4-17
Figure 4.10. Total Lead Concentration Versus Average Lead Activity, Experiment Performed 13 Sept 97.....	4-19
Figure 4.11. Average Lead Activity Versus Average Toxicity Function, Experiment Performed 8 Aug 97.....	4-21
Figure 4.12. Square-root of Average Lead Activity Versus Average Toxicity Function, Experiment Performed 8 Aug 97	4-21
Figure 4.13. Average Lead Activity Versus Average Toxicity Function, Experiment Performed 30 Aug 97.....	4-22

Figure 4.14. Square Root of the Average Lead Activity Versus Average Toxicity Function, Experiment Performed 30 Aug 97	4-23
Figure 4.15. Average Lead Activity Versus Average Toxicity Function, Experiment Performed 13 Sept 97.....	4-24
Figure 4.16. Average Lead Activity Versus Average Toxicity Function, Experiment Performed 13 Sept 97.....	4-24
Figure 4.17. Total Lead Concentration Versus Adjusted Potential Reading, Microbial Mass = 4.04 mg DW = Dilution Water; DW + M. = Dilution Water with Microorganisms, Experiment Performed 17 Sept 97	4-27
Figure 4.18. Lead Activity Versus Lead Adsorbed per Microbial Mass, Experiment Performed 17 Sept 97.....	4-27
Figure 4.19. Total Lead Concentration Versus Adjusted Potential Reading DW = Pure Dilution Water; DW + M. = Dilution Water with Microorganisms, Experiment Performed 22 Sept 97	4-28
Figure 4.20. Least Squares Fit of Lead Activity Versus Lead Adsorbed per Dry Weight for Experiments Performed 17 Sept, 22 Sept, and 7 Oct.....	4-29
Figure 4.21. Least Squares Fit of Distribution Coefficient (DC) Versus Dry Mass.....	4-30
Figure 4.22. Distribution coefficient versus pH.....	4-31
Figure 4.23. Average Lead Activity Versus Lead Adsorbed per Microorganism Mass. Experiment Performed 7 Oct 97	4-32
Figure 4.24. Lead Activity Versus Lead Adsorbed by Microorganisms, Experiment Performed 7 Oct 97.....	4-32
Figure 4.25. Case II, Lead Activity Versus Predicted & Actual Toxicity Function (Experiment Performed 8 Aug 97)	4-33
Figure 4.26. Ratio of predicted to actual toxicity response as a function of final pH (experiment performed 8 Aug 97)	4-35
Figure 4.27. Case II, Lead Activity Versus Predicted & Actual Toxicity Function (Experiment Performed 30 Aug 97)	4-36
Figure 4.28. Ratio of predicted to actual toxicity response as a function of final pH (experiment performed 30 Aug 97)	4-37

Figure A.1. Bioreactor Set-up.....	A-1
Figure C.1. Total copper versus normalized metabolic activity for 31 July experiment.....	C-2
Figure C.2. Total copper versus toxicity function value for 31 July experiment	C-3
Figure C.3. Total copper versus NMA for 13 Aug experiment	C-4
Figure C.4. Total copper versus toxicity function value for 13 Aug experiment	C-5
Figure C.5. Total copper versus ANMA for 28 Aug experiment	C-6
Figure C.6. Total copper versus toxicity function value for 28 Aug experiment	C-7
Figure C.7. Total cadmium versus NMA for 31 July experiment	C-9
Figure C.8. Total cadmium versus toxicity function for 31 July experiment	C-9
Figure C.9. Total cadmium versus NMA for 14 Aug experiment	C-11
Figure C.10. Total cadmium versus toxicity function for 14 Aug experiment.....	C-11
Figure C.11. Total cadmium versus NMA for 20 Aug experiment.....	C-13
Figure C.12. Total cadmium versus toxicity function for 20 Aug experiment.....	C-14
Figure C.13. Total cadmium versus ANMA for 12 Sept experiment.....	C-15
Figure C.14. Total cadmium versus toxicity function for 12 Sept experiment.....	C-16

List of Tables

	Page
Table 3.1. Nutrients in growth medium	3-2
Table 3.2 Nutrients in dilution water	3-3
Table 4.1. Dissolved oxygen consumption rate reproducibility test performed 24 July 97	4-4
Table 4.2. Dissolved oxygen consumption rate reproducibility test performed 3 Sept 97.....	4-5
Table 4.3. Dissolved oxygen (DO) consumption rate, average do consumption rate, standard deviation , and coefficient of variation, experiment performed 2 Sept 97.....	4-6
Table 4.4. Innoculum volume, organism mass, and dissolved oxygen (DO) consumption rate, experiment performed 5 Oct 97.....	4-8
Table 4.5. Uncorrected electrode potential, experiment performed 8 Aug 97	4-12
Table 4.6. Corrected electrode potential, experiment performed 8 Aug 97	4-13
Table 4.7. Lead activity, dissolved oxygen (DO) consumption rate, normalized metabolic activity (NMA) and toxicity function, experiment performed 8 Aug 97.....	4-14
Table 4.8. Total lead concentration, lead activity, dissolved oxygen (DO) consumption rate, normalized average metabolic activity (NAMA), experiment performed 30 Aug 97	4-16
Table 4.9. Total lead concentration, lead activity, dissolved oxygen consumption rate, normalized average metabolic activity (NAMA), average toxicity function, experiment performed 13 Sept 97	4-18
Table 4.10. R-squared values for correlation between lead activity and toxicity response.....	4-25
Table 4.11 Lead distribution coefficients determined in three separate experiments	4-29

Table 4.12. Average lead activity, final pH, predicted toxicity response, actual toxicity response and ratio of predicted to actual toxicity response (experiment performed 8 Aug 97).....	4-34
Table 4.13. Average lead activity, final pH, predicted toxicity response, actual toxicity response and ratio of predicted to actual toxicity response (experiment performed 30 Aug 97).....	4-36
Table B.1. Lead complexed as determined using AAS and ISE techniques (7 Oct experiment).....	B-2
Table C.1. Total Cu ²⁺ , DO consumption rate, NMA, and toxicity function value for trial 1 of the 31 July experiment.....	C-1
Table C.2. Total Cu ²⁺ , DO consumption rate, NMA, and toxicity function value for trial 2 of the 31 July experiment.....	C-2
Table C.3. Total Cu ²⁺ , DO consumption rate, NMA, and toxicity function value for trial 1 of the 13 Aug experiment.....	C-3
Table C.4. Total Cu ²⁺ , DO consumption rate, NMA, and toxicity function value for trial 2 of the 13 Aug experiment.....	C-4
Table C.5. Total Cu ²⁺ , DO consumption rate, NMA, and toxicity function value for 28 Aug experiment.....	C-6
Table C.6. Total Cd ²⁺ , DO consumption rate, NMA, and toxicity function value for trial 1 of the 31 July experiment.....	C-8
Table C.7. Total Cd ²⁺ , DO consumption rate, NMA, and toxicity function value for trial 2 of the 31 July experiment.....	C-8
Table C.8. Total Cd ²⁺ , DO consumption rate, NMA, and toxicity function value for trial 1 of the 14 Aug experiment.....	C-10
Table C.9. Total Cd ²⁺ , DO consumption rate, NMA, and toxicity function value for trial 2 of the 14 Aug experiment.....	C-10
Table C.10. Total Cd ²⁺ , DO consumption rate, NMA, and toxicity function value for trial 1 of the 20 Aug experiment.....	C-12
Table C.11. Total Cd ²⁺ , DO consumption rate, NMA, and toxicity function value for trial 2 of the 20 Aug experiment.....	C-12

Table C.12. Total Cd²⁺, DO consumption rate, NMA, and toxicity function value for trial 3 of the 20 Aug experiment C-13

Table C.13. Total Cd²⁺, DO consumption rate, NMA, and toxicity function value for the 12 Sept experiment C-15

Abstract

A dissolved oxygen probe and an ion specific electrode were used to study the lead-induced metabolic inhibition in a toluene-enriched microbial population. Predicted toxicity values were compared to the actual toxicity responses using a free metal ion toxicity model (TM) which linked metabolic inhibition with lead activity. Experimentally derived values for the model parameters (lead activity and a lead distribution coefficient) were used in the TM. It was postulated that cellular metabolism is disrupted by the conformational changes to the cell's plasma membrane produced by lead ion adsorption.

The predicted toxicity values were higher than the actual toxicity response. This is expected since the TM did not distinguish between essential and non-essential cellular ligands. Moreover, lead-induced metabolic inhibition appears to be pH dependent as the TM predicted.

An adsorption experiment suggested that the microbial mass has two lead binding sites: tightly bound ligands and loosely bound ligands. The tightly bound ligand sites appeared to be saturable. No evidence of saturation was observed in the loosely bound ligand sites. Contrary to expectations, the loosely bound ligand sites appear to be more essential to cellular metabolism than the tightly bound ligand sites.

**METABOLIC INHIBITION OF A TOLUENE-ENRICHED MICROBIAL
POPULATION DUE TO LEAD (Pb²⁺):**

VERIFICATION OF A FREE METAL ION TOXICITY MODEL

I. Introduction

Background

Heavy metals in the environment are a concern since they can disrupt important microbe assisted processes. Microorganisms respond to metals in varying ways. Several natural biological processes such as growth, metabolism, and natural fluorescence may be inhibited. Furthermore, damage to the cell membrane or cell lysis may occur (Beveridge and Doyle, 1989:39-44).

This study extended the work performed by Scott Hansen (1995) which examined metabolic inhibition in a slow growing, toluene-selected microbial population due to treatments of first row transition metal ions (Cu²⁺, Co²⁺, Zn²⁺, Mn²⁺, and Fe³⁺) under varying pH and nutrient conditions. He found a toxicity trend which correlated with phosphate binding affinity. Competition of hydrogen ions and non-toxic metal ions reduced the toxicity of the transition metal ions. Metabolic inhibition was measured as the ratio of oxygen consumption of treated samples to the oxygen consumption of untreated samples. The ratio was referred to as the Normalized Metabolic Activity (NMA).

This work focused on the metabolic inhibition due to lead ions (Pb²⁺), a third row main group metal. It was expected that the response to lead may be different than to first row transition metal ions. Lead is not essential to microorganisms at any amount unlike

the first row transition metals which are essential at low concentrations and toxic at higher concentrations.

To explain Hansen's findings a mathematical model relating metabolic inhibition with the metal adsorbed to microorganisms was developed by Burggraf, Hansen, and Bleckmann (1997). This model is based on the free-ion activity model (Morel, 1983) which assumes that the free metal ions are the bio-active metal species responsible for the toxic response. The model developed by Burggraf et al. will be referred hereafter as the toxicity model (TM). The development of the TM will be discussed in Chapter 2.

The TM postulates "that metabolic inhibition is proportional to cell membrane damage inherent with transition metal ion chemisorption at phosphatic cell membrane sites" (Burggraf *et al.*, 1997). The metabolic inhibition in a toluene selected microbial population can be predicted as a function of metal activity if the metal distribution coefficient (DC) of the microbial population is determined. The TM is pH dependent and predicts two cases of toxicity response depending on how well protons compete with metal ions for essential cellular ligand sites.

In Case I, protons do not compete well with metal ions. Metal ions are assumed to form bi-chelated complexes with essential cellular ligands. Conformational changes occur in the cellular membrane which result in cell damage or death. The toxicity response is assumed to be directly proportional to the product of the DC and metal activity.

In Case II, protons do compete well with metal ions. The protons which bind to the cellular ligands limit the formation of multi-ligand/metal complexes. The toxicity

response is assumed to be directly proportional to the product of the DC and the square root of the metal activity.

Importance of Research

Numerous studies compared the relative toxicity responses of microorganisms to various metals (Bitton, Jung, Koopman, 1994; Codina *et al.*, 1993; Fargasova, 1994). Few studies are found which link metal adsorption with toxicity, much less, studies offering an empirical or theoretical model to explain the findings.

The TM is unique since it allows for the prediction of a specific toxic response for a given microbial population. The model explains well the findings presented in Hansen's work, however, the model parameters, DC and metal activity, were not explicitly determined in the experiments. This thesis effort evaluated the predictive value of the TM by comparing the predicted and actual toxicity response of a toluene selected microbial population treated with lead ions. The DC and lead activity were explicitly measured. This work helped bridge the gap in current works by linking a specific biological response to a predictive model.

Problem Statement

This thesis attempted to answer the question: Can the lead-induced metabolic inhibition in a toluene-enriched microbial population be accurately predicted using the TM, if the parameters DC and lead activity are determined?

Research Objectives

There were three main objectives for this thesis effort:

1. Determine the metabolic inhibition in a toluene-enriched microbial population due to lead treatments using a dissolved oxygen probe and meter.
2. Develop a methodology using ion-selective electrodes to determine the lead activity in test solutions and the DC of the test microorganisms.
3. Evaluate the predictive value of the Burggraf model by comparing the toxic response predicted by the model with the actual toxic response.

Thesis Overview

In general, this thesis was organized according to the table of contents. However, special attention was given to the development of the TM in Chapter 2. The materials, techniques, and procedures used in the experiment were discussed in Chapter 3. The data was reported and discussed in Chapter 4, and in Chapter 5, a conclusion and future research suggestions were offered.

Appendices A, B and C are referenced in the chapters and include additional information and experimental results. Appendix A describes the set-up of the bioreactor. Data obtained from a single atomic adsorption experiment was included in Appendix B. Results from metabolic inhibition experiments involving copper and cadmium ions are included in Appendix C.

II. Literature Review

Introduction

This chapter will discuss basic bacteria morphology; the aerobic degradation of toluene; the metal adsorption to cellular components; the mechanisms responsible for metabolic inhibition; and the development of the toxicity model (TM).

Bacteria Morphology

This section will focus on the differences of the gram-negative and gram-positive bacteria outer membrane. The outer membrane plays a significant role in a bacteria's defense system. The cellular membrane serves as an osmotic barrier which allows essential nutrients to enter the cell, but prevents the entrance of deleterious substances including heavy metals.

Gram-positive and gram-negative microorganisms are distinguished by staining a smear with the basic dye crystal violet. A microorganism is classified as gram-positive if it remains crystal violet when de-colored with an organic solvent such as ethanol. Gram-negative bacteria lose the crystal violet and become colorless (Prescott *et al.*, 1990:29,G12).

This study used a microbial population selected in an aerobic, toluene-enriched bioreactor (Reference Appendix A). The population consisted primarily of gram-negative microorganisms, but a small percentage of gram positive-microorganisms were also present (Goodbody, 1997).

In general, the gram-negative and gram-positive bacteria are similar in that each have a capsule, cell wall, periplasmic space, and plasma membrane. The primary difference between the classifications is that the outer membrane, periplasmic space and plasma membrane of the gram-negative bacteria is much more complex chemically and structurally than the gram-positive bacteria (Beveridge, 1989:14). The differences in the outer structure of gram-negative and gram-positive bacteria are well documented (Beveridge, 1989:ch.1; Inouye, 1979:ch.1). The distinguishing characteristics of each type of bacteria is outlined below.

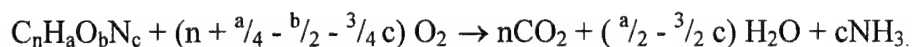
Gram Negative Morphology. The outer membrane of a gram-negative bacteria contains approximately 20-25% phospholipids, 30% lipopolysaccharide (LPS), and 45-50% protein (Beveridge 1981: 265). The hydrophilic LPS is appropriated to the external face of the membrane, whereas the hydrophobic phospholipid aligns along the inner face (Beveridge and Doyle, 1989:14). Proteins, in the form of polypeptides, are distributed throughout the membrane and can be oriented on either surface or can span it completely (Beveridge and Doyle, 1989:14). Other important polypeptides are matrix or porin proteins. These proteins appear to be coded for by independent genes, and their relative amounts vary greatly with growth conditions (Inouye, 1979:7). The function of the matrix proteins is to form passive diffusion pores which presumably, metallic ions would be free to diffuse through to reach the underlying periplasm (Beveridge and Doyle, 1989:15, Inouye 1981:7).

Gram-positive bacteria. The gram-positive cell wall consists of a low-ordered matrix about 20-25 nm thick which contains cross-linked and uncross-linked peptidoglycan strands with covalently attached teichoic acids (Beveridge, 1981:242). A combination of free carboxyl and phosphoryl groups within the wall fabric usually imparts an overall electronegative charge density to them (Beveridge and Doyle, 1989:14).

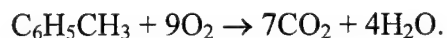
Aerobic Degradation of Toluene

The aerobic degradation of toluene occurs through different pathways for different strains of bacteria (Duetz *et al.*, 1994:2858). The metabolic pathways will not be discussed in this paper. However, it is important to note that the toluene metabolic pathway, referred to as the TOL pathway, is an enzymatic process involving toluene dioxygenase as well as monooxygenase systems (Duetz *et al.*, 1994:2858; Wackett, *et al.* 1989:185).

Oxygen consumption was determined to be a convenient measurement indicative of hydrocarbon metabolism by bacteria (Naziruddin, Grady, Tabak, 1995). The amount of oxygen required to convert organic molecules to carbon dioxide, water, and ammonia is described by the general stoichiometric relationship (Sawyer, McCarty, and Parkin, 1995):



Hence, for toluene,



Toluene Transport into the Cytoplasm. Toluene must enter the cell's interior, or cytoplasm, to begin the TOL pathway. A large molecule, such as toluene, is most likely transported into the cell's cytoplasm via active transport or group translocation, however passive diffusion and facilitated diffusion of toluene may also occur.

Passive diffusion is the process in which a molecule simply crosses the plasma membrane from a region of higher concentration to one of lower concentration (Prescott *et al.*, 1990:97). The passive diffusion rate is dependent upon the size of the concentration gradient between a cell's exterior and interior. The process is inefficient and is not employed extensively by microorganisms in nutrient uptake. Passive diffusion typically works in conjunction with other transport mechanisms.

Facilitated diffusion is similar to passive diffusion in that the process operates only when the nutrient concentration outside the cell is greater than the concentration inside the cell. However, facilitated diffusion involves the use of carrier proteins, called permeases, which greatly increases the uptake nutrients.

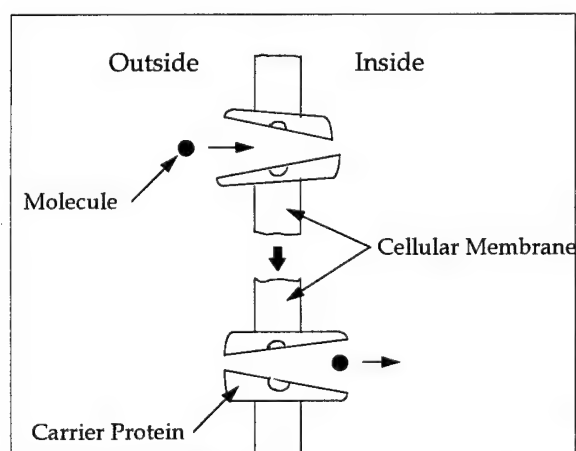


Figure 2.1. A model of facilitated diffusion. Adapted from Prescott *et al.* (1990:98)

In facilitated diffusion, the carrier protein changes conformation in order to bind an external molecule and subsequently release it into the cytoplasm as shown in Figure 4.1. The protein then returns to the outward oriented position and is ready to transport other molecules. The carrier proteins are selective and will transport only specific molecules or related solutes (Prescott *et al.*, 1990:98).

Active transport is similar to facilitated diffusion in that the process involves carrier proteins. However, metabolic energy is needed in the active transport process since solute molecules is moved to higher concentrations, or against a concentration gradient. The energy source is ATP, although other high-energy phosphate compounds may drive uptake in some transport systems. Moreover, proton and sodium ion gradients are involved in the transport process in what is known as protonmotive force (Prescott *et al.*, 1990:98-99).

Finally, molecules can be transported and be chemically altered in a single process known as group translocation. A well known group translocation system is the phosphoenolpyruvate: sugar phosphotransferase system (PTS) which is inherent in many prokaryotes. The PTS transports a variety of sugars into the cells while simultaneously phosphorylating them using phosphoenolpyruvate (PEP) as the phosphate donor. The PTS is quite complex and involves the use of enzymes and proteins in various numbers, depending on the microorganism strain. Group translocation of toluene may follow a similar process to that of the PTS system (Gottschalk, 1979:13).

Metal Adsorption to Cellular Components

Much work has been done on the metal binding abilities of the bacterial cell wall and outer membrane components (Hoyle and Beveridge, 1983; Coughlin *et al.*, 1983; Doyle *et al.*, 1980). Studies using nuclear magnetic resonance (NMR) suggest that the most abundant reactive electronegative sites in the outer membrane capable of binding metal cations are the LPS phosphoryl groups and phospholipids (Beveridge and Doyle, 1989:307)

In a proton titration experiment performed by Plette *et al.* (1996), three different types of binding sites were distinguished by the median value of the intrinsic proton affinity constant (K_H) for each site : carboxylic ($\log K_H = 4.6$), phosphatic ($\log K_H = 7.8$), and amino-type sites ($\log K_H = 10.0$). Moreover, in a metal ion sorption experiment performed by Plette *et al.* (1996), it was observed that specifically bound protons, calcium, and metal ions compete for the same binding sites on gram-positive soil bacterium cell wall. The metal ion sorption increased with increasing pH and calcium ions and protons were released from the cell wall material as a result of metal ion sorption.

Similar results were observed from an earlier experiment performed by Doyle *et al.* (1980) involving the Mn^{2+} adsorption by the cell walls of *Bacillus subtilis*. As the pH was raised, an increase in the apparent association constant between the metal and the cell wall occurred. However, over the same pH range the number of binding sites increased only slightly. Therefore, hydrogen ions altered the strength of the association between the

cell wall and metals but did not significantly alter the stoichiometry of the interaction. This suggest that the metal and protons bind to the same cell wall site(s).

Experiments determining the adsorption of Ag^+ , La^{3+} , Cu^{2+} , and Cd^{2+} by four different bacteria types suggest the adsorption of Cu^{2+} and Cd^{2+} is modeled well using Freundlich isotherms (Mullen *et al.*, 1989). Proton and copper ion uptake experiments using alga (Crist *et al.*, 1988) suggest that proton adsorption is characterized by a fast surface reaction followed by a slow diffusion of protons into cell. The metal ion adsorption behavior was quantitatively represented by the Langmuir adsorption isotherm.

The works reviewed used isolated cell components. Certainly, metal adsorption characteristics may be different for intact microorganisms. However, an essential understanding is gained about the different cellular binding sites and the expected metal adsorption behavior onto a cellular surface.

Mechanisms Resulting in Metabolic Inhibition

Assuming that cell membrane deformation is the cause of acute toxicity, metabolic inhibition in a microbial population may be attributed to two mechanisms: toluene transport process disruption and cell lysis.

Disruption of the Toluene Transport. Metabolic inhibition may result from a disruption or stoppage in the toluene transport process or processes. Conformational changes to the cellular membrane may result from metal ion adsorption. The conformational changes may act to inhibit toluene transport. Consequently, metabolic inhibition would occur.

Published works addressing the conformational changes in the cellular membrane of intact microorganisms due to metal binding were not found. However, a study performed by Rothstein (1970) supports the notion that the transport pathway involved in metabolism may be disrupted by metal ion adsorption.

Rothstein studied the fermentation inhibition in yeast due to uranyl ion adsorption. The sugar fermentation by yeast is described as a group translocation process involving the simultaneous transport and phosphorylation of the sugar. Membrane phosphoryl and carboxyl sites are involved in the sugar transport. However, glucose fermentation is associated primarily with the phosphoryl sites.

Rothstein concluded that uranyl ions inhibit the entry of sugars into the cell's metabolic system by blocking sugar transfer through the cell membrane. The rate of glucose fermentation was inhibited 90 percent if the phosphoryl sites were fully occupied by uranyl ions. The remaining 10 percent was inhibited only if the of uranyl ion concentration was increased to levels that resulted in carboxyl site saturation. The relationship between the uranyl ion-binding and the inhibition was one to one.

The conclusions made by Rothstein were extended to *E. coli* since the bacteria metabolizes sugar using a similar process as yeast. Likewise, the disruption of the toluene metabolic process is offered as a possible mechanism of metabolic inhibition due to lead ion toxicity.

Cell Lysis. Cell lysis, or the release of cellular constituents after a cell's plasma membrane ruptures, are generally observed after extended contact with metal ions

(Walum *et al.*, 1990:76). Cell lysis is generally viewed as the endpoint of an increasingly severe, toxicological effect progression. For example, in a study using the algae strain, *Chlorella saccharphila* (Folsom *et al.*, 1986), morphological events (vacuolation, cell wall thinning and cell lysis) advanced in stages as the cell died over a 5 day period.

Cell lysis is a possible, but an unlikely mechanism responsible for the metabolic inhibition observed in the acute toxicity experiments. The metabolic inhibition due to lead ions occurred rapidly (<5 min) and may be explained more accurately by a disruption in the cell's metabolic process. Structural changes in the cytoplasmic membrane due to lead adsorption may inhibit conformation changes required for protein transport functions.

Viability and Metabolic Inhibition. Metabolic inhibition does not necessarily imply cellular death. A microorganism may still be viable despite exhibiting metabolic inhibition. However, metabolic inhibition in a microbial population may also be the result of cell lysis in which case cell death is inevitable. The metabolic inhibition observed in this thesis' experiments may be a result of one or both of the mechanisms discussed. The concurrent work of Goodbody (1997), attempts to establish whether the metabolic inhibition is due primarily to cell death, or by the disruption of the cell's metabolic process.

Development of the Toxicity Model (TM)

Model Assumptions. The TM is based on the following three assumptions (Burggraf *et al.* 1997):

(1) Only free (hydrated) metal ions interacting with cells produce toxic effects.

Metal ion toxicity is changed by reactions which change equilibrium activities of free metal ions in solution.

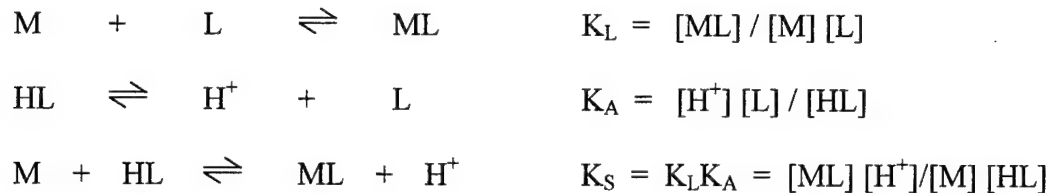
(2) Acute toxicity is produced by metal ions binding at phospholipid ligand membrane sites, characterized by a single binding constant. Metal ions and hydrogen ions compete for these saturable membrane chemisorption sites.

(3) Substitution of toxic transition metal ions at multiple chelated phosphate membrane sites change phospholipid ligand conformations producing local denaturation and proportionately diminished metabolic function.

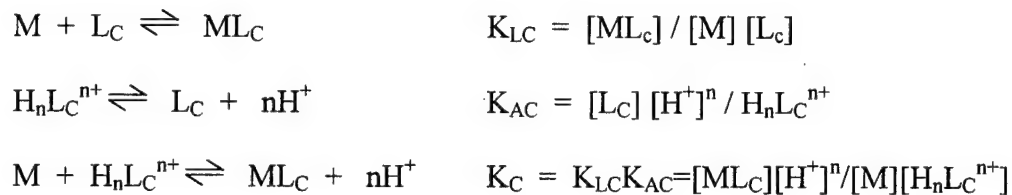
By the first assumption, the TM implies that the toxic effects will be a function of the free metal ion concentration, or metal activity. The second assumption implies that all cellular binding sites at which a metal complexes will contribute to metabolic inhibition. Moreover, the degree to which a metal complexes with the binding sites is pH dependent. The final assumption postulates a metabolic inhibition mechanism. Metabolic inhibition is caused by conformational changes in the cellular membrane resulting from metals complexing with cellular ligand sites. Furthermore, metabolic inhibition is manifested in proportion to the conformational changes.

Equilibrium Equations. The equilibrium equations governing the TM are based on two sets of competitions. The equations are generalized, and thus do not show the charge for all ions.

The first set is the competition between protons (H) and free metal cation (M) for ligands in solution (L):



The second set is the competition between free metal cations and protons for ligand sites on the cellular membrane (L_C)



The mass balance equations for total metal concentration is the following equation is:

$$M_T = M + ML + ML_C.$$

In the case where metal ions are strongly bound to membrane phosphate relative to hydrogen ions, it is assumed that a single metal cation can complex with one or two surface-immobilized ligands due to the chelate effect and the proximity of the ligands. Complexes comprised of more than two surface ligands are deemed to be structurally unreasonable (Burggraf *et al.*, 1997). The toxicity model is further developed with the following arguments:

The mass balance equation for the total essential ligand sites is: $L_{C\text{ total}} = L_C + HL_C + ML_C$. The normalized metabolic activity is taken to be equal to the fraction of membrane ligands unaffected by metal ion chemisorption, f_c , where $f_c = L_C / (L_C + HL_C + ML_C)$.

Substituting the appropriate formation constants defined previously,

$$f_c = (1 + \alpha_1[M])^{-1} \quad (1)$$

where: $\alpha_1 = K_{LC}K_{AC} / ([H^+]^n + K_{AC}) \quad (2)$

When there is excess solution ligand, f_c has a form similar to equation (1):

$$f_c = (1 + \alpha_{1L}[ML])^{-1} \quad (3)$$

where: $\alpha_1 = \{K_{LC}K_{AC}([H^+]) + K_A\} / \{K_LK_A\bar{C}_L([H^+]^n + K_{AC})\} \quad (4)$

n = the proton substitution number for the membrane ligand sites

If $NMA = f_c$, in the presence of excess solution ligand, the toxicity function is proportional to the total metal concentration by:

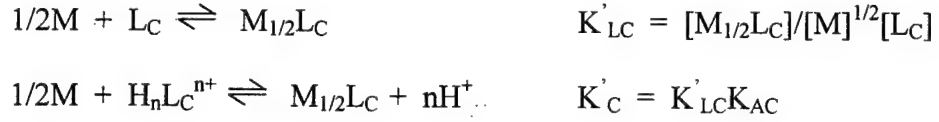
$$(NMA^{-1} - 1) = \beta_1 [ML^{2+}] \quad (5)$$

where, $\beta_1 = \alpha_1$.

In this relationship, $(NMA^{-1} - 1)$ will be referred to as the toxicity function. The toxicity function is used in subsequent analysis to determine the toxicity response to lead ions. The relationship implies that the toxicity response will be proportional to the lead adsorbed by the microorganisms for strongly bound metal ions.

If hydrogen ions compete well with metal ions for membrane phosphate, such that $([M]K_{LC} < ([H^+](K_{AC})^{-1}))$, it is assumed that cellular ligands will be protonated. Bi-chelate complexation in this situation is unlikely since the formation of a bi-phosphate complex

would require two independent deprotonated ligands. In this case, metal ion will be complexed with only a single cellular ligand. Thus, the equilibrium equation defining metal-cellular ligand complex formation is changed to the following equations:



and equations (1) and (2) are changed to:

$$f_c = (1 + \alpha_2[M]^{1/2})^{-1} \quad (6)$$

where: $\alpha_{2L} = \{K'_{LC}K_{AC}/([H^+] + K_{AC})\} \quad (7)$

When there is excess solution ligand, f_c has a form similar to equation (1):

$$f_c = (1 + \alpha_{2L}[ML]^{1/2})^{-1} \quad (8)$$

where: $\alpha_{2L} = \{K'_{LC}K_{AC}([H^+] + K_A)^{1/2}\}/\{(K_LK_{AC}C_L)^{1/2}([H^+]^n + K_{AC})\} \quad (9)$

And the toxicity function is proportional to the square root of the total metal ion concentration:

$$(NMA^{-1}-1) = \beta_2 [ML]^{1/2} \quad (10)$$

Equations (5) and (10) are further simplified to eliminate the need to measure K_{AC} directly. If the pH is low enough, the free metal ion activity will roughly equal the total metal concentration M_{total} . If the test medium contains no ligands other than the microorganisms, the metal-microorganism interaction can be simplified to a single equilibrium equation:



where Γ is the distribution coefficient (DC) defining the fraction of metal absorbed on the microorganisms per dry mass of microorganism. The distribution coefficient is valid

for any pH in which the majority metal specie is the free ion. The DC can be determined for microorganisms in solution at any pH, however, the DC can only be applied to predict the toxicity response in similar pH solutions.

The toxicity function can now be arranged to reflect the DC as shown below for the case in which protons do not compete well with lead ions:

$$(NMA^{-1}-1) = \Gamma [M], \quad (11)$$

and in cases in which protons do compete well with lead ions:

$$(NMA^{-1}-1) = \Gamma [M]^{1/2}. \quad (12)$$

In this case, metal ion toxicity will not be proportional to metal adsorption.

III. Methodology

Overview

This chapter is organized into three sections: Materials, Standard Techniques, and Experimental Procedures. The Materials and Standard Techniques sections present a general discussion on the materials and procedures used in some or all of the experiments. The Experimental Procedures section describes in detail the six experiment types performed.

Materials

This section is a general description of the materials used repeatedly throughout the experimental process. The materials described in this section will be referred to by name in subsequent discussions regarding standard techniques and experimental procedures.

Microcosm. A microcosm is the standard test unit consisting of dilution water (DW) and innoculum. The microcosm contents is contained in a standard 300-mL BOD bottle (Wheaton).

Innoculum. Innoculum consists of microorganisms and growth solution used as the test mixture in the experiments. A microorganism consortium was selected for its ability to degrade toluene under aerobic conditions. It was derived from an activated sludge mixed liquor sample taken from the effluent end of an aeration basin at the Fairborn Water

Reclamation Center. One liter of the activated sludge was added to 3-L growth medium within a bioreactor. The growth medium was a 1:1 dilution of a Hach BOD Buffer pillow and 20 ppm potassium nitrate. The growth medium's inorganic nutrient composition is shown in Table 3.1. Toluene was the microbial population's only source of carbon. A continuous flow of toluene-saturated air was fed into the bioreactor at a rate of 2-mL of toluene per hour. The nutrients in the bioreactor were replenished daily by replacing at least 300-mL of the inoculum with an equal growth medium volume. The inoculum's microorganisms were characterized as being predominantly gram-negative bacteria with a small percentage of gram-positive bacteria (Goodbody, 1997).

TABLE 3.1. NUTRIENTS IN GROWTH MEDIUM

Nutrient	Conc. ppm
NO_3^-	12.3
K^+	19.9
PO_4^{3-}	29.6
Cl^-	19.7
Na^{+2}	5.7
NH_4^+	0.6
Mg^{+2}	2.2
SO_4^{2-}	8.8
Ca^{+2}	9.9
Fe^{+3}	0.5

Dilution Water (DW). DW is a solution of K^+ , Na^{2+} , Ca^{2+} , and Mg^{2+} in deionized water. DW provides the osmotic gradient necessary for the microorganisms' survival in a microcosm.

One liter of DW water consisted of 5.0-mL potassium nitrate stock solution, 5.0-mL sodium nitrate stock solution, 6.0-mL calcium nitrate stock solution, and 3.0-mL magnesium nitrate stock solution. The DW was pH adjusted to 5.0 using dilute nitric

acid and dilute sodium hydroxide. DW was prepared for each experiment one day prior and left at room temperature in a covered reagent bottle. The nutrient concentration in one liter of DW is shown in Table 3.2.

The stock solutions consisted of 10,000 ppm potassium nitrate, sodium nitrate, calcium nitrate, and magnesium nitrate and were prepared from their respective nitrate salts in de-ionized water.

TABLE 3.2. NUTRIENTS IN DILUTION WATER

Nutrients	Concentration (ppm)
NO_3^-	98.7
K^+	19.3
Na^{+2}	13.5
Mg^{+2}	2.8
Ca^{+2}	10.2

Metal Treatment. A 1000 ppm standard lead stock solution in a nitric acid matrix was used in the preparation of all metal treatments one day prior to an experiment. DW was used to dilute lead stock solution to prepare metal treatments at specific lead concentrations. The DW containing the metal treatment was pH adjusted to 5.0 and left at room temperature in a closed reagent bottle.

Filtering Apparatus. Microcosms were vacuum filtered using Whatman GF/A, binder-free glass fiber filters (particle retention 1.6 μm) with a Fisherbrand, 47mm diameter vacuum filter holder, gasket, and flange.

Dissolved Oxygen (DO) Meter and BOD Probe. Dissolved oxygen in the microcosms was measured using either a Yellow Springs Instruments (YSI) Model 5100 DO meter with a YSI 5010 self stirring BOD probe, or a YSI Model 58 with a YSI 5730 self stirring BOD probe and a Kipp & Zonen Dual Channel model BD 112 flatbed recorder.

Lead Selective Electrode and Meter. The lead activity was determined using an Orion Model 920 Benchtop pH/ISE meter with a combination reference, Orion Model 9682 ionplus™ series lead electrode, in which the sensing electrode and reference electrode were housed in one unit.

Standard Techniques

This section describes the preparation and measurement techniques that were used repeatedly throughout the experimental process. These techniques are referred to in the Experimental Procedures section.

Standard Preparation of Microcosms. Typically, 15 to 18 microcosms were prepared for a single experiment. 260-mL aliquots of DW (with or without metal treatment) were distributed in standard 300-mL BOD bottles (Wheaton). The volume of DW used varied with the volume of inoculum used.

A single draw of inoculum was continuously stirred in a 1-L glass beaker at medium to high speed for 5 to 10 minutes. The floc and filamentous formations within the inoculum were dispersed by the stirring. The inoculum was then vacuumed filtered

through a 100-mm diameter, fixed perforated plate porcelain funnel to eliminate large microbial formations (>1.5mm) that could have lead to large variations in the distribution of microorganisms.

The inoculum was continuously stirred while it was distributed in a pseudo-random pattern into 50-mL glass beakers in two passes to ensure each microcosm received an estimated equal mass of microorganisms. The inoculum was introduced into the BOD bottles and an additional 5-mL of untreated DW was added to eliminate any headspace in the BOD bottle. The microorganisms were then allowed to acclimate in the microcosm for 5 to 10 minutes prior to testing.

Special Preparation of Microcosm. A special preparation procedure was followed to eliminate all inorganic complexing agents from the microcosm. The entire inoculum was centrifuged; the supernatant was removed; the remaining pellet was rinsed twice using DW; and the pellet was resuspended using DW equilibrated with toluene.

Blanks. DW blanks were used to measure the dissolved oxygen probe accuracy and the possible cross-contamination effects. Other microcosms, not treated with lead, were used to establish a baseline dissolved oxygen consumption rate.

Filtering and Weighing Technique. Each glass fiber filter paper was placed in an aluminum weigh boat and dried in a convection oven for 24 hours at 104° C. The filters

were removed and placed in a desiccator to cool for at least 45 minutes. The tarred initial dry weight of the filters was measured using a Mettler Toledo analytical balance.

After vacuum filtering the microcosm contents; the filter paper was again dried for 24 hours; cooled in a desiccator for 45 minutes; and then the final dry weight was measured.

DO Measurement Technique. The BOD probe was rinsed with de-ionized water prior to all DO measurements. The probe was inserted into the BOD bottle firmly to ensure an air tight seal. The probe was allowed to stir in the BOD bottle for two minutes prior to recording the DO measurement. Measurements were then performed in a random fashion to eliminate bias due to the sampling sequence.

Lead Activity Measurement Technique. Solutions were continuously stirred while performing lead activity measurements. The electrode potential was allowed to stabilize (1 to 5 minutes depending on the lead activity) prior to recording three consecutive readings. The temperature and pH of each microcosm was measured and recorded after the activity measurement.

Lead Activity Calibration Procedure. A 100-mL volume of DW was pH adjusted to 5.0 (± 0.02). A 100 ppm lead standard solution was added incrementally to the DW, and the electrode potential at each addition was recorded. A semi-logarithmic plot of the

electrode potential as a function of total lead was constructed to calibrate subsequent lead activity measurements.

The DW, at its final lead concentration, was measured before and after each series of microcosm measurements to adjust for slight differences in the solutions' matrix composition.

Experimental Procedures

This section describes the procedures used in each experiment reported in Chapter IV, Findings and Analysis.

DO Consumption Rate Linearity Experiment. A single microcosm was prepared using 40-mL of inoculum and untreated DW. The DO consumption rate was monitored using a flatbed recorder. The data obtained from this procedure was used to show evidence that the DO consumption rate of an untreated microcosm is linear over the duration of a typical experiment (70 to 80 minutes).

DO Consumption Rate Reproducibility Experiments. Two experiments (24 July and 3 Sept) were performed to determine the DO consumption rates of 18 untreated microcosms. The microcosms tested included three blanks. The total inoculum volume used for each experiment was drawn from the bioreactor at one time. Three DO measurements were recorded for each microcosm over a 30 to 60 minute period. Simple linear regression was used to determine each microcosm's DO consumption rate.

In the 24 July experiment, six microcosms were prepared and tested in three separate trials. Each microcosm contained 30-mL of inoculum. In the 3 Sept experiment, all 18 microcosms were prepared and tested in a single trial. The microcosms in the 3 Sept experiment contained 50-mL of inoculum. The data, obtained from the two DO reproducibility experiments, was used to quantify the coefficient of variation in the DO consumption rate using slightly different procedures.

Various Inoculum Volume Experiments. Two experiments (2 Sept and 5 Oct) were performed to determine the DO consumption rates of microcosms containing different inoculum volumes.

The experiment performed on 2 Sept consisted of preparing and testing 18 microcosms containing 0, 20, 30, 40, 50, and 60-mL of inoculum in triplicate. The toluene source for each microcosm was increased proportionally to the inoculum volume.

In the 5 Oct experiment, 12 microcosms containing 10, 20, 30, and 40-mL of inoculum in triplicate were prepared using the special preparation procedures. The toluene content was kept constant for each microcosm. Each microcosm tested in the 5 Oct experiment was filtered and weighed.

Data obtained was used to demonstrate the relationship between inoculum volume and DO consumption rate. The mass data gathered from the 5 Oct experiment established a mass-DO consumption rate relationship as well as a mass-inoculum volume relationship.

Activity Measurement Reproducibility Experiment. Three consecutive electrode potential measurements of four DW samples containing 15.15, 30.3, 60.6 and 122.1 ppm total lead were recorded. The measurements were performed in three separate trials. Between each trial a set of microcosms were measured.

The data obtained from this experiment was used to quantify the electrode potential measurement precision and to demonstrate an acceptable way to correct for electrode response offsets.

Metabolic Inhibition Experiments. Three experiments (8 Aug, 30 Aug, and 13 Sep) were performed to determine the metabolic inhibition due to lead ions. In each experiment, microcosms were treated with various concentrations of lead. The initial DW pH used in each microcosm was adjusted to 5.0. The DO consumption rate and lead activity was determined for each microcosm.

Twelve microcosms, which included two blank microcosms and two untreated microcosms, were prepared and tested during the 8 Aug experiment. Microcosms containing total lead concentrations of 13.2, 26.3, 52.6, and 105.3 ppm were tested in duplicate. The final pH ranged from 4.6 in the microcosms containing 105.3 ppm lead to 5.8 in the untreated microcosms.

Fifteen microcosms, which included three blank microcosms and three untreated microcosms, were prepared and tested during the 30 Aug experiment. Microcosms containing total lead concentrations of 0.9, 4.4, and 8.7 ppm were tested in triplicate. The

final pH ranged from 5.13 in the microcosms containing 8.7 ppm lead to 5.6 in the untreated microcosms.

Twelve microcosms, which included three untreated microcosms, were prepared and tested during the 13 Sept experiment. Microcosms containing total lead concentrations of 0.9, 8.7, and 43.3 ppm were tested in triplicate. The final pH of the microcosms were not recorded for this experiment.

The data obtained from the three experiments was used to determine a relationship between lead activity and metabolic inhibition in the microcosms.

Lead Adsorption Experiment. Three experiments (17 Sep, 22 Sep, and 7 Oct) were performed to determine the amount of lead adsorbed to a microbial mass. In the experiment, the lead activity calibration procedure was first performed. Then, using a DW/microorganism mixture, the calibration procedure was repeated.

The DW/microorganism mixture was prepared by centrifuging 80-mL of innoculum and removing the supernatant. It was necessary to remove the supernatant because the liquid contained organic and inorganic complexing agents. The remaining pellet was rinsed twice and re-suspended with DW. The suspended material was then added to 600-mL of DW. In the 17 Sept and 22 Sep experiment, the pH was 5.0 in the DW solution and in the DW/microorganism mixture. In the 7 Oct experiment, the DW solution was 4.3 and the DW/microorganism mixture was 5.6.

The data obtained from the three experiments was used to estimate three lead coefficient values.

IV. Findings and Analysis

Overview/Introduction

The experimental findings and analysis are presented in four main sections: Experimental Measurements, Metabolic Inhibition Experiments, Metal Complexation Experiments, and Predicted Versus Actual Toxicity Response.

Experimental Measurements presents the experimental results used to establish test parameters. Metabolic Inhibition Experiments discusses the relationship between metabolic inhibition and lead activity. The Metal Complexation Experiments reports the distribution coefficients (DC) which define the lead amount presumably adsorbed to microbial mass as a function of lead activity. Moreover, evidence suggesting two cellular binding sites will be presented in this section. The final section, Actual Versus Predicted Toxicity Response, compares the actual toxicity response observed in two metabolic inhibition experiments with the predicted toxicity responses determined by the Case II equation of the TM.

Experimental Measurements

The purpose of the experiments described in this section was to establish certain test parameters. First, the linearity of the DO consumption rate was demonstrated. Next, the DO consumption rate reproducibility was quantified. Then, the linear relationship between microbial mass and DO consumption rate was established. Finally, the lead activity reproducibility was determined.

DO Consumption Rate Linearity Experiments. The DO consumption rate for the microcosm tested was linear over a period of 190 minutes as shown in Figure 4.1. A least squares fit line indicated a high correlation ($R^2 = 0.9996$) with a simple linear model. In this case, the DO consumption rate was the slope of the regression line ($0.0223 \text{ (mg/L)/min}$).

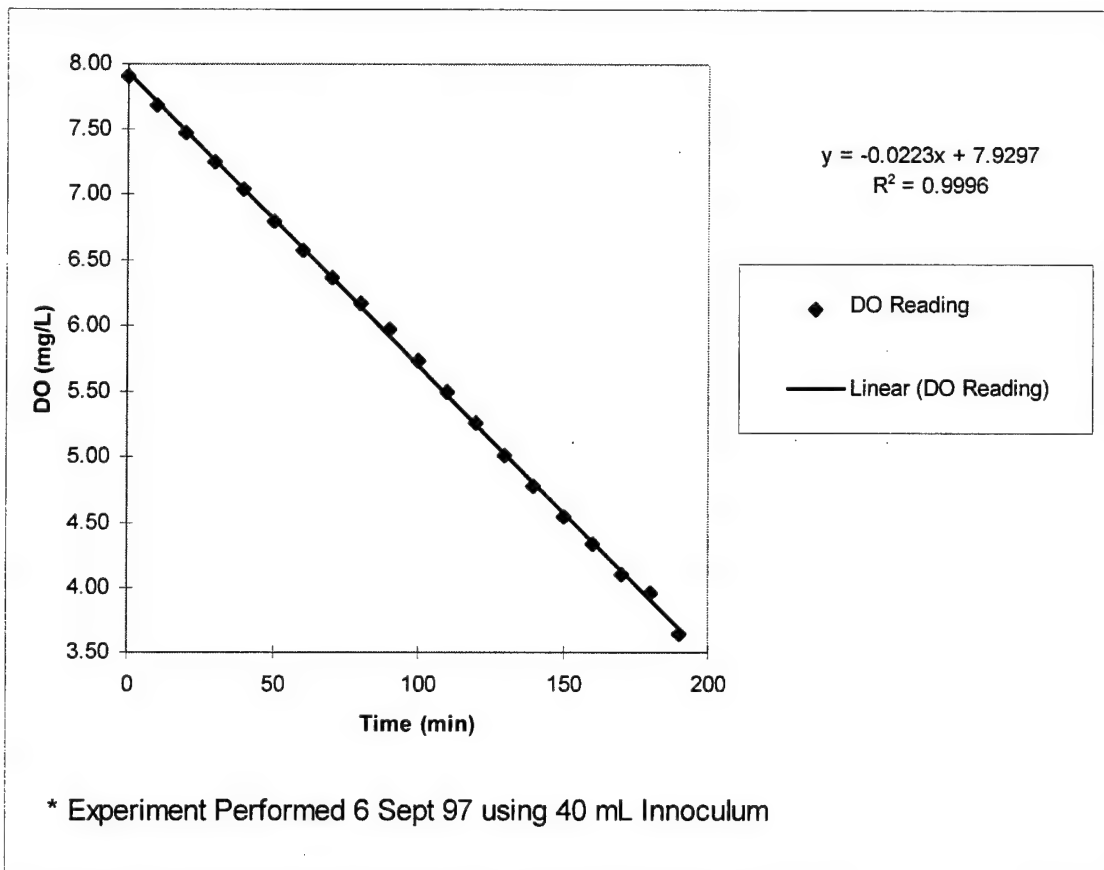


Figure 4.1. Time Versus Dissolved Oxygen (DO) Reading

The linearity of the DO consumption rate suggested that the test microbial population was slow growing, and that a first order rate of oxygen consumption could be used to describe the selected culture metabolic activity (Hansen, 1995:66). The DO

consumption rate for lead treated microcosms was determined to be linear over the test period (not shown) using linear regression. A high degree of correlation was found between time and DO consumption rate in the metal treated microcosms measured.

The DO consumption rates determined in subsequent experiments were determined by simple linear regression of at least three measurements taken over a 30 to 80 minute period.

DO Consumption Rate Reproducibility Experiments. An experiment typically required the use of 15 to 18 microcosms. It was important that each microcosm exhibited a metabolic activity that was nearly the same. Identical metabolic activities between each microcosm was impossible due to microorganism distribution variation within the inoculum.

In an experiment performed on 24 July, a coefficient of variation (CV) of 7.95% was achieved for 15 microcosms as reported in Table 4.1. A CV of 6.60% was achieved for 15 microcosms tested on 3 Sept as shown in Table 4.2.

The experiment performed on 3 Sept resulted in a smaller CV, but bias due to sampling was evident. Table 4.2 lists the microcosms in the order in which they were tested. The DO consumption rate decreased slightly for each microcosm further in the order. Random sampling was used in subsequent experiments to reduce sampling bias.

The DO consumption rate of the three blank microcosms (not shown) was 0.00 for each experiment which suggest little occurrence of cross-contamination between microcosms. The lack of DO consumption in the blanks also demonstrated that the

instrumental error in the DO probe was not large enough to effect the DO consumption rate.

Each microcosm in the 24 July experiment contained 30-mL of inoculum resulting in an average DO consumption rate of 0.033 (mg/L)/min. In the 3 Sept experiment the microcosms tested contained 50-mL of inoculum, but produced an average DO consumption rate of only 0.027 (mg/L)/min. The most probable reason for this occurrence was that the 24 July experiment inoculum may have had a greater microorganism concentration. Despite the smaller volume of microcosm, the microorganism concentration in the 3 Sept experiment may have been large enough to produce a relatively high DO consumption rate. The relationship between inoculum volume, microbial mass, and DO consumption rate is discussed in the next section.

TABLE 4.1. DISSOLVED OXYGEN CONSUMPTION RATE REPRODUCIBILITY TEST PERFORMED 24 JULY 97 (APPROXIMATELY 30 MINUTE PERIOD)

Bottle # (In sequence of measurement)	DO Rate, mg/L/min
1	0.0315
2	0.0365
3	0.0319
4	0.0319
5	0.0346
6	0.0375
7	0.0328
8	0.0325
9	0.0307
10	0.0327
11	0.0353
12	0.0267
13	0.0334
14	0.0313
15	0.0314
Average	0.033
St. Dev.	0.003
CV	7.95%

TABLE 4.2. DISSOLVED OXYGEN CONSUMPTION RATE REPRODUCIBILITY TEST PERFORMED 3 SEPT 97.

Bottle # (In sequence of measurement)	DO Rate, mg/L/min
1	0.0302
2	0.0298
3	0.0293
4	0.0288
5	0.0282
6	0.0284
7	0.0277
8	0.0283
9	0.0272
10	0.0277
11	0.0258
12	0.0261
13	0.0258
14	0.0243
15	0.0246
Mean	0.027
St. Dev.	0.002
CV	6.60%

Various Innoculum Volume Experiments. Data obtained from two experiments, performed 2 Sept and 5 Oct, were used to establish the relationship between inoculum volume and DO consumption rate. Furthermore, the relationship between microbial mass, inoculum volume, and DO consumption rate was made from the 5 Oct experiment data.

Data obtained from the two experiments was used to explain variations in the DO consumption rate between microcosms; to establish the ideal inoculum volume for subsequent experiments; and to better understand the relationship between the metabolic inhibition and the microbial mass reduction.

The 2 Sept experiment data summary is shown in Table 4.3. Each triplicate CV was within 10%, except for the microcosms containing 20-mL of inoculum (20.38%). The smallest CV was observed in the microcosms using 50-mL of inoculum (1.22%). Hence, an inoculum volume must be selected which will produce a DO consumption rate large enough to minimize the CV.

The DO consumption rate for the blanks, or microcosm containing no inoculum, shown on Table 4.3, suggested that the effects of any cross-contamination or variations in the DO probe reading was not significant enough to influence the DO consumption rate.

TABLE 4.3. DISSOLVED OXYGEN (DO) CONSUMPTION RATE, AVERAGE DO CONSUMPTION RATE, STANDARD DEVIATION , AND COEFFICIENT OF VARIATION, EXPERIMENT PERFORMED 2 SEPT 97.

Innoculum Volume, mL	DO Rate, mg/L/min	Ave. DO Consumption Rate	Std Dev.	Coefficient of Variation
60 60 60	0.0383 0.0367 0.0340	0.036	0.002	5.98%
50 50 50	0.0267 0.0261 0.0262	0.026	0.000	1.22%
40 40 40	0.0178 0.0186 0.0168	0.018	0.001	5.09%
30 30 30	0.0102 0.0103 0.0086	0.010	0.001	9.83%
20 20 20	0.0037 0.0036 0.0025	0.003	0.001	20.38%
0 0 0	0.0003 0.0002 0.0003	0.000	0.000	NA

In Figure 4.2, the inoculum volume is plotted against the 2 Sept experiment microcosm DO consumption rates. The least squares polynomial fit suggested that the relationship between inoculum volume and the DO consumption rate was not linear for increasing volumes of inoculum. The DO consumption rate appeared to increase disproportionately with increasing inoculum volume. This non-linearity may be due to the greater toluene amount introduced in the microcosm which accompanies larger inoculum volumes.

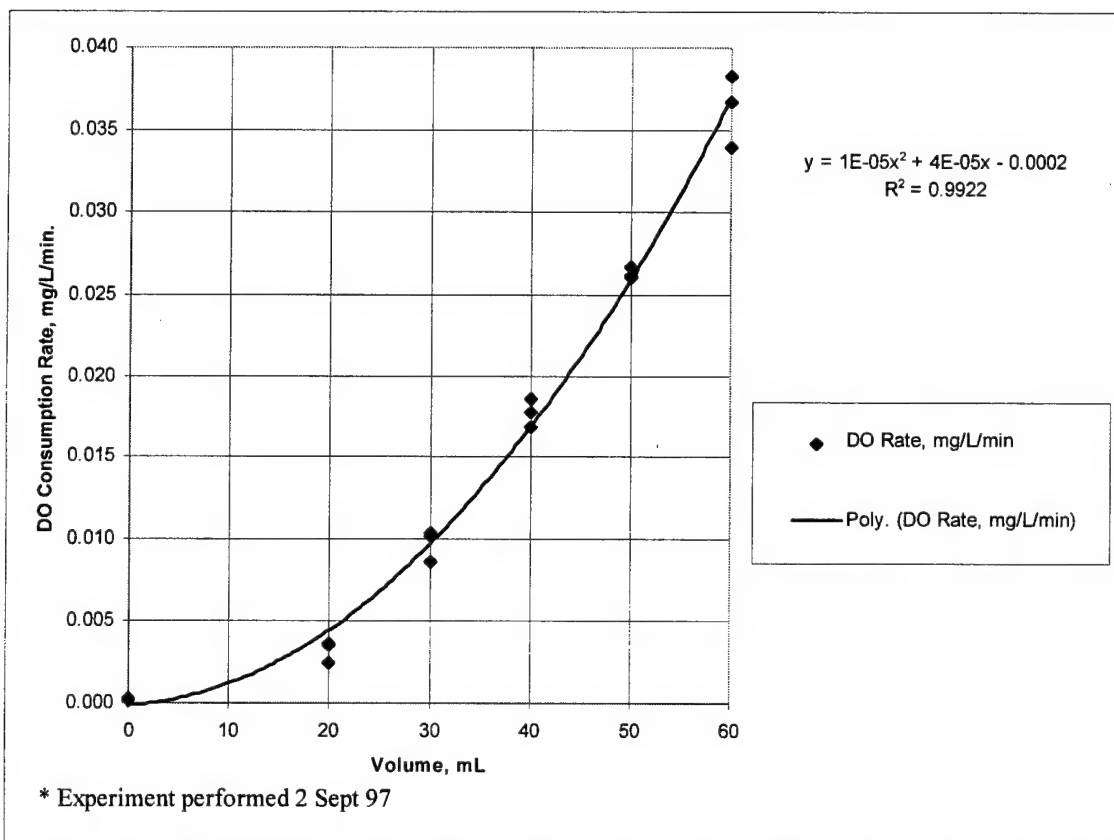


Figure 4.2. Inoculum Volume Versus Dissolved Oxygen (DO) Consumption Rate, Experiment performed 2 Sept 97.

The toluene concentration was held constant for the microcosm tested on 5 Oct. The test results summary is listed in Table 4.4. The average DO consumption rates were similar in the 5 Oct and 2 Sept experiments for microcosms containing similar volumes of inoculum (no statistics applied). The CV for the average 5 Oct DO consumption rates were generally higher than that of the 2 Sept values. A CV larger than 10% (16.55%) was achieved when the average DO consumption rate was 0.010 (mg/L)/min. The smallest CV occurred when the average DO consumption rate was only 0.006 (mg/L)/min. The larger CV values may be attributed to the additional preparation performed in the 5 Oct experiment.

TABLE 4.4. INNOCULUM VOLUME, ORGANISM MASS, AND DISSOLVED OXYGEN (DO) CONSUMPTION RATE, EXPERIMENT PERFORMED 5 OCT 97

Innoculum Volume (mL)	Organism Mass (mg)	Ave Mass (mg)	Mass stdev	Mass CV	DO Rate (mg/L/min)	Ave DO Rate	Rate Stdev	Rate CV
40	8.03	8.81	0.720	8.18%	0.0117	0.013	0.001	7.37%
40	8.95				0.0132			
40	9.45				0.0134			
30	7.03	6.96	0.762	10.95%	0.0095	0.010	0.002	16.55%
30	6.17				0.0085			
30	7.69				0.0118			
20	4.88	5.17	0.317	6.13%	0.0063	0.006	0.000	3.17%
20	5.51				0.0061			
20	5.13				0.0060			
10	2.56	2.61	0.104	4.00%	0.0044	0.004	0.001	15.45%
10	2.73				0.0032			
10	2.54				0.0042			

In Figure 4.3, the inoculum volumes are plotted against the 5 Oct experiment DO consumption rates. The data correlated well ($R\text{-squared} = 0.968$) with a least squares

linear fit line. A one-half inoculum volume decrease resulted in an approximate one-half DO consumption rate reduction. The close to ideal results achieved in this experiment may have resulted from ensuring a constant toluene concentration in each microcosm.

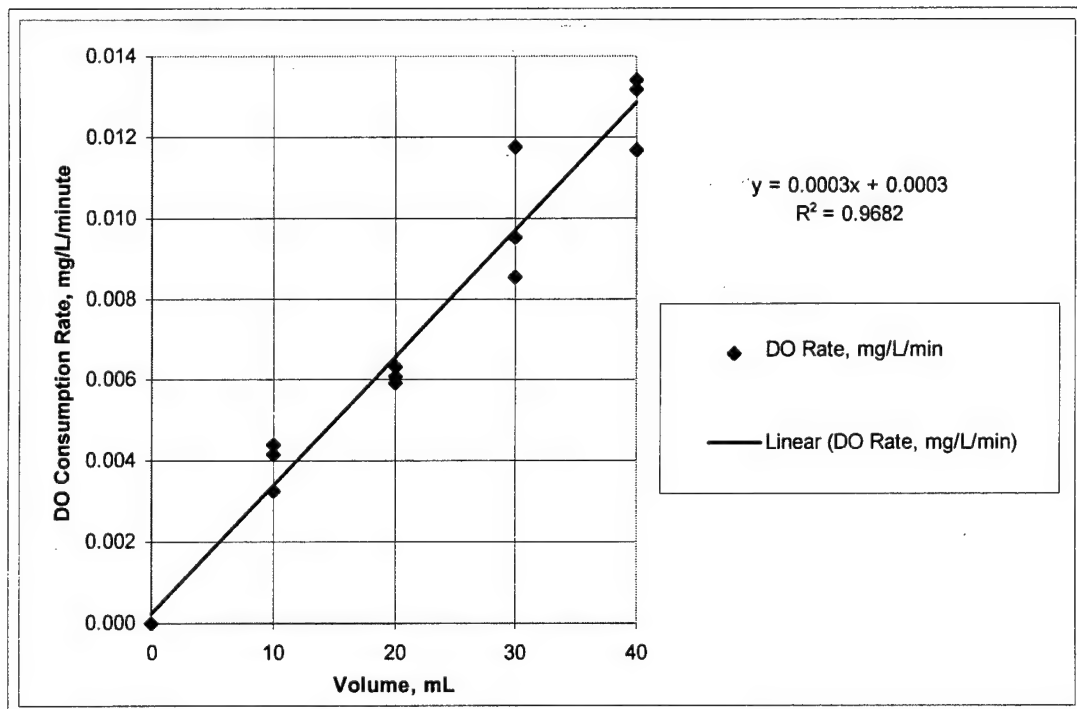


Figure 4.3. Inoculum Volume Versus Dissolved Oxygen (DO) Consumption Rate, Experiment Performed 5 Oct 97

In Figure 4.4, the microbial mass is plotted against the DO consumption rate in each microcosm tested in the 5 Oct experiment. The data correlates well (R -squared = 0.976) with a least squares linear fit line. Furthermore, a linear relationship (R -squared 0.975) between inoculum volume and microbial mass is illustrated in Figure 4.5.

It was expected that the microbial population would change over time within the bioreactor. These changes may have resulted in variations in the microbial concentration

in the inoculum. Figures 4.3, 4.4 and 4.5, are useful in comparing data from different experiments, and in explaining variations in the results. Since a strong linear relationship exists between microbial mass and DO consumption rate, the estimated dry microbial mass or the microcosms used in subsequent metabolic experiments were extrapolated from Figure 4.4 using the average DO consumption rate of the untreated microcosms.

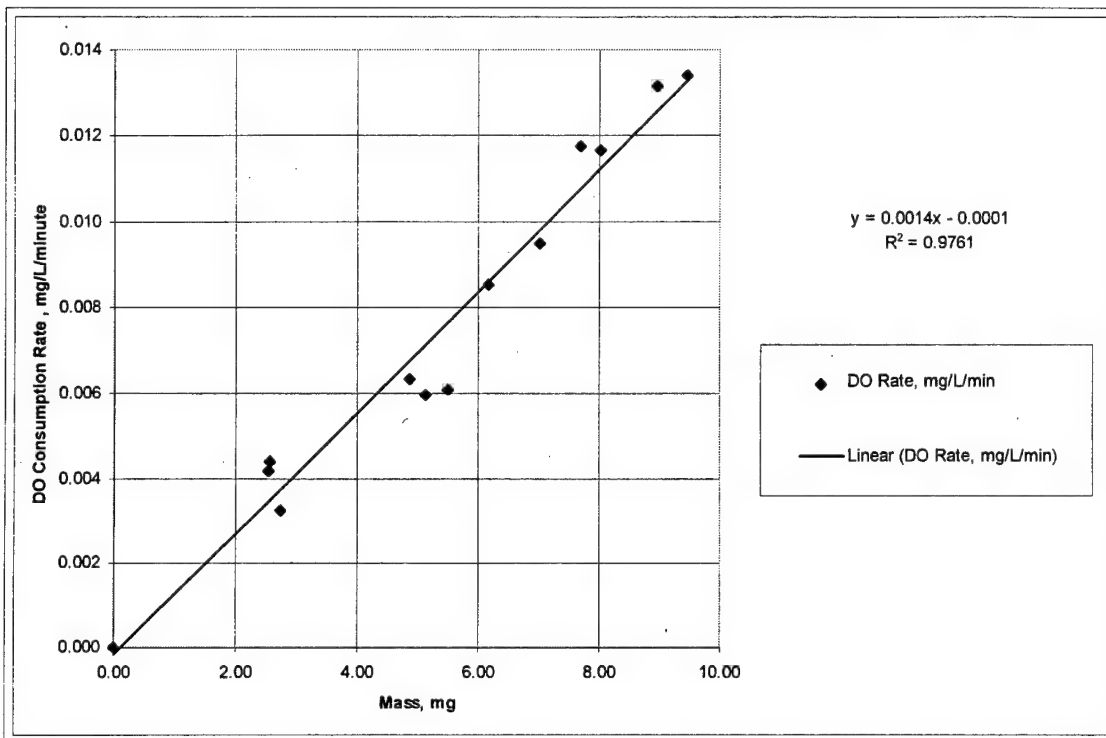


Figure 4.4. Microbial Mass Versus Dissolved Oxygen (DO) Consumption Rate, Experiment Performed 5 Oct 97

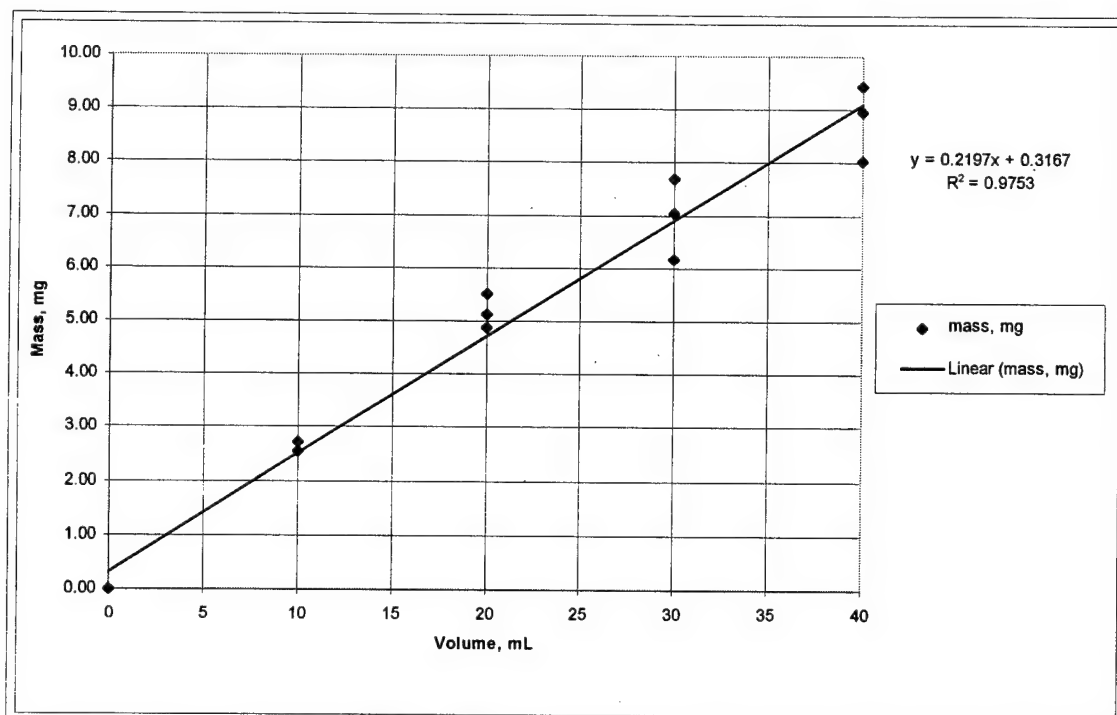


Figure 4.5. Innoculum Volume Versus Microbial Mass, Experiment Performed 5 Oct 97

Activity Measurement Reproducibility Experiment. The measurement precision of the lead ion selective electrode was tested on 8 Aug. Table 4.5 lists electrode potential values of four lead standards during three measurement trials. A value of 500 was added to the “raw” electrode potential values in order to transform the negative mV potential values to a positive number. Figure 4.6 illustrates that the potential readings were offset slightly after measuring a microcosm set between each trial. The CV for each measurement set was less than 1%. This error was well within the probe tolerance of 4%. However, Table 4.6 and Figure 4.7 demonstrate that greater precision (<0.2%) could be achieved if the offset between each set of measurements was corrected.

TABLE 4.5. UNCORRECTED ELECTRODE POTENTIAL, EXPERIMENT PERFORMED 8 AUG 97

Trial # Ave. Adjusted Potential	15.15 ppm standard	30.3 ppm standard	60.6 ppm standard	121.2 ppm standard
1	231.0	238.3	245.4	251.1
2	229.1	236.6	243.3	249.5
3	227.9	235.6	242.4	248.4
Mean	229.4	236.9	243.7	249.7
Stdev	1.57	1.39	1.53	1.36
CV	0.69%	0.59%	0.63%	0.55%

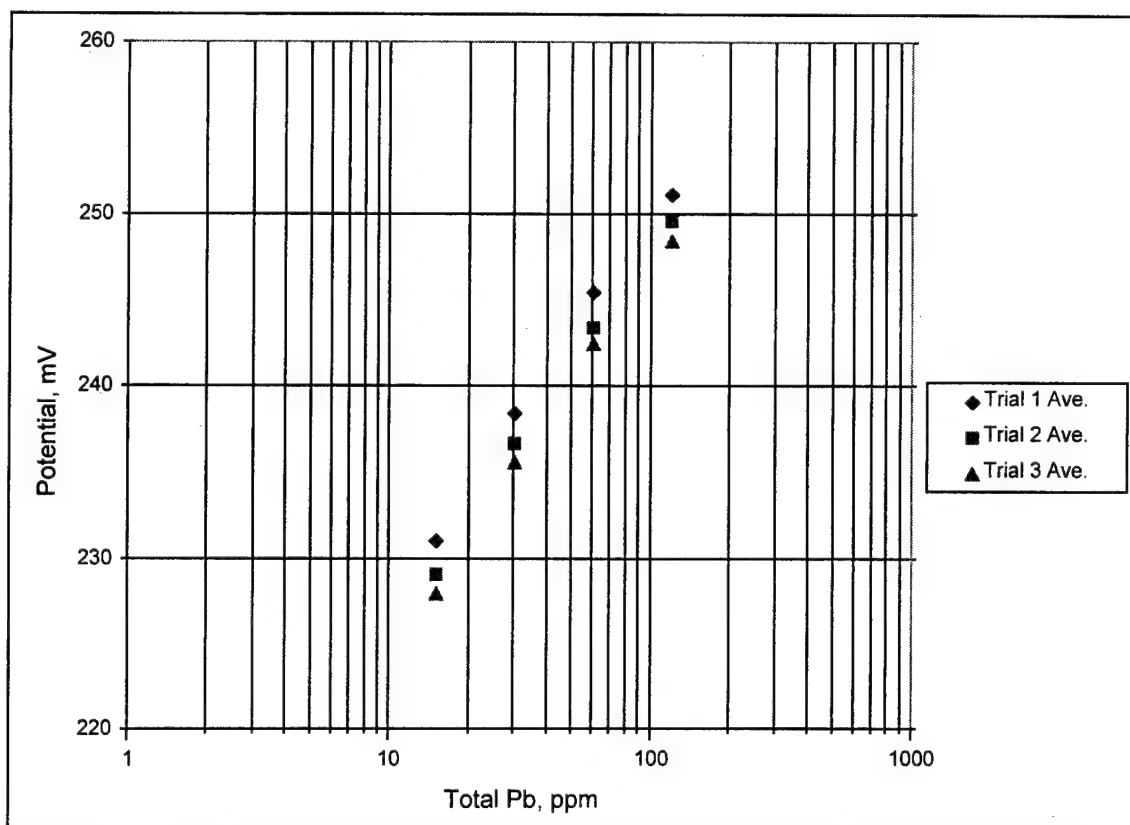


Figure 4.6. Total Lead Concentration Versus Electrode Potential, Uncorrected Data, Experiment Performed 8 Aug 97.

The offset in the electrode response was applied equally to all measurements.

Therefore, the offset can be corrected by subtracting the difference in potential readings

from a designated standard solution. In this case, the 121.2 ppm lead solution was the designated standard that was used to correct all measurements made in a single trial. This technique for correcting the offset in electrode potential measurements was applied in the experiments where lead activity measurements were performed.

TABLE 4.6. CORRECTED ELECTRODE POTENTIAL, EXPERIMENT PERFORMED 8 AUG 97

Trial # Ave. Adjusted Potential	15.15 ppm standard	30.3 ppm standard	60.6 ppm standard	121.2 ppm standard
1	231.1	238.4	245.4	251.1
2	230.7	238.2	244.9	251.1
3	230.7	238.3	245.2	251.1
Mean	230.8	238.3	245.2	251.1
Stdev	0.22	0.06	0.26	0.00
CV	0.10%	0.03%	0.11%	0.00%

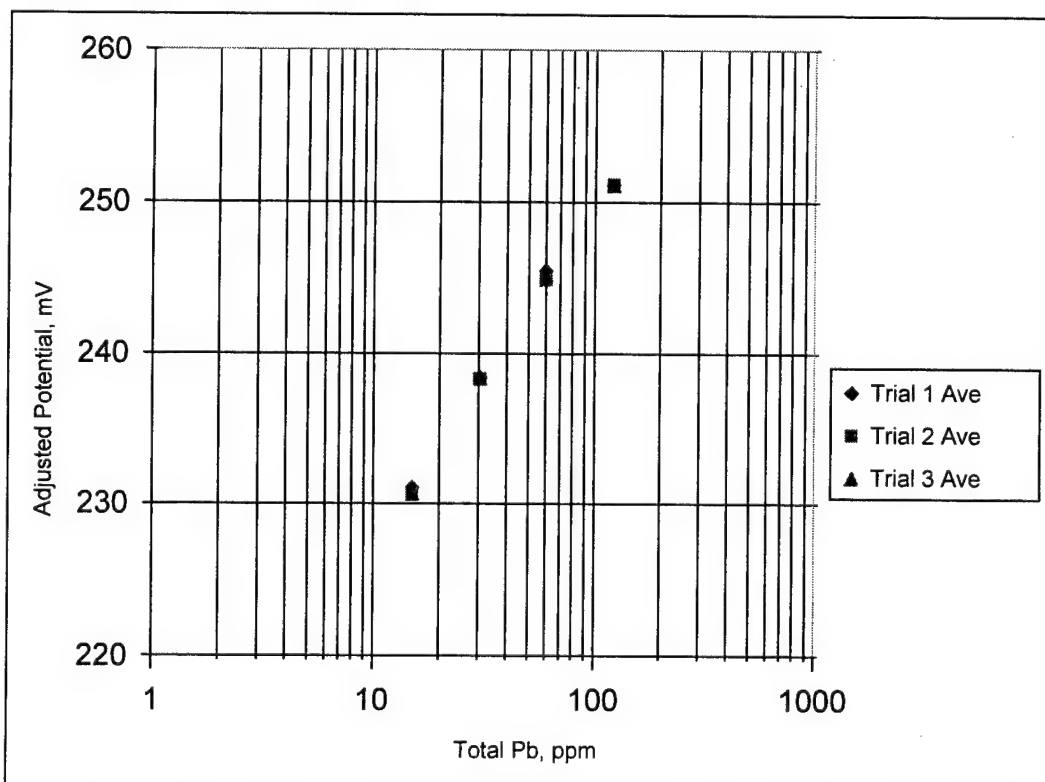


Figure 4.7. Total Lead Concentration Versus Electrode Potential, Corrected Data, Experiment Performed 8 Aug 97.

Metabolic Inhibition Experiments.

The purpose of the metabolic inhibition experiments was to determine if the relationship between the toxicity response and lead activity followed case I or case II behavior. The data obtained from these experiments served as the basis for subsequent comparisons between the actual and predicted toxicity response values.

TABLE 4.7. LEAD ACTIVITY, DISSOLVED OXYGEN (DO) CONSUMPTION RATE, AVERAGE NORMALIZED METABOLIC ACTIVITY (ANMA) AND TOXICITY FUNCTION, EXPERIMENT PERFORMED 8 AUG 97.

Total Pb conc. ppm	Ave Pb Act.	Ave DO Rate	ANMA	Ave Tox. Func	Ave. Final pH
13.16	6.1 (± 0.424)	0.012 (± 0.0018)	0.666 (± 0.086)	0.52 (± 0.197)	5.0
26.33	20.5 (± 0.424)	0.010 (± 0.0011)	0.558 (± 0.046)	0.80 (± 0.148)	4.9
52.65	46.4 (± 0.071)	0.007 (± 0.0001)	0.411 (± 0.002)	1.43 (± 0.011)	4.8
105.30	98.7 (± 0.849)	0.005 (± 0.0000)	0.300 (± 0.007)	2.33 (± 0.079)	4.6
0.00	0.0	0.018 (± 0.0004)	1.000 (± 0.000)	0.00 (± 0.000)	5.8
Untreat					
0.00	0.0	0.000 (± 0.0004)	0.025 (± 0.020)	NA	4.8
Blank					

* 30-mL of inoculum per microcosm

* Estimated 12.9 mg of microbial mass based on DO consumption rate of untreated microcosm

* () is one standard deviation from the mean

Table 4.7 shows the average lead activity, average DO consumption rate, average normalized metabolic activity (ANMA), average toxicity function value, and average pH for the microcosms tested in the 8 Aug experiment. The total lead concentration ranged from 0 to 105 ppm. The lead activity ranged from 0 to 98.7 ppm. The final pH ranged

from 4.6 in the microcosms containing 105.3 ppm total lead to 5.8 in the untreated microcosm. Each microcosm contained 30-mL of inoculum with exception to the blank, and each lead treatment was run in duplicate.

Table 4.7 also shows that the average DO rate of the untreated microcosm was 0.018 (mg/L)/min. Regardless of the inoculum volume used, the microbial mass can be determined based on the DO consumption rate by extrapolating the least squares fit line from Figure 4.4. In doing this the approximate mass in each microcosm is roughly 12.9 mg.

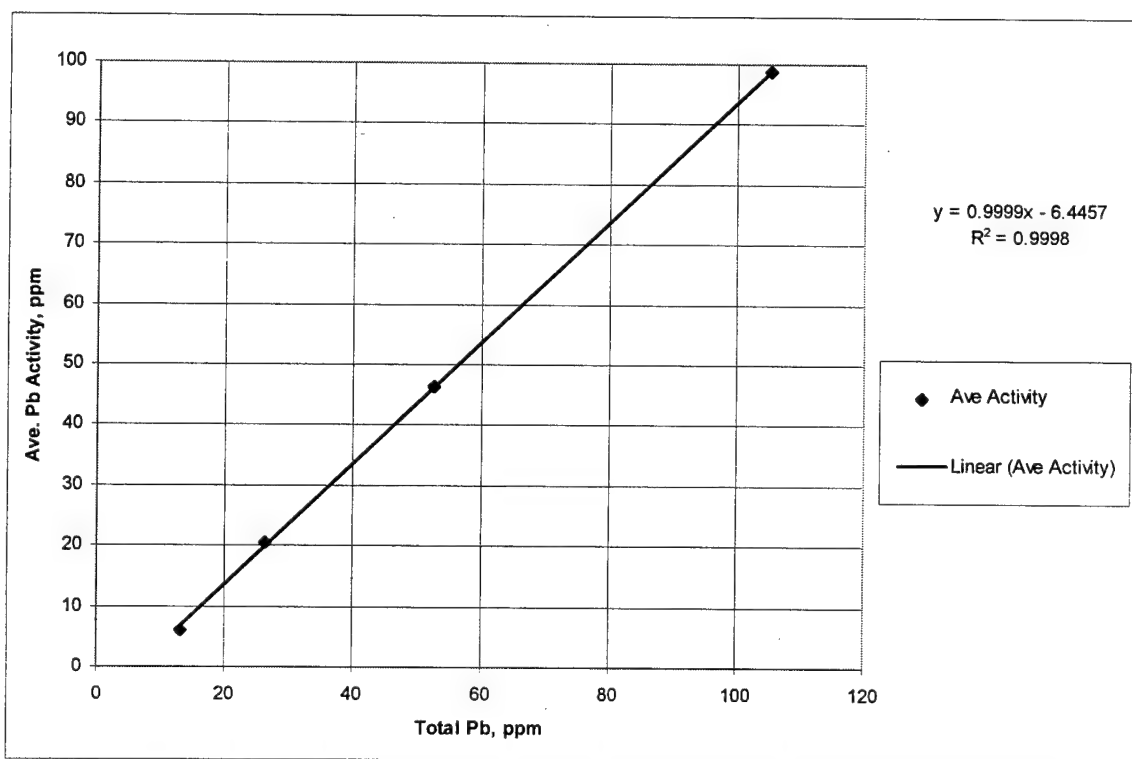


Figure 4.8. Total Lead Concentration Versus Average Lead Activity, Experiment Performed 8 Aug.

In Figure 4.8 the total lead concentration is plotted versus the average lead activity in each microcosm tested on 8 Aug. The data was fit with high correlation (R-squared = 0.999) with a simple linear regression line. The x-intercept in this case is 6.45 ppm and represents the equivalent amount of lead titrated by ligands.

The inorganic complexing agents in each microcosm included PO_4^{3-} , Cl^- , and SO_4^{2-} in concentrations of 2.91, 1.94, and 0.86 ppm, respectively. The lead equivalent for PO_4^{3-} , Cl^- , and SO_4^{2-} is 1.94, 3.88, and 0.86 ppm, respectively. The total lead equivalent value (6.68 ppm) nearly matches the x-intercept value (6.45 ppm) determined from Figure 4.8.

TABLE 4.8. TOTAL LEAD CONCENTRATION, LEAD ACTIVITY, DISSOLVED OXYGEN (DO) CONSUMPTION RATE, AVERAGE NORMALIZED METABOLIC ACTIVITY (ANMA), EXPERIMENT PERFORMED 30 AUG 97.

Total Lead Conc ppm	Average Lead Activity ppm	Average DO Consum. Rate	ANMA	Ave. Toxicity Function	Ave. Final pH
0.87	0.04 (± 0.008)	0.016 (± 0.002)	0.71	0.42	5.64 (± 0.02)
4.42	0.21 (± 0.016)	0.014 (± 0.001)	0.61	0.65	5.22 (± 0.02)
8.69	2.10 (± 0.125)	0.008 (± 0.001)	0.36	1.80	5.12 (± 0.01)
0.00	0.00	0.023 (± 0.000)	1.00	0.00	5.68 (± 0.08)
Untreat					
0.00	0.00	0.000 (± 0.000)	0.02	na	na
Blank					

* 30-mL of inoculum per microcosm

* Estimated 16.5 mg of microbial mass based on DO consumption rate of untreated microcosm

* () is one standard from the mean

Table 4.8 shows the average lead activity, average DO consumption rate ANMA, average toxicity function values, and pH for the microcosms tested in the 30 Aug experiment. The total lead concentration ranged from 0 to 8.7 ppm. The corresponding lead activity ranged from 0 to 2.10 ppm. The final pH ranged from 5.13 in the microcosms containing 8.7 ppm lead to 5.6 in the untreated microcosms. Each microcosm contained 30-mL of inoculum except the blank. Each lead treatment was run in triplicate. The average untreated microcosm DO consumption rate shown was 0.023 (mg/L)/min. The estimated microbial mass was 16.5 mg.

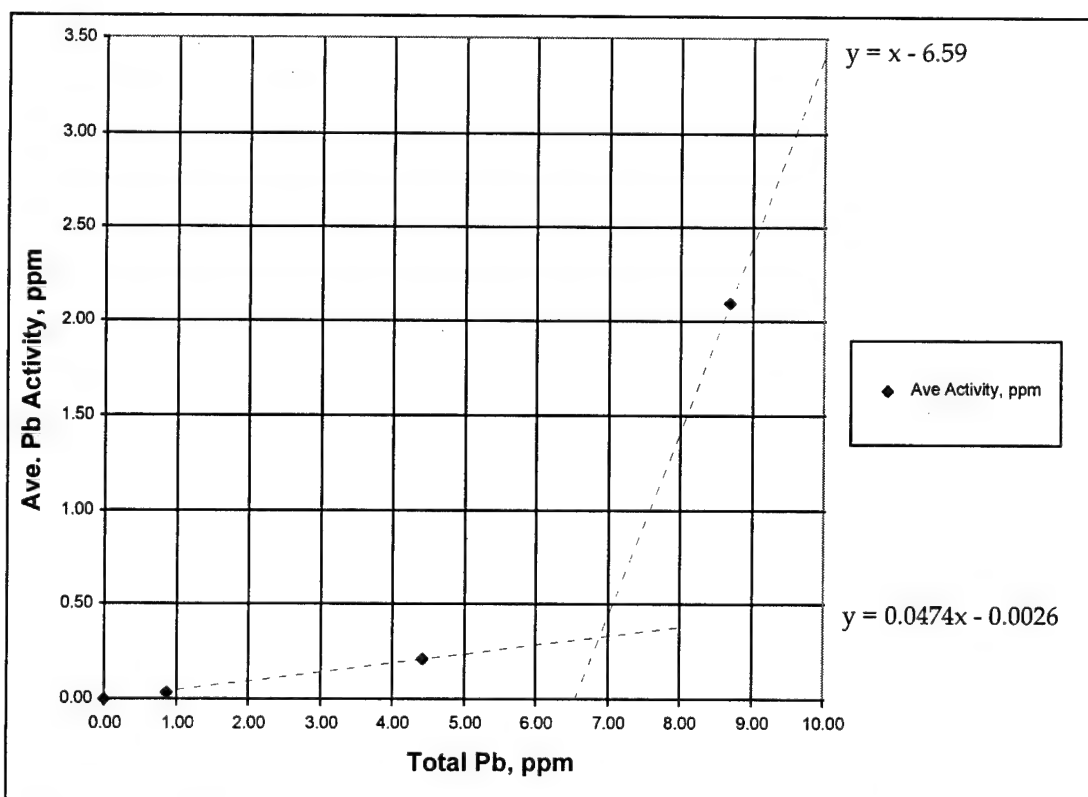


Figure 4.9. Total Lead Concentration Versus Average Lead Activity, Experiment Performed 30 Aug.

In Figure 4.9, the total lead concentration is plotted versus the average lead activity in each microcosm tested on 30 Aug. The amount of lead complexed by ligands is approximately 6.92 ppm. The value was determined by plotting the theoretical slope ($y=x-6.59$) and the least squares linear fit line ($y = 0.0474 x - 0.0026$). The point at which the two lines intersect represents the lead complexed by ligands. Again, the amount of lead complexed is reasonable since each microcosm contained PO_4^{3-} , Cl^- , and SO_4^{2-} in concentrations of 2.91, 1.94, and 0.86, respectively. The amount of inorganic ligands is roughly equivalent to 6.68 ppm lead.

TABLE 4.9. TOTAL LEAD CONCENTRATION, LEAD ACTIVITY, DISSOLVED OXYGEN CONSUMPTION RATE, AVERAGE NORMALIZED METABOLIC ACTIVITY (ANMA), AVERAGE TOXICITY FUNCTION, EXPERIMENT PERFORMED 13 SEPT 97.

Total Lead Conc. (ppm)	Ave. Pb Activity (ppm)	Ave DO Consum. Rate	ANMA	Ave. Toxicity Funct.
0.87	0.01 (± 0.001)	0.009 (± 0.0005)	0.86	0.16
8.67	0.49 (± 0.037)	0.008 (± 0.0004)	0.75	0.33
43.33	30.14 (± 1.700)	0.004 (± 0.0003)	0.41	1.46
0.00	0.00	0.010 (± 0.0006)	1.00	0.00
untreated.				

* 40-mL of inoculum per microcosm

* Estimated 7.21 mg of microbial mass based on DO consumption rate of untreated microcosm

* () is one standard deviation from the mean

Table 4.9 shows the average lead activity, average DO consumption rate, ANMA, and average toxicity function values for the 13 Sept experiment. The total lead concentration ranged from 0 to roughly 43 ppm with a corresponding lead activity of 0 to 30.14 ppm. Each microcosm contained 40-mL of inoculum, and each lead treatment was run in triplicate. The final microcosm pH was not recorded for this experiment. The average untreated microcosm DO consumption rate shown in Table 4.9 was 0.010 (mg/L)/min. The estimated microbial mass was 7.21 mg.

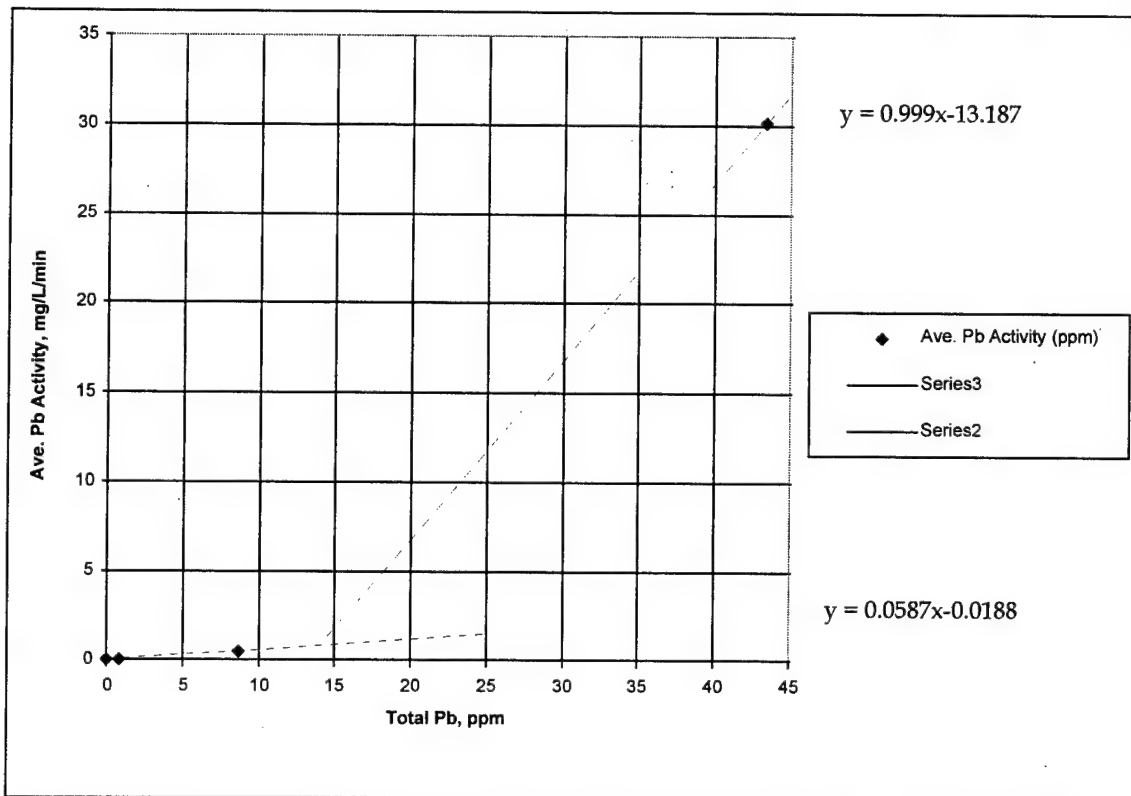


Figure 4.10. Total Lead Concentration Versus Average Dissolved Oxygen (DO) Consumption Rate, Experiment Performed 13 Sept 97.

In Figure 4.10, the total lead concentrations were plotted versus the average lead activity in each microcosm tested on 13 Sep. Approximately 14 ppm lead was complexed. The value was determined by plotting the theoretical slope ($y=0.999x-$

13.187) and the least squares linear fit line ($y=0.0587-0.0188x$). The intersection of the two lines represents the amount of lead complexed. The concentration for PO_4^{3-} , Cl^- , and SO_4^{2-} in each microcosm was 3.89, 2.58, and 1.15 ppm, respectively. The lead equivalent of the three inorganic ligands is 8.90 ppm.

The lead complexed in the 30 Aug and 13 Sept experiments were greater than the inorganic ligand lead equivalent. This suggests lead is complexed by other ligands other than PO_4^{3-} , Cl^- , and SO_4^{2-} . It is reasonable to expect that lead is complexed by dissolved organic material secreted by the microorganisms.

The average toxicity function values listed on Table 4.7 are plotted as a function of the average lead activity, and the square-root of the average lead activity in Figures 4.11 and 4.12, respectively. It was shown in the figures that a higher correlation ($R^2 = 0.984$) was achieved when the average toxicity function was plotted as a function of the average lead activity square-root rather than as a function of the average lead activity ($R^2 = 0.962$).

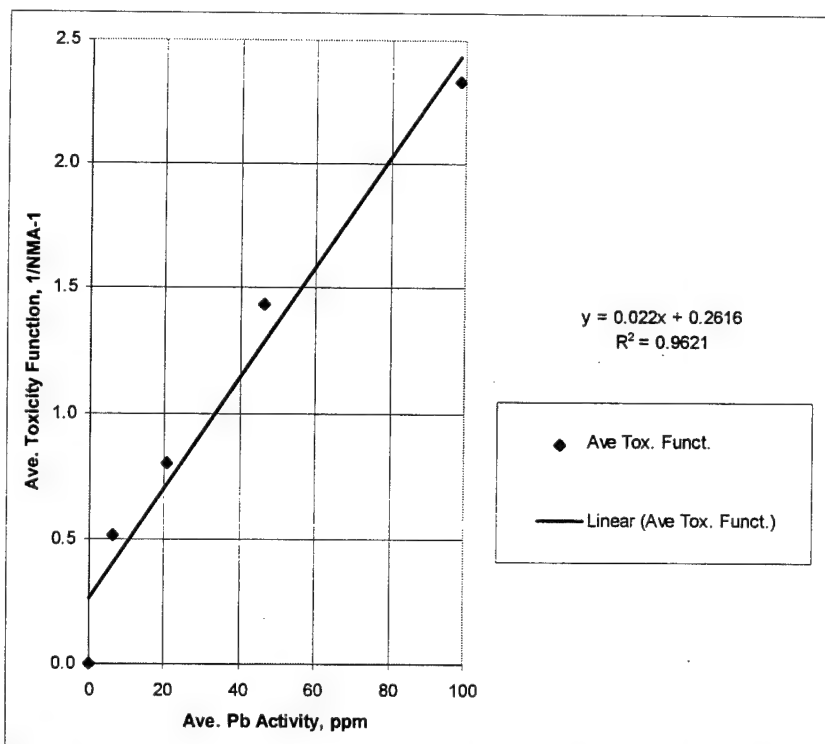


Figure 4.11. Average Lead Activity Versus Average Toxicity Function, Experiment Performed 8 Aug 97.

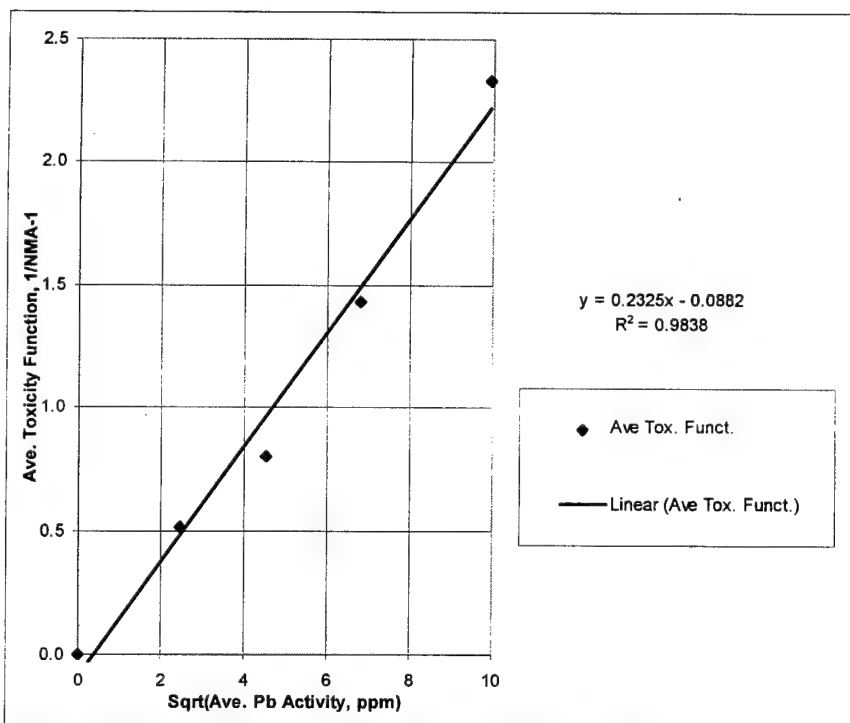


Figure 4.12. Square-root of Average Lead Activity Versus Average Toxicity Function, Experiment Performed 8 Aug 97

Likewise, the average toxicity function values shown in Table 4.8 are plotted as a function of the average lead activity in Figure 4.13, and as a function of the square-root of the average lead activity in Figure 4.14. The toxicity function values are correlated better with a least squares linear fit when plotted as a function of the average lead activity square root ($R^2 = 0.989$), rather than a function of simply the average lead activity ($R^2 = 0.922$).

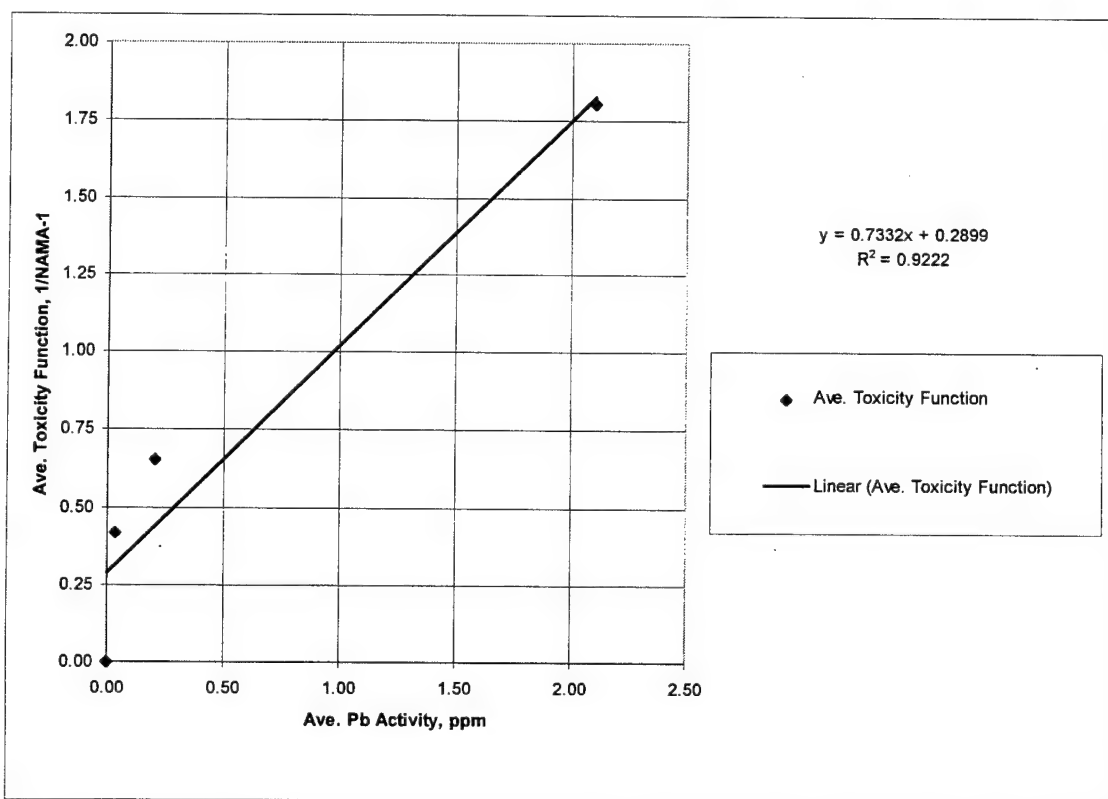


Figure 4.13. Average Lead Activity Versus Average Toxicity Function, Experiment Performed 30 Aug 97

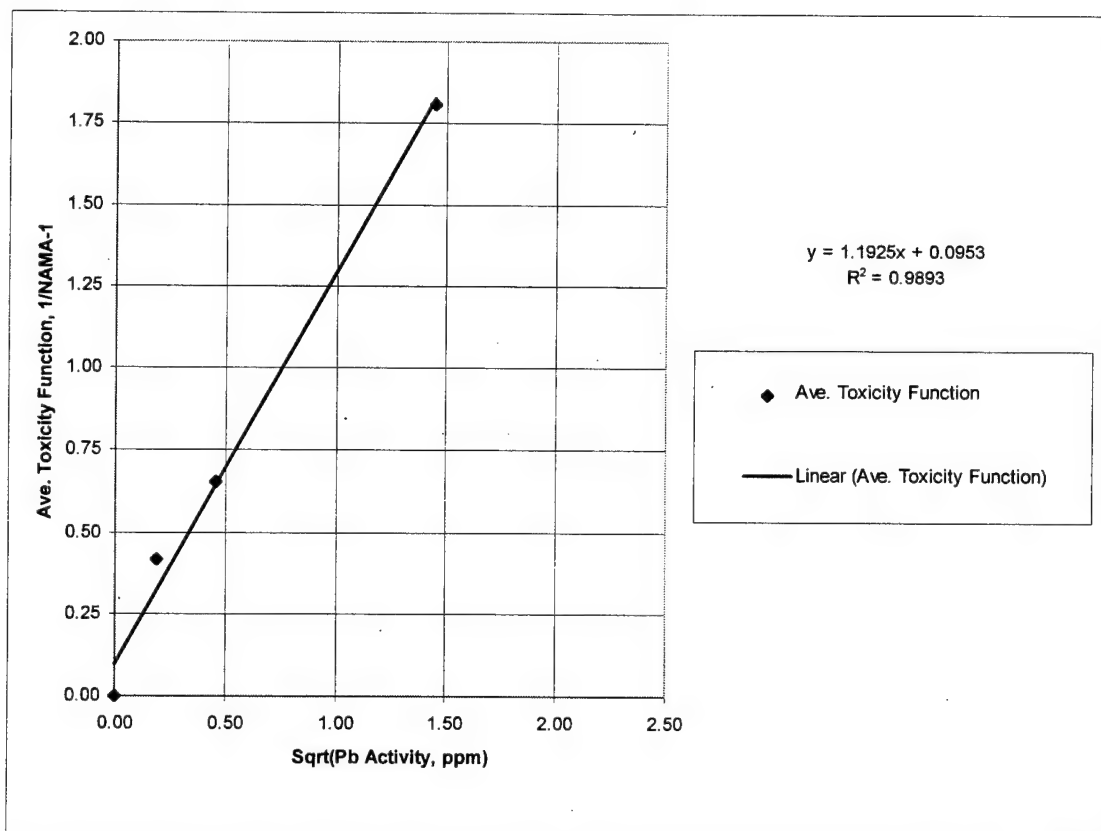


Figure 4.14. Square Root of the Average Lead Activity Versus Average Toxicity Function, Experiment Performed 30 Aug 97

Finally, the toxicity function values shown in Table 4.9 are plotted as a function of the average lead activity in Figure 4.15 and as a function of the square-root of the average lead activity in Figure 4.16. Again, the toxicity function values are correlated better with a least squares linear fit when plotted as a function of the average lead activity square root (R -squared = 0.989), rather than a function of the average lead activity (R -squared = 0.963).

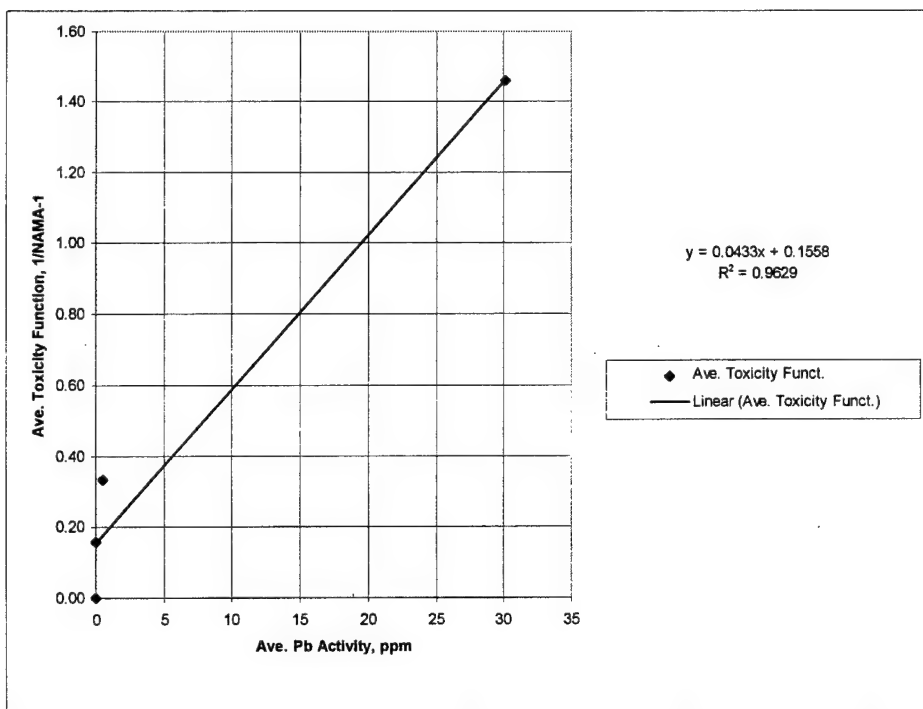


Figure 4.15. Average Lead Activity Versus Average Toxicity Function, Experiment Performed 13 Sept.

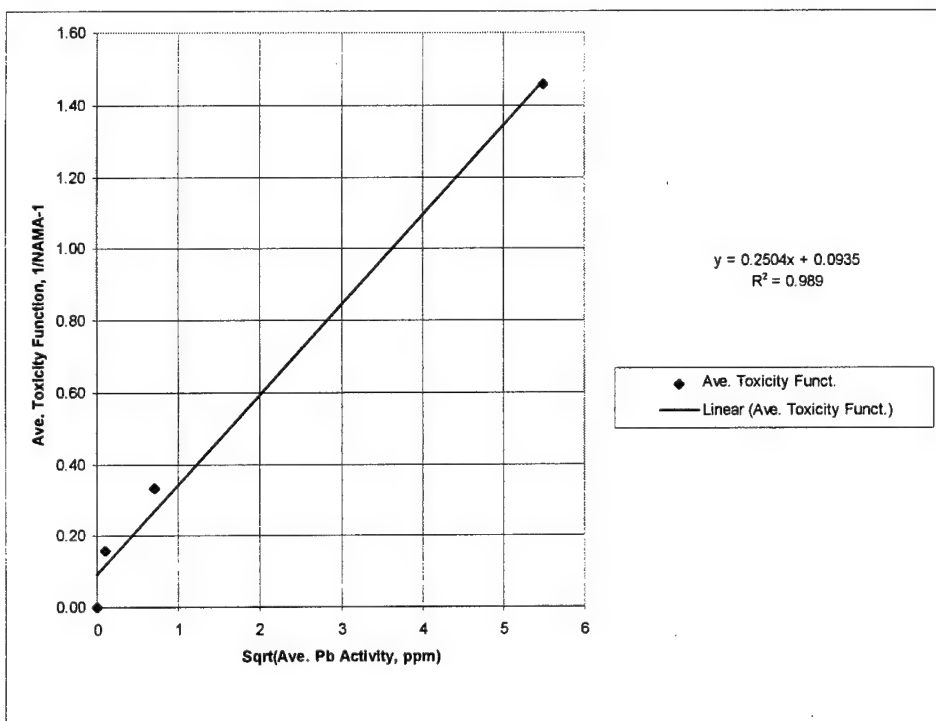


Figure 4.16. Average Lead Activity Versus Average Toxicity Function, Experiment Performed 13 Sept.

The R-squared values for each experiment are summarized in Table 4.10. The data suggests that the average toxicity function value is better correlated with the square root of the average lead activity. This suggests the toxicity response follows Case II of the TM in which protons compete well with lead ions for cell ligand sites.

TABLE 4.10. R-SQUARED VALUES FOR CORRELATION BETWEEN LEAD ACTIVITY AND TOXICITY RESPONSE

Experiment	<u>Case I</u> Correlate with Pb Activity (R-Squared Value)	<u>Case II</u> Correlate with Square Root of Pb Activity (R-Squared Value)
8 Aug	0.962	0.984
30 Aug	0.922	0.989
13 Sept	0.963	0.989

Metal Complexation Experiments

The purpose of the metal complexation experiments was to derive the distribution coefficient (DC) of lead with microorganisms. Three experiments were performed in which the amount of lead complexed by a microbial mass was measured. It is assumed that the metal complexed was adsorbed entirely by the microbial mass. However, data from a single experiment using graphite furnace atomic adsorption spectroscopy (AAS) suggested otherwise (Reference Appendix B). The lead amount retained by the microbial mass may be a fraction of the total lead complexed. The remaining lead amount may be complexed to organic substances secreted by the microorganisms or washed off the microbial mass during the sample preparation process.

In each of the experiments, a calibration curve was established by titrating pure DW with lead standard solution. Since the DW contains no significant inorganic complexes, and the DW's pH was 5.0 or below, it was assumed that the lead activity in pure DW equaled its total lead concentration.

The lead complexed by the microbial mass was assumed to be the difference between the total lead concentration and its corresponding lead activity. For example, in Figure 4.17, a total lead concentration of 4 ppm had a corresponding lead activity of nearly 3 ppm. The lead adsorbed by the microbial mass was assumed to be 1 ppm. The amount of lead adsorbed was calculated at each total lead concentration. This value was then divided by the estimated dry mass of the microorganisms and plotted as a function of lead activity. The lead AC was assumed to be the slope of the least squares fit line for the data.

The calibration curves for the 17 Sept, 22 Sept, and 7 Oct experiments are shown in Figures 4.17, 4.18, and 4.19, respectively. The relative linearity of the calibration curves shown in Figure 4.18 was not expected since the lead electrode response for concentrations less 1.0 ppm were expected to be non-linear. A more ideal electrode response is shown in Figure 4.19. In Figure 4.17, the electrode response at the lower concentration region was not known due to a lack of data points. In Figure 4.18, lead carbonate precipitate may have formed at 11 ppm total lead which resulted in the apparent decrease in lead activity.

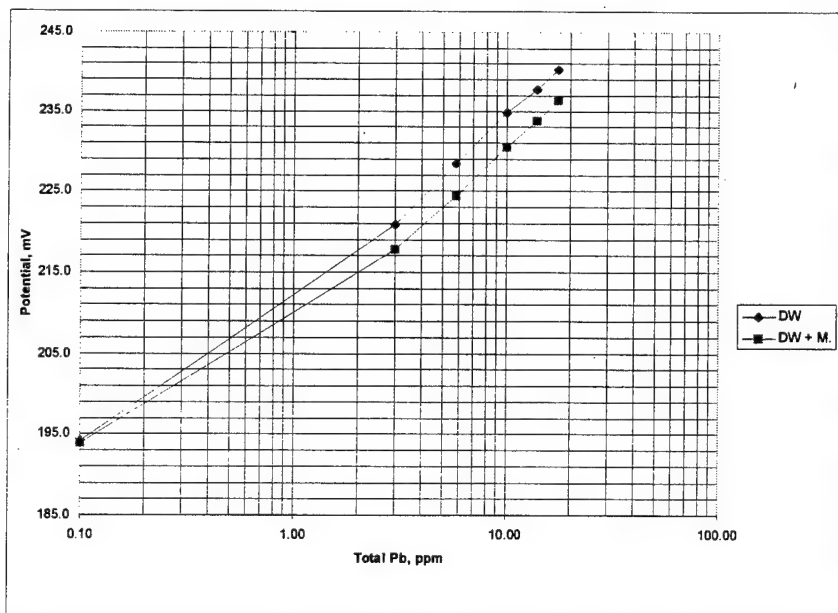


Figure 4.17. Total Lead Concentration Versus Adjusted Potential Reading, Microbial Mass = 4.04 mg; DW = Dilution Water; DW + M. = Dilution Water with Microorganisms, Experiment Performed 17 Sept.

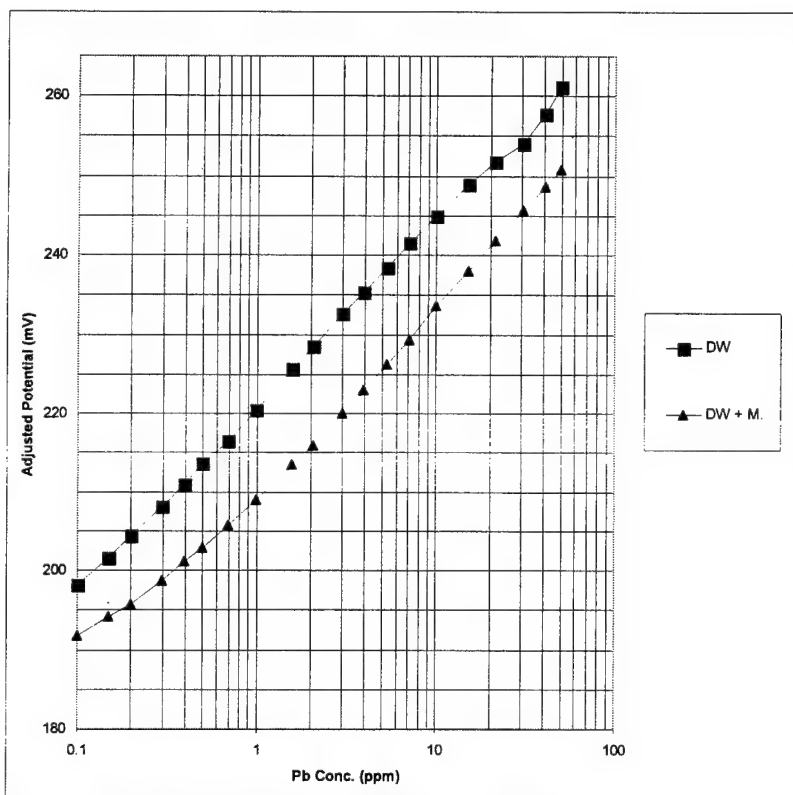


Figure 4.18. Total Lead Concentration Versus Adjusted Potential Reading DW = Pure Dilution Water; DW + M. = Dilution Water with Microorganisms, Experiment Performed 22 Sept.

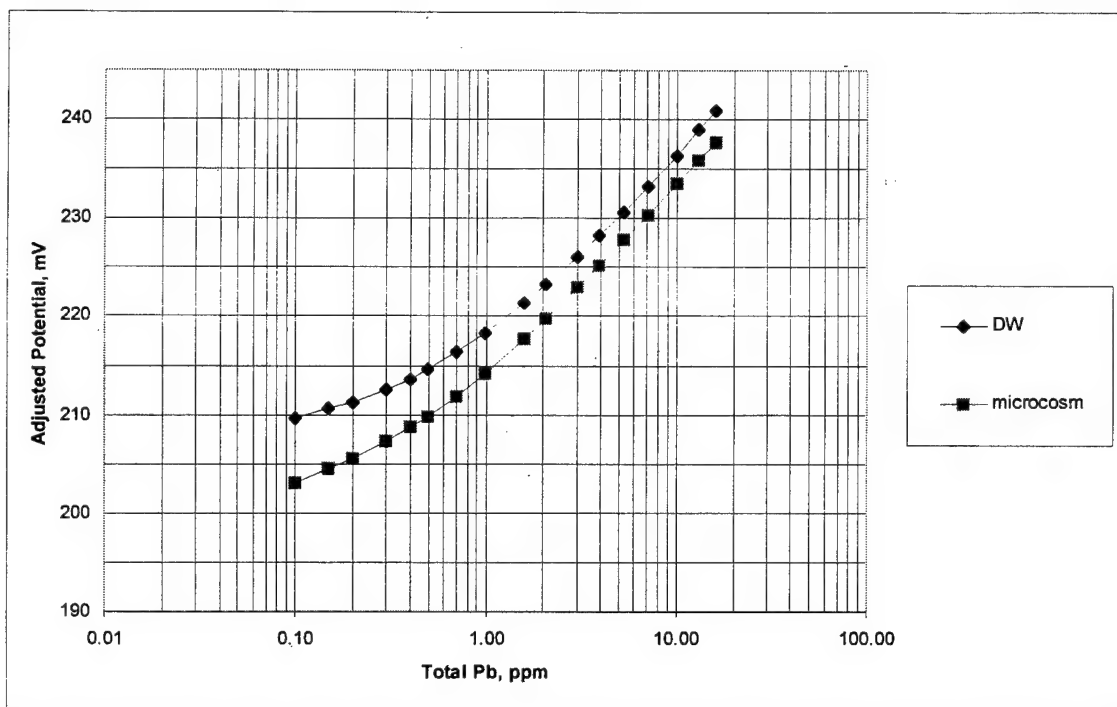


Figure 4.19. Total Lead Concentration Vs. Transformed Potential Readings, Corrected for Electrode Response Offset, DW = Pure Dilution Water; DW + M = DW and microorganisms, Experiment Performed 7 Oct 97)

Figure 4.20 shows the lead adsorbed by the microbial mass plotted as a function of lead activity for the 17 Sept, 22 Sept, and 7 Oct experiments. In the 17 Sept experiment, lead activities less than 2 ppm were not plotted due to a lack of data points. In all cases, the data correlated well using a linear least squares fit. The DC values were taken to be the slope of the least squares fit line. The average pH, dry microbial mass, and DC values for each experiment is summarized in Table 4.11.

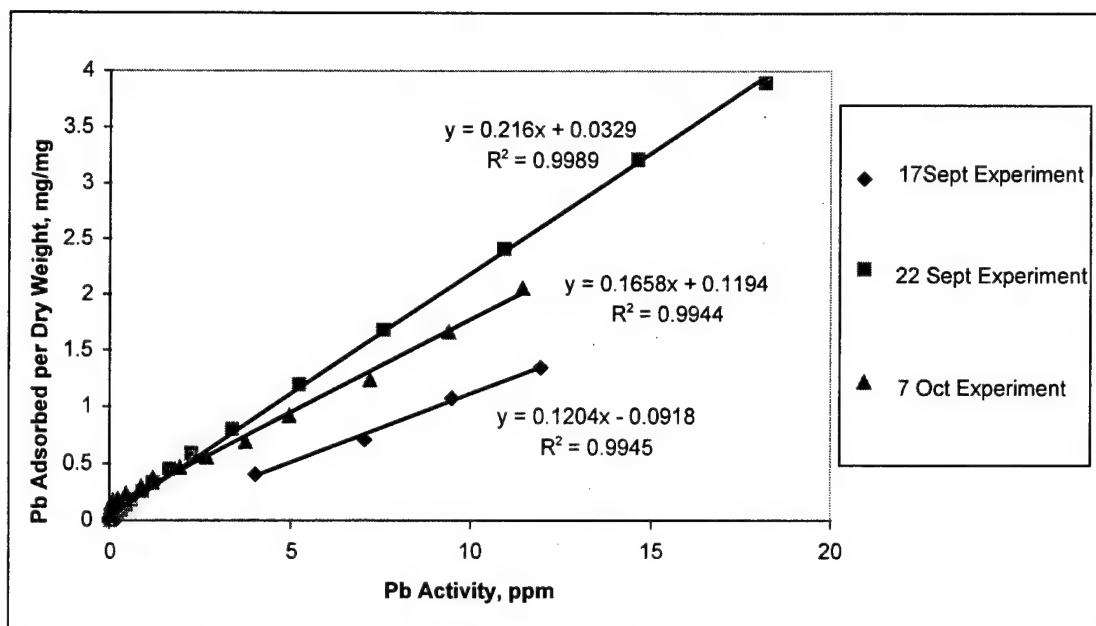


Figure 4.20. Least Squares Fit of Lead Activity Versus Lead Adsorbed per Dry Weight for Experiments Performed 17 Sept, 22 Sept, and 7 Oct

TABLE 4.11. LEAD DISTRIBUTION COEFFICIENTS DETERMINED IN THREE SEPARATE EXPERIMENTS

Experiment Date	Untreated, Dry Microbial Mass mg	Lead Distribution Coefficient (DC) mg Pb/mg Dry Weight	Average pH in DW/Microorganism Mixture
17 Sept 97	4.04	0.120	5.00 (±0.01)
22 Sept 97	8.14	0.216	5.14(±0.09)
7 Oct 97	6.72	0.166	5.68(±0.17)

The difference in the DC values may be attributed to differences in the microbial mass used in each experiment. In Figure 4.21, good correlation (R-squared = 0.960) was made between the DC values and microbial mass. The mass dependence may be attributed to a disproportionate increase in available binding sites with increased

microbial mass. Microorganisms may also secrete organic compounds which complex lead.

Alternatively, the DC values may not be the thermodynamic constant, K_{LC} , specified in the development of the TM (Chapter 2). Moreover, the activity of binding sites may not be proportional to mass.

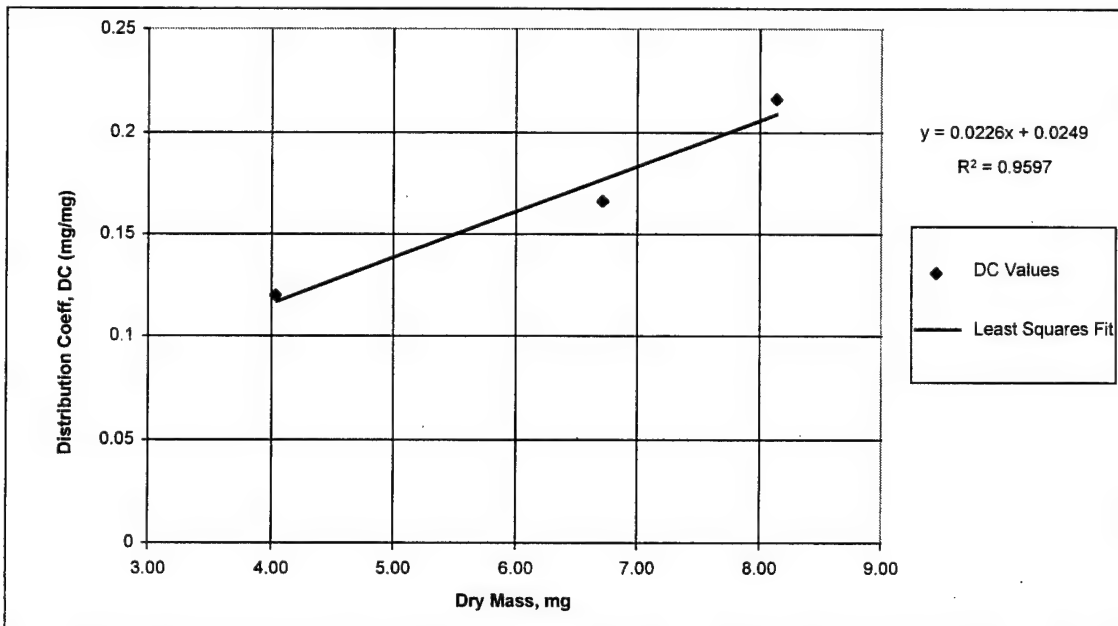


Figure 4.21. Least Squares Fit of Distribution Coefficient (DC) Versus Dry Mass. The DC values appear to be mass dependent.

Poor correlation (R -squared = 0.029) was made between the DC values and pH as shown in Figure 4.22. The results was contrary to expectations. The DC values were expected to correlate well with pH, however, it is not unreasonable to assume that the DC values may be more greatly affected by the microbial mass.

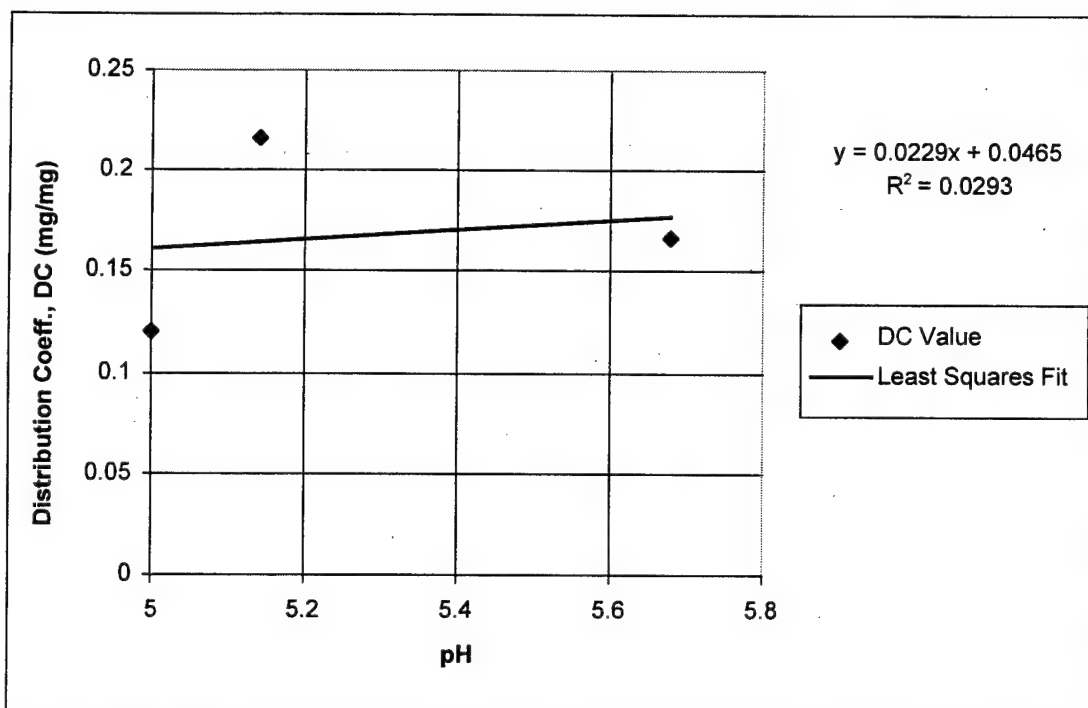


Figure 4.22. Distribution coefficient versus pH. The DC values do not appear to be pH dependent.

Langmuirian Adsorption Behavior. Langmuirian adsorption behavior is observed when a surface's binding sites are saturable and constant binding site affinity. As complexes form at surface ligand sites, the number of sites available to form new complexes become scarce, and eventually, all available ligand sites are occupied. Consequently, the adsorption behavior is a logarithmic curve which is characterized by a value that represents the maximum amount of cation adsorbed to the surface.

The adsorption curve for the 7 Oct experiment exhibited saturable behavior at low concentrations (<0.30 ppm) as seen in Figure 4.23. The log plot in Figure 4.24 suggests that in the microbial mass, two binding sites are present: tightly bound ligand sites and loosely bound ligand sites. The tightly bound sites appear to be saturable. The loosely bound sites show no evidence of saturation. It is proposed that the tightly bound ligand

allow the formation of multiple-ligand complexes. The loosely bound ligand sites allow the formation of single-ligand complexes. Conformational changes in the cell membrane would be expected to occur more greatly with the tightly bound ligands. Contrary to expectations, the metabolic inhibition occurred at higher lead concentrations. This suggests that metabolic inhibition is better correlated with the loosely bound ligand sites.

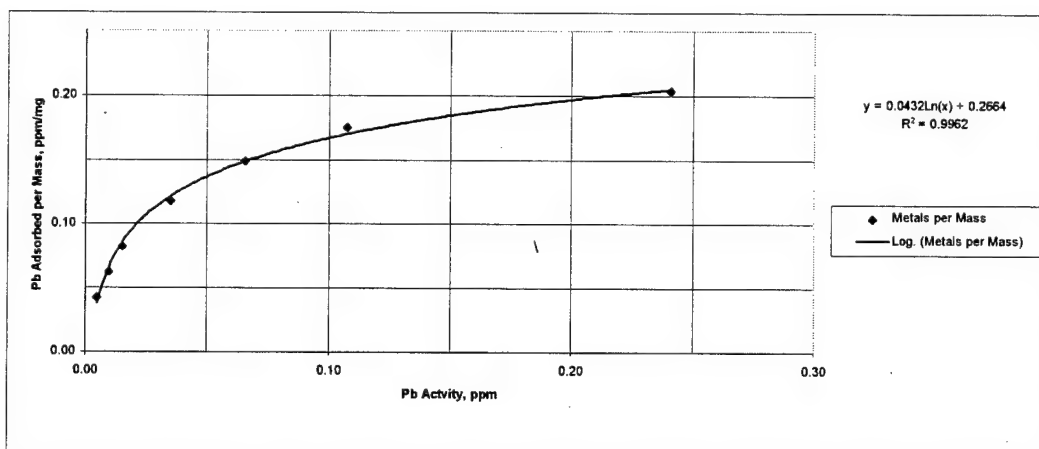


Figure 4.23. Average Lead Activity Versus Lead Adsorbed per Microorganism Mass. Experiment Performed 7 Oct 97

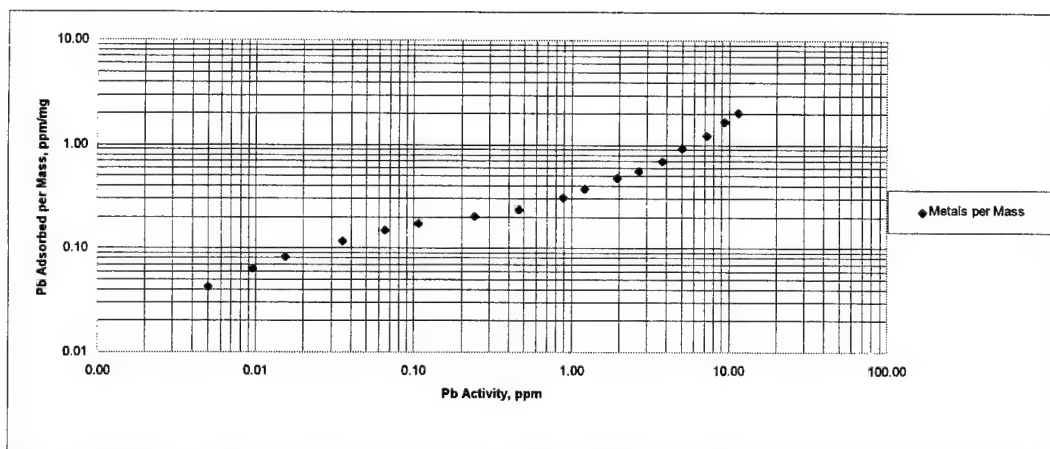


Figure 4.24. Lead Activity Versus Lead Adsorbed by Microorganisms, Experiment Performed 7 Oct 97

Predicted Toxicity Response

This section compares the predicted toxicity response to the actual response observed in the 8 Aug and 30 Aug experiments. The toxicity response was predicted using the Case II relationship with the experimentally derived parameter values: DC and lead activity. The DC values were extrapolated from Figure 4.21 in each experiment. The average lead activity measurements were calculated in each experiment and used for the lead activity values.

In Figure 4.25, the predicted and actual toxicity function values are plotted as a function of lead activity for the 8 Aug experiment. The estimated untreated mass per microcosm was 12.9 mg and the estimated DC value was 0.32. Table 4.12 lists the average lead activity, final pH, predicted toxicity response, actual toxicity response, and the predicted to actual response ratio. In this experiment, the pH measurement of one microcosm per metal treatment was determined as the representative pH value.

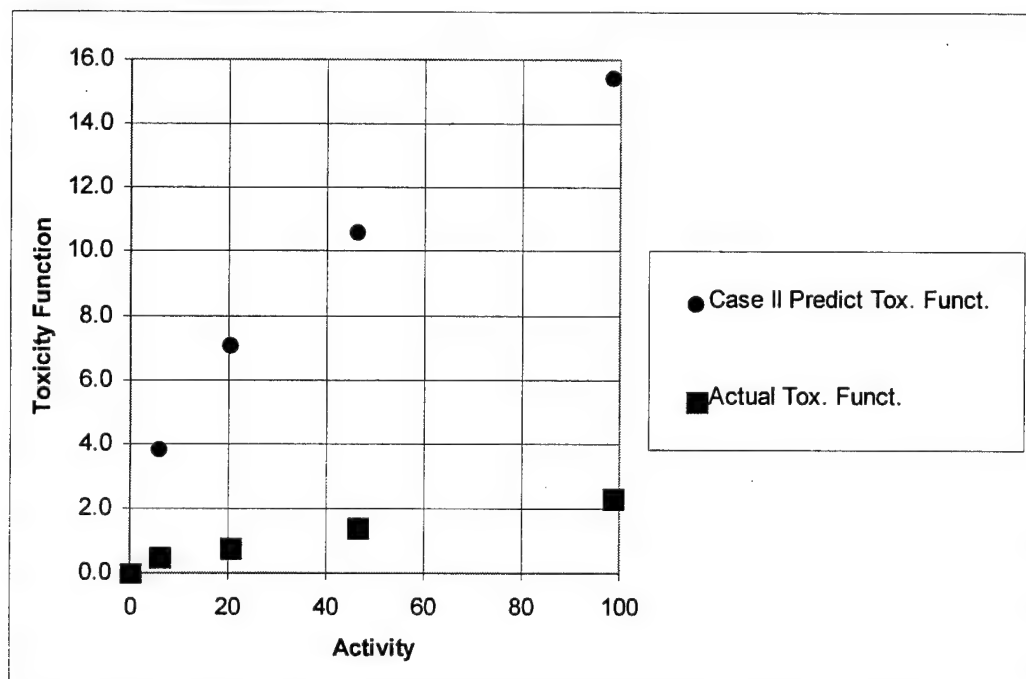


Figure 4.25. Case II, Lead Activity Versus Predicted & Actual Toxicity Function
estimated untreated mass = 12.9 mg, Inoculum Volume = 30 mL, Estimated DC = 0.32,
(Experiment Performed 8 Aug 97)

TABLE 4.12. AVERAGE LEAD ACTIVITY, FINAL PH, PREDICTED TOXICITY RESPONSE, ACTUAL TOXICITY RESPONSE AND RATIO OF PREDICTED TO ACTUAL TOXICITY RESPONSE (EXPERIMENT PERFORMED 8 AUG 97).

Average Pb Activity	Final pH	Predicted Toxicity Response	Actual Toxicity Response	Predicted to Actual Toxicity Response Ratio
6.1	5.0	10.08	0.52	19.57
20.5	4.9	18.48	0.80	23.14
46.4	4.8	27.79	1.43	19.40
98.7	4.6	40.55	2.33	17.38
0.0	5.8	0.00	0.00	NA

* Estimated microbial mass is 12.9 mg based on DO consumption rate of untreated microcosm

* Estimated DC is 0.32 based on the microbial mass

The predicted toxicity response, as shown in Figure 4.25, was consistently larger than the actual toxicity response. The difference between the predicted and actual toxicity response value per metal treatment was quantified using a predicted to actual toxicity response ratio. The ratio represents the factor by which the actual toxicity response value must be multiplied to equal the predicted value. A ratio larger than one would indicate that the predicted toxicity value was larger than the actual toxicity response. It was observed that the ratio increased slightly with decreasing pH values. However, as Figure 4.26 shows, the predicted to actual toxicity response ratio in this experiment was poorly correlated ($R\text{-squared} = 0.389$) with pH.

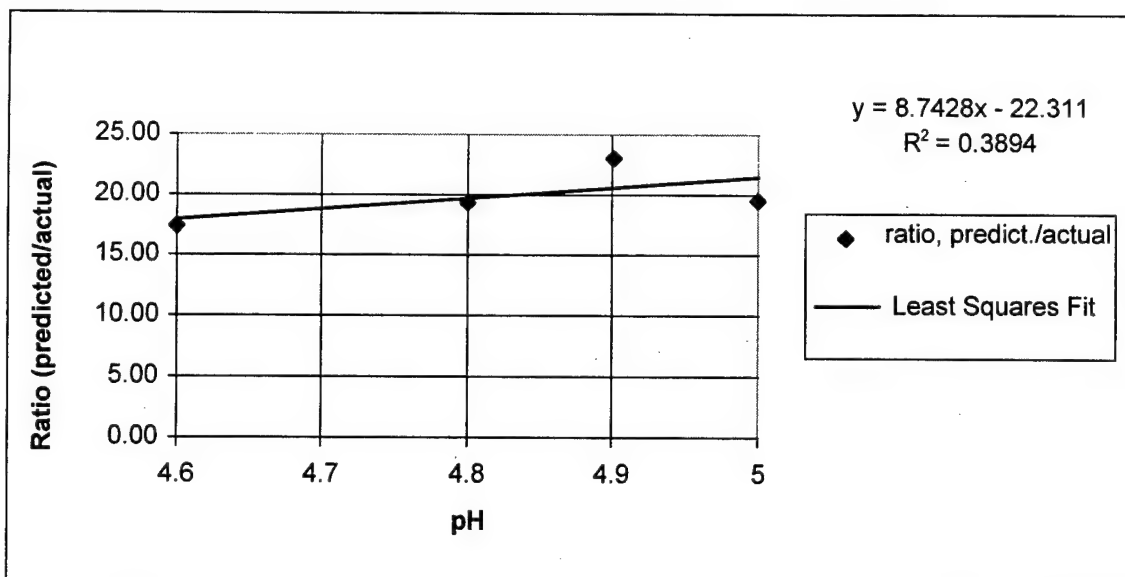


Figure 4.26. Ratio of predicted to actual toxicity response as a function of final pH estimated untreated mass = 12.9 mg, estimated DC = 0.32, (Experiment Performed 8 Aug 97)

In Figure 4.27, the predicted and actual toxicity function values are plotted as a function of lead activity for the 30 Aug experiment. The estimated untreated mass per microcosm was 16.5 mg and the estimated DC value was 0.40. Table 4.13 lists the average lead activity, average final pH, predicted toxicity response, actual toxicity response, and the predicted to actual response ratio. In this experiment, the average pH value per treatment level is recorded in the table. The pH variations were attributed to the metal's natural acidity.

As in the previous experiment, the predicted toxicity response, as shown in Figure 4.27, was consistently larger than the actual toxicity response. However, the predicted to actual toxicity response ratio appears to be pH dependent as indicated by the high correlation achieved ($R^2 = 0.990$) by the least squares linear fit shown in Figure 4.28. As the pH increased the ratio decreased as expected. This suggested that protons may have a protective effect on the microorganisms.

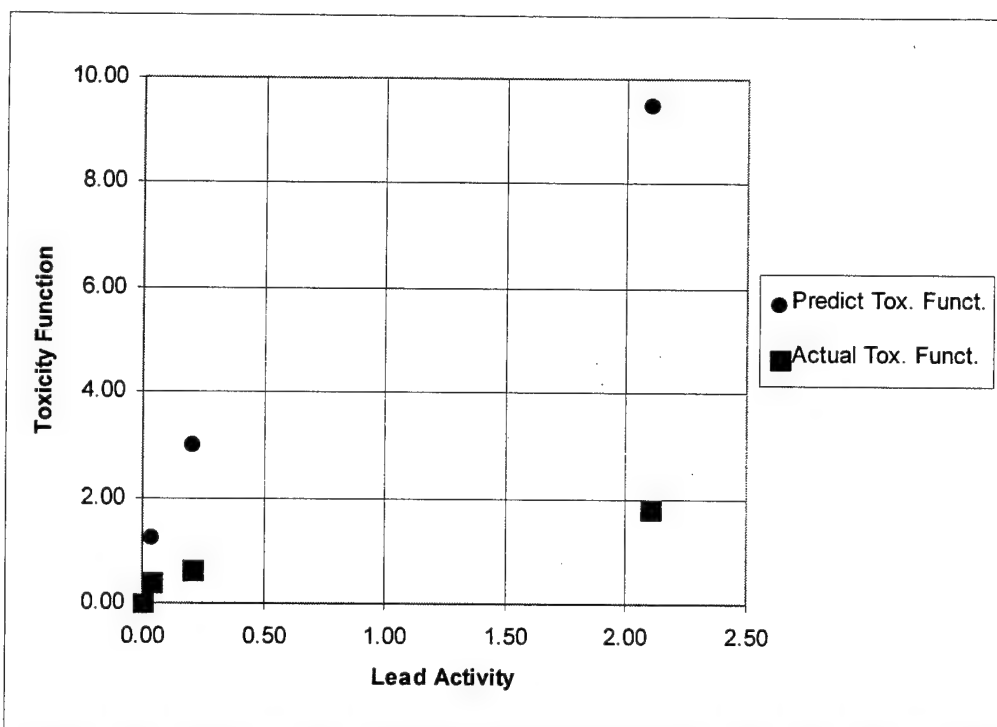


Figure 4.27. Case II, Lead Activity Versus Predicted & Actual Toxicity Function estimated untreated mass = 16.5 mg, Inoculum Volume = 30 mL, estimated DC = 0.40, (Experiment Performed 30 Aug 97).

TABLE 4.13. AVERAGE LEAD ACTIVITY, FINAL PH, PREDICTED TOXICITY RESPONSE, ACTUAL TOXICITY RESPONSE AND RATIO OF PREDICTED TO ACTUAL TOXICITY RESPONSE (EXPERIMENT PERFORMED 30 AUG 97)

Average Lead Activity ppm	Ave. Final pH	Predicted Toxicity Function	Actual Ave. Toxicity Function	Predicted to Actual Toxicity Response Ratio
0.04	5.64(±0.02)	1.23	0.42	2.95
0.21	5.22(±0.02)	2.99	0.65	4.58
2.10	5.12(±0.01)	9.51	1.80	5.27
0.00	5.68(±0.08)	0.00	0.00	NA
Untreated				

* Estimated microbial mass is 16.5 mg based on DO consumption rate of untreated microcosm

* Estimated DC is 0.40 based on microbial mass.

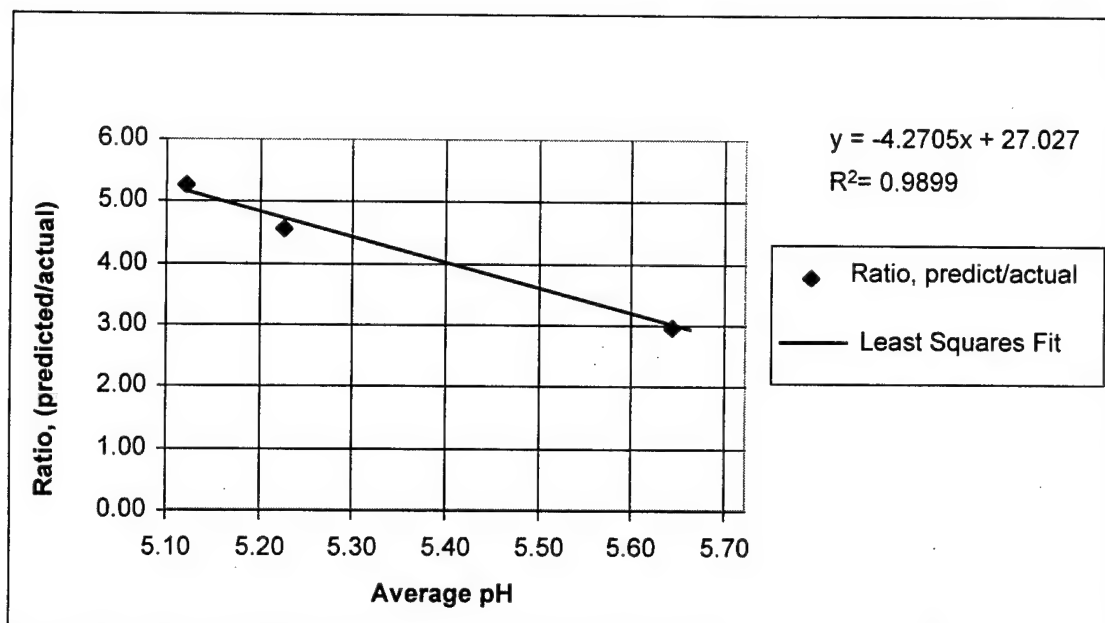


Figure 4.28. Ratio of predicted to actual toxicity response as a function of Average pH, estimated untreated mass = 16.5 mg, Inoculum Volume = 30 mL, estimated DC = 0.40, (Experiment Performed 30 Aug 97).

In both experiments, the predicted toxicity response values were larger than the actual values. Two explanations may account for the difference in the values.

First, the TM assumes that the metal complexed in the microcosm are bound entirely to cellular ligand sites essential to the microorganism's metabolism, however, this may not be the case. As suggested in Figures 4.23 and 4.24, the cellular membrane appears to have two binding sites: tightly bound ligands and loosely bound ligands. The DC values represent lead binding to both types of ligand sites equally. If metabolic inhibition is effected primarily by the complexes formed with tightly bound sites, the toxicity values predicted using the TM would overestimate the actual values. Moreover, metal may have complexed with the small concentration of inorganic ligands in the microcosm introduced with the inoculum.

Second, the DC values used to calculate the predicted toxicity response was assumed to be independent of pH. However, the data shown in Figure 4.28 suggested the toxicity response was pH dependent. If the DC values were actually pH dependent, as the TM derivation suggests, the differences between the predicted and actual toxicity response values could be accounted for by the pH difference.

In general, protons appear to have a greater protective effect at lower pH. However, when the pH drops below 5.0, the acidity of the solution may adversely affect the microorganisms. This may have been the case for the data shown in Figure 4.28.

The predicted to actual toxicity response ratios are greater in the 8 Aug experiment than in the 30 Aug experiment. For the 8 Aug experiment, the treated microcosms had a pH of 5.0 or less, and in the 30 Aug experiment, the pH ranged from 5.43 to 5.12. The overall difference in pH values between experiments may explain the greater ratio values observed in the 8 Aug experiment.

Chapter V. Conclusion

Conclusion

Metabolic inhibition was observed to be rapid (< 5 minute), suggesting that the toxic effects were due to chemisorption rather than a slower kinetic process. The observations suggested that the metabolic inhibition mechanism due to lead was similar to that involving first row transition metal ions.

A high degree of correlation was found between the untreated microcosm DO consumption rate and the dry microbial weight. Moreover, high correlation was determined between dry microbial weight and the lead DC value.

The toxicity response observed in the metabolic inhibition experiments fit Case II of the TM, and suggested that protons competed well with lead for cellular ligand sites. This assumption seemed reasonable since the experiments were performed under acidic conditions.

The DC values gained from the metal complexation experiments suggested that the DC values were dependent on microbial mass but independent of pH. The DC values increased with increasing microbial mass. Apparently, an increase in microbial mass resulted in a disproportionate increase in metal binding sites (perhaps from organic material excreted from the microorganisms).

Furthermore, the metal complexation experiments produced evidence of two cellular binding sites: tightly bound ligands and loosely bound ligands. It is reasonable to assume that conformational changes in the cellular membrane would be more greatly associated with multi-ligand complexes (tightly bound sites) rather than complexes

involving only a single ligand. Contrary to expectations, metabolic inhibition appeared to correlate better with the loosely bound sites since metabolic inhibition occurred at higher lead concentrations.

The toxicity response values predicted by the TM are larger than the actual values. This is not surprising since the TM does not differentiate between essential and non-essential ligand sites. The TM assumes that all complexes formed with a cellular ligand site will contribute to metabolic inhibition. However, if metabolic inhibition is associated with only a fraction of the complexes formed, then it is reasonable to expect that the TM will overestimate the actual toxicity response.

The predicted to actual toxicity response ratio was calculated to determine the factor by which the TM overestimated the actual toxicity response value. This ratio appeared to be pH dependent. The ratio decreased with increasing pH when pH values ranged from 5.12 to 5.64. The observation suggested that lead was more toxic at higher pH values than at lower pH values. This was consistent with the TM predictions. The ratio values did not follow this trend for pH levels below 5.0. Perhaps at low pH, the toxicity response was influenced by the solution's acidic effects.

Finally, a concurrent study which measured the test organism's viability after exposure to lead was performed by Goodbody (1997). He compared the toxicity response in terms of the microorganism's ability to reproduce to the toxicity response in terms of metabolic inhibition. It was observed that metabolic inhibition indicated a greater toxicity response at low lead activity (<0.50 ppm) relative to the viability measurements. However, as the activity increased, the viability measurements indicated a greater

toxicity response relative to metabolic inhibition. The mechanisms affecting cell viability and metabolic inhibition may not be the same. The distinction between the two measurements of toxicity should be further explored.

Further Research

Many opportunities exist to further the study of metal's toxic effects on microorganisms. The following is a list of a few possible follow-on projects.

1. Test further the pH dependence suggested by the TM.
2. Characterize the toxicity response among species of microorganisms possessing different levels of exo-polymer material.
3. It is assumed that all metal complexed is adsorbed by the microbial mass. There is evidence that this may not be the case. Use atomic absorption spectroscopy to evaluate the assumption that metal complexed in DW is actually adsorbed by the microbial mass.
4. Correlate the fraction of tightly bound ligand sites with the predicted and observed toxicity response.
5. Perform experiments to further study the mechanisms involved with cell viability. Compare the toxicity response measured in terms of metabolic inhibition with the toxicity response measured in terms of cell viability.

Appendix A: Bioreactor

Bioreactor

The inoculum used for all experiments was cultured in a 2.5 gallon capacity plastic container (i.e. a gas can) referred to as the bioreactor. Toluene was used as the microorganism's sole carbon source. Toluene saturated air was continuously pumped into the bioreactor using an aquarium pump as shown Figure A-1.

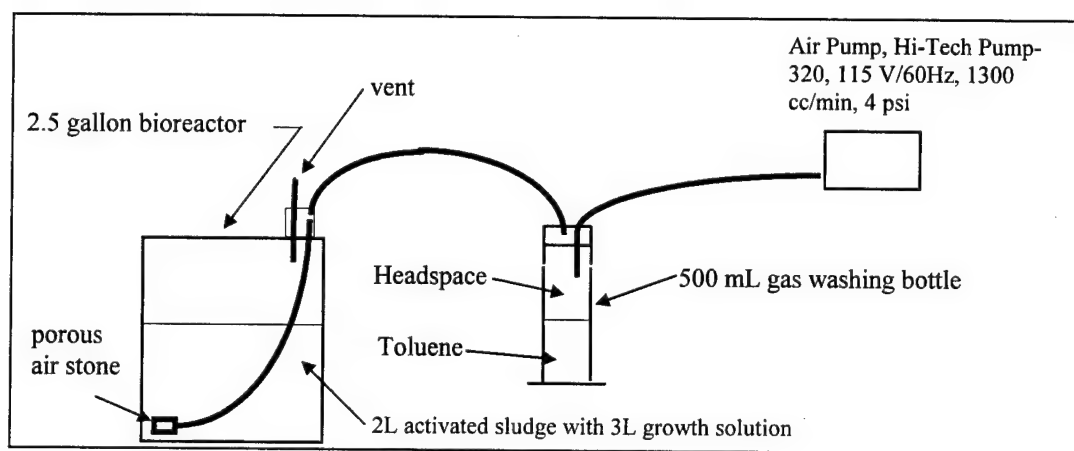


Figure A.1. Bioreactor set-up

Toluene Source.

Three grades (reagent, commercial, HPLC) of toluene were used during the course of the experiment. It was assumed that the toluene grade did not alter the microorganisms significantly. No more than 100 mL of toluene was kept in the gas washing bottle at one time. The toluene container was filled approximately every two days.

Growth Solution.

Initially, 1 liter of the activated sludge was placed into the bioreactor with 3 liters of growth solution consisting of a 1:1 mixture of a Hach premixed BOD buffer pillow and 20 ppm of potassium nitrate. Roughly 300 mL of inoculum was replaced with 300 mL of fresh growth solution on non experimental days to prevent the build-up of toxic organic substances secreted by the microorganisms and to provide additional growth nutrients. On experimental days, the inoculum volume used in the experiments were replaced with growth solution.

Appendix B: Atomic Adsorption Spectroscopy

Atomic Adsorption Spectroscopy (AAS) using a solid graphite furnace technique was performed by GBC Scientific Equipment, Inc, to analyze the lead adsorbed in six specimens taken from the 7 Oct metal adsorption experiment. In this appendix, the sample preparation procedures for the AAS analysis will be described. The values determined using AAS will be compared to the values obtained using the ISE technique.

Sample Preparation:

The contents of six microcosms were filtered and weighed in accordance to the procedures described in Chapter 3. After the final weigh-in, a nitric acid digestion procedure (American Public Health Association *et al.*, 1981) was used to digest the microbial mass. The steps in the digestion procedure included the following:

1. A 50 mL volume of deionized water and 5 mL of concentrated nitric acid was added to the filtered sample in a beaker.
2. The sample was heated on a hotplate and allowed to boil slowly until the volume decreased to roughly 25 mL.
3. A 5 mL volume of concentrated nitric acid was added. The beaker was covered with a watch glass and refluxing action was observed until all carbon material was dissolved. Roughly 15 to 20 mL of solution remained.
4. The remaining solution was filtered and diluted in a 100 mL volumetric flask.

Results:

Table B-1 list the total lead in the microcosm, the lead complexed as determined from the AAS analysis, and the lead complexed as determined from the ISE technique. As shown in the table, the values determined from the ISE technique are greater than the values determined using AAS. This may be the result of lead being complexed, but not retained on the microbial mass. Further work is needed to justify the discrepancy between the two values.

TABLE B.1. LEAD COMPLEXED AS DETERMINED USING AAS AND ISE TECHNIQUES (7 OCT EXPERIMENT)

Identification #	Total Lead (ppm)	Lead (ppm) Complexed Determined from AAS (Adjusted for Dilution)	Lead (ppm) Complexed Determined from ISE
FN23	0	none detected	0
* FN24	16.14	0.952	4.61
FN26	1.73	0.461	1.36
FN28	4.33	0.661	2.26
FN33	9.53	0.951	3.83
FN35	13.87	0.758	4.72

* The sample was taken from the calibration procedures in which 100 mL of untreated microcosm was titrated with a standard lead solution. The final lead concentration was 16.14 ppm.

Appendix C: Cu²⁺ and Cd²⁺ Metabolic Inhibition Experiments

This appendix reports the results from metabolic inhibition experiments involving Cu²⁺ and Cd²⁺ without further analysis.

Cu²⁺ Metabolic Inhibition Experiments:

Three metabolic inhibition experiments involving Cu²⁺ were performed 31 Jul, 13 Aug, and 28 Aug. The metabolic inhibition experiments were performed similar to the lead experiments except the metal activity was not measured.

31 Jul Experiment. The 31 Jul experiment consisted of two trials with 5 microcosms per trial. A single draw of inoculum was used to provide the microorganisms for each trial. The trials were performed concurrently using two different DO instruments. The untreated microcosm's DO consumption rate was used to normalize the metabolic activities. The total metal concentration, DO consumption rate, NMA, and toxicity function value for trial one and trial two are summarized in Table C-1 and Table C-2, respectively. The NMA and toxicity function values are plotted as a function of total copper in Figures C-1 and C-2, respectively.

TABLE C.1. TOTAL Cu²⁺, DO CONSUMPTION RATE, NMA, AND TOXICITY FUNCTION VALUE FOR TRIAL 1 OF THE 31 JULY EXPERIMENT

Bottle #	Total Cu ²⁺ (ppm)	DO Consum. Rate (mg/L/min)	NMA	Toxicity Function Value
14	0.00	0.121	1.00	0.00
11	4.50	0.004	0.04	26.57
22	22.50	0.004	0.03	32.69
6	45.00	0.001	0.01	100.08

TABLE C.2. TOTAL Cu^{2+} , DO CONSUMPTION RATE, NMA, AND TOXICITY FUNCTION VALUE FOR TRIAL 2 OF THE 31 JULY EXPERIMENT

Bottle #	Total Cu^{2+} (ppm)	DO Consum. Rate (mg/L/min)	NMA	Toxicity Function Value
14	0.00	0.121	1.00	0.00
18	4.50	0.002	0.02	51.74
16	22.50	0.004	0.03	32.69
10	45.00	0.001	0.01	150.63

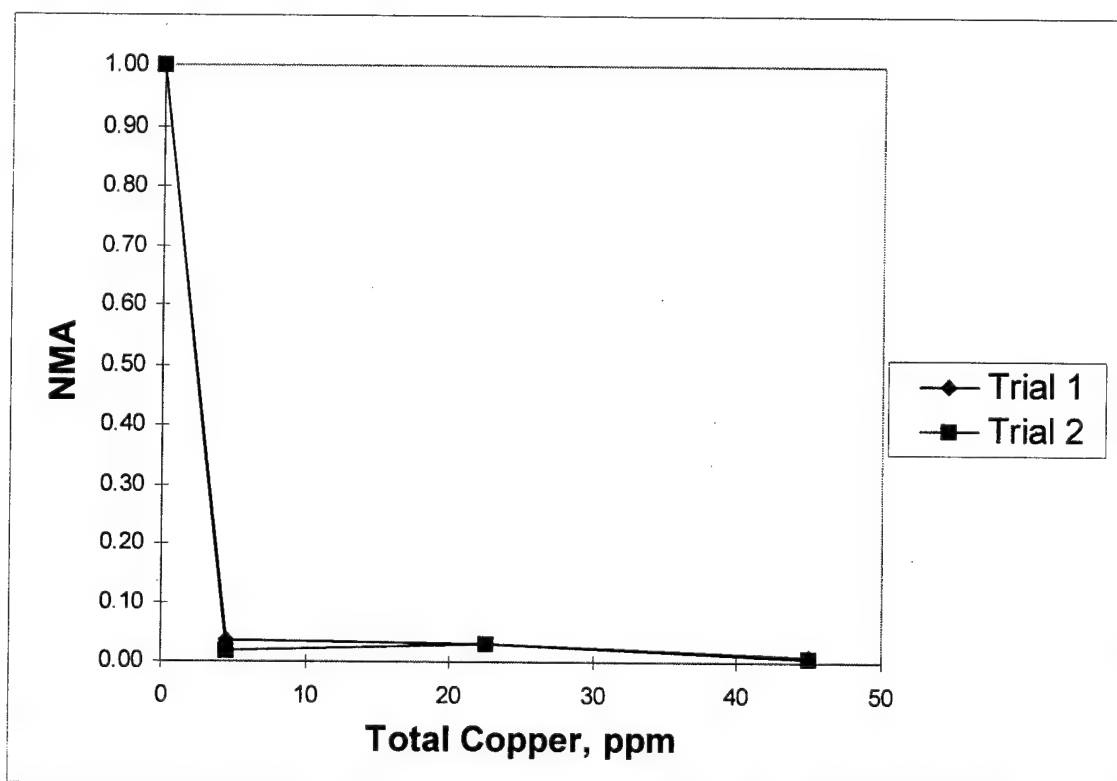


Figure C.1. Total Copper versus normalized metabolic activity (NMA) for 31 July experiment.

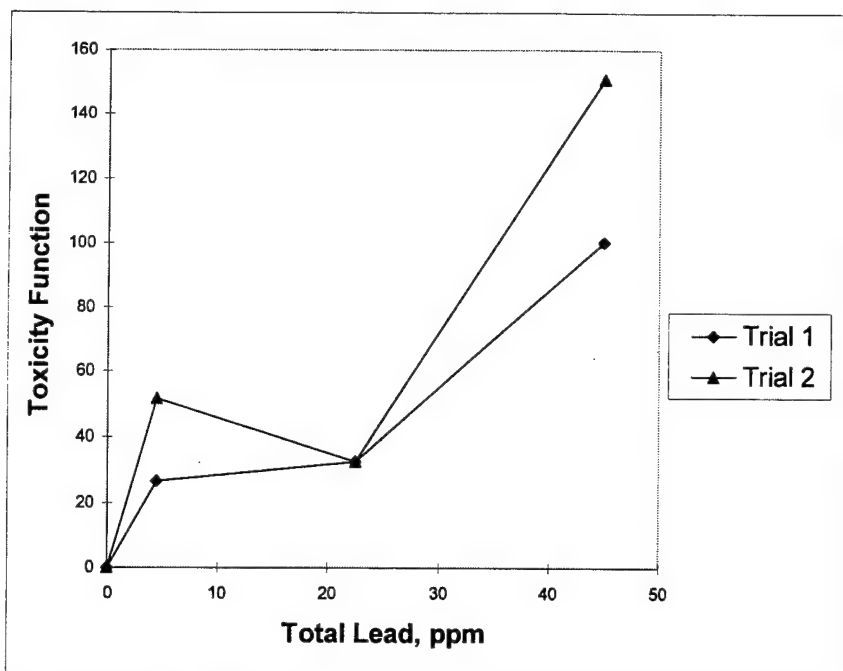


Figure C.2. Total Copper versus toxicity function value for 31 July experiment.

13 Aug Experiment. The 13 Aug experiment was performed in two trials similar to the 31 Jul experiment. Six microcosms were tested per trial. The total metal concentration, DO consumption rate, NMA, and toxicity function value for trial one and trial two are summarized in Table C-3 and Table C-4, respectively. The NMA and toxicity function values are plotted as a function of total copper in Figures C-3 and C-4, respectively.

TABLE C.3. TOTAL Cu^{2+} , DO CONSUMPTION RATE, NMA, AND TOXICITY FUNCTION VALUE FOR TRIAL 1 OF THE 13 AUG EXPERIMENT

Bottle #	Total Cu^{2+} (ppm)	DO Consum. Rate (mg/L/min)	NMA	Toxicity Function Value
14	0.00	0.0147	1.00	0.00
3	0.50	0.0112	0.76	0.31
22	1.25	0.0078	0.53	0.88
21	2.50	0.0052	0.35	1.83
7	5	0.0041	0.28	2.59
0	blank	0.0009	0.06	15.33

TABLE C.4. TOTAL Cu^{2+} , DO CONSUMPTION RATE, NMA, AND TOXICITY FUNCTION VALUE FOR TRIAL 2 OF THE 13 AUG EXPERIMENT

Bottle #	Total Cu^{2+} (ppm)	DO Consum. Rate (mg/L/min)	NMA	Toxicity Function Value
16	0.00	0.0187	1.00	0.00
23	0.50	0.0127	0.68	0.47
11	1.25	0.0076	0.41	1.46
1	2.50	0.0048	0.26	2.90
19	5	0.0028	0.15	5.68
4	blank	0.0023	0.12	7.13

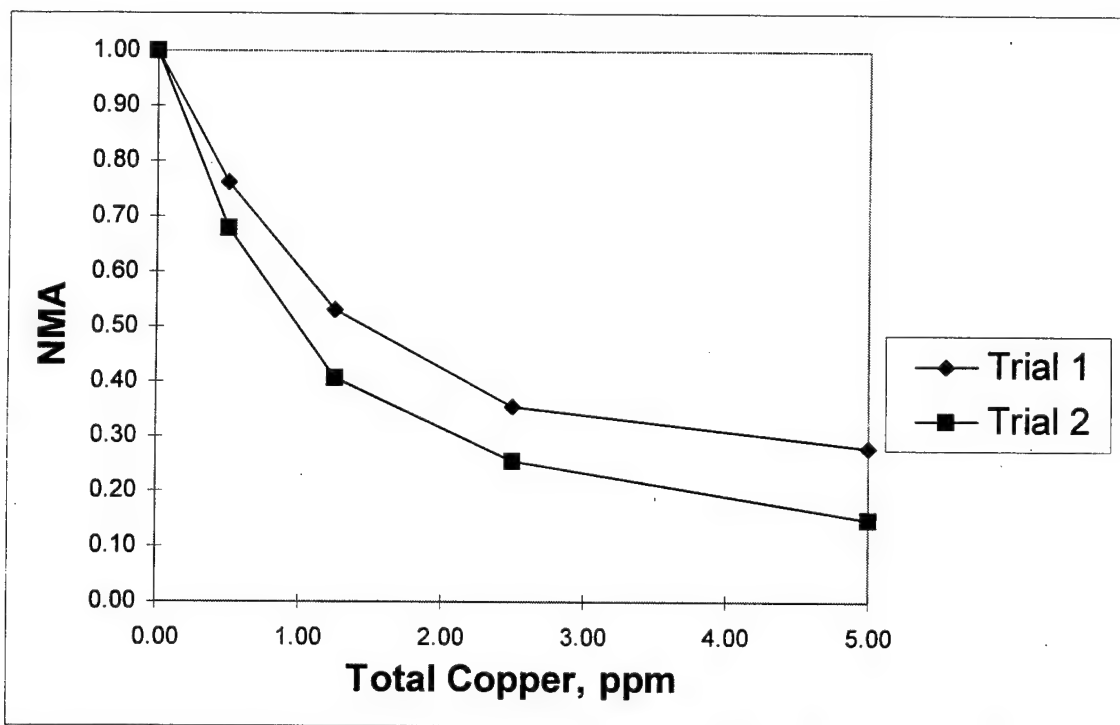


Figure C.3. Total Copper versus NMA for 13 Aug experiment.

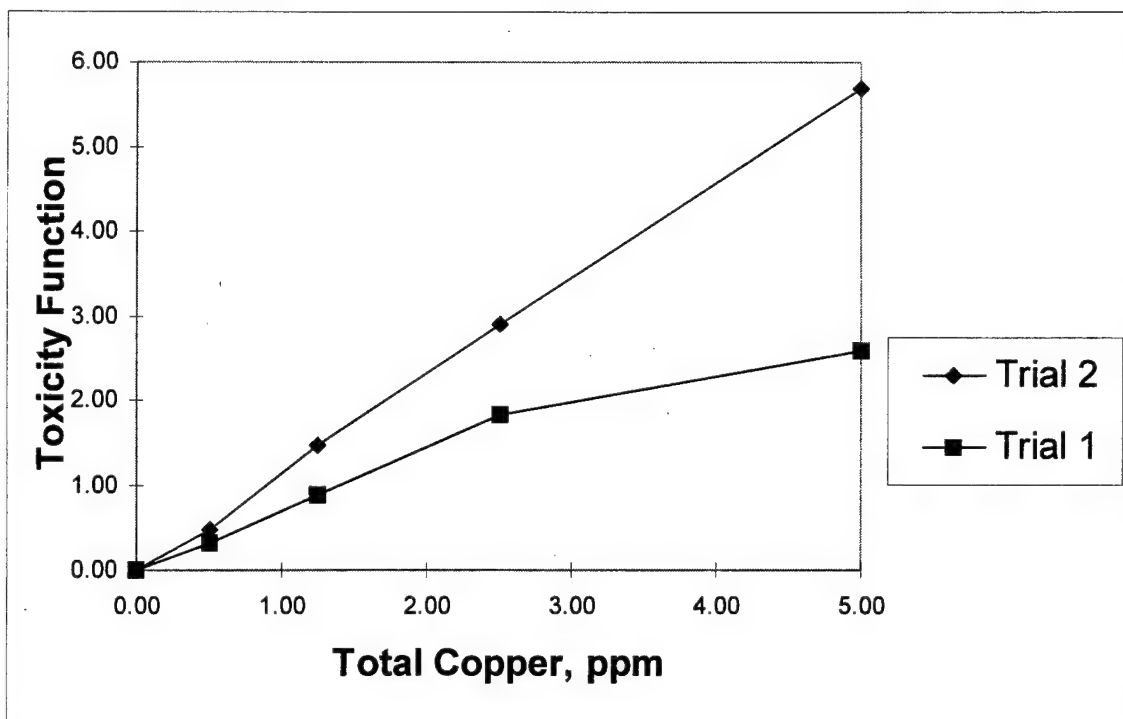


Figure C.4. Total Copper versus toxicity function value for 13 Aug experiment.

28 Aug Experiment. Eighteen microcosms were tested in the 28 Aug experiment in a single trial. The average untreated DO consumption rate was used to normalize the average DO consumption rates per metal treatment. The total metal concentration, DO consumption rate, ANMA, and average toxicity function value for the experiment is summarized in Table C-5. The NMA and toxicity function values are plotted as a function of total copper in Figures C-5 and C-6, respectively.

TABLE C.5. TOTAL Cu^{2+} , DO CONSUMPTION RATE, NMA, AND TOXICITY FUNCTION VALUE FOR THE 28 AUG EXPERIMENT

Bottle #	Total Cu^{2+} (ppm)	DO Consum. Rate (mg/L/min)	Ave DO rate (mg/L/min)	ANMA	Ave Toxicity Function
17 3 23	0.00	0.0298 0.0313 0.0305	0.031	1.000	0.000
4 14 21	0.13	0.0108 0.0069 0.0084	0.009	0.285	2.507
7 13 20	0.25	0.0044 0.0045 0.0039	0.004	0.140	6.127
11 219 40	0.50	0.0030 0.0027 0.0024	0.003	0.089	10.251
91 0 51	1.00	0.0013 0.0021 0.0017	0.002	0.056	16.904
204 208 210	0.00 blank	0.0010 0.0008 0.0011	0.001	0.032	30.579

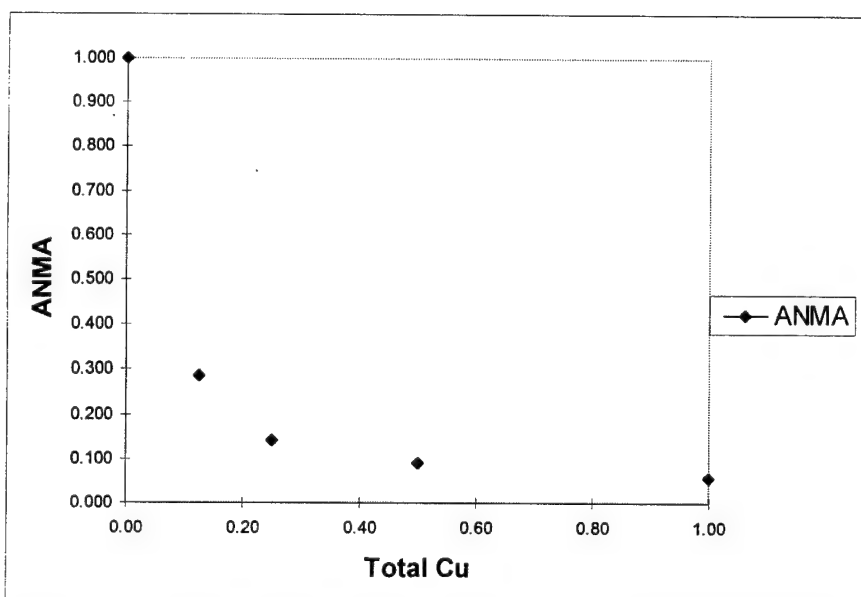


Figure C.5. Total Copper versus ANMA for 28 Aug experiment.

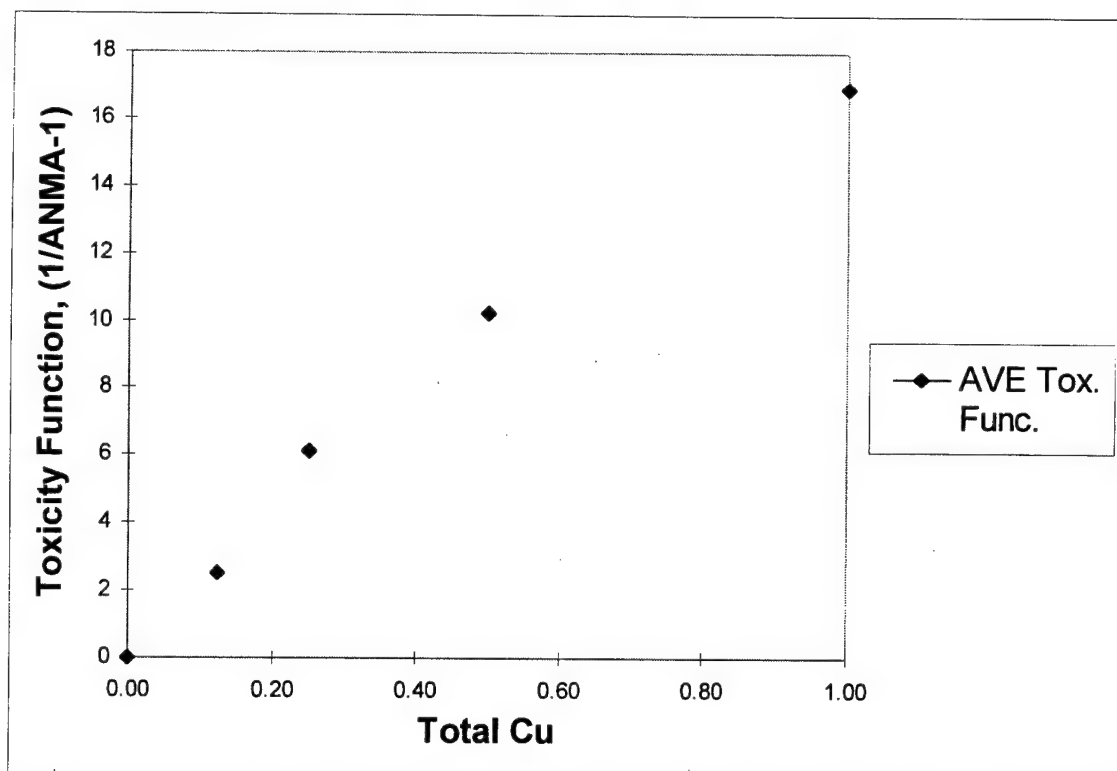


Figure C.6. Total Copper versus average toxicity function value for 28 Aug experiment.

Cd²⁺ Metabolic Inhibition Experiments:

Four metabolic inhibition experiments involving Cd²⁺ were performed 31 Jul, 14 Aug, 20 Aug, and 12 Sept. The metabolic inhibition experiments were performed similar to the lead experiments except the metal activity was not measured.

31 Jul Experiment. The 31 Jul experiment consisted of two trials with 5 microcosms per trial. A single draw of inoculum was used to provide the microorganisms for each trial. The trials were performed concurrently using two different DO instruments. The untreated microcosm's DO consumption rate was used to normalize the metabolic activities. The total metal concentration, DO consumption rate, NMA, and toxicity function value for trial one and trial two are summarized in Table C-6 and Table C-7,

respectively. The NMA and toxicity function values are plotted as a function of total copper in Figures C-7 and C-8, respectively.

TABLE C.6. TOTAL Cd^{2+} , DO CONSUMPTION RATE, NMA, AND TOXICITY FUNCTION VALUE FOR TRIAL 1 OF THE 31 JULY EXPERIMENT

Bottle #	Total Cd^{2+} (ppm)	DO Consum. Rate (mg/L/min)	NMA	Toxicity Function Value
15	0.00	0.0859	1.00	0.00
51	4.50	0.0300	0.35	1.86
3	22.50	0.0172	0.20	4.01
4	45.00	0.0142	0.17	5.06
20	0 (blank)	0.0008	0.01	102.46

TABLE C.7. TOTAL Cd^{2+} , DO CONSUMPTION RATE, NMA, AND TOXICITY FUNCTION VALUE FOR TRIAL 2 OF THE 31 JULY EXPERIMENT

Bottle #	Total Cd^{2+} (ppm)	DO Consum. Rate (mg/L/min)	NMA	Toxicity Function Value
7	0.00	0.1166	1.00	0.00
1	4.50	0.0371	0.32	2.15
21	22.50	0.0218	0.19	4.34
91	45.00	0.0171	0.15	5.84
19	0 (Blank)	0.0021	0.02	55.07

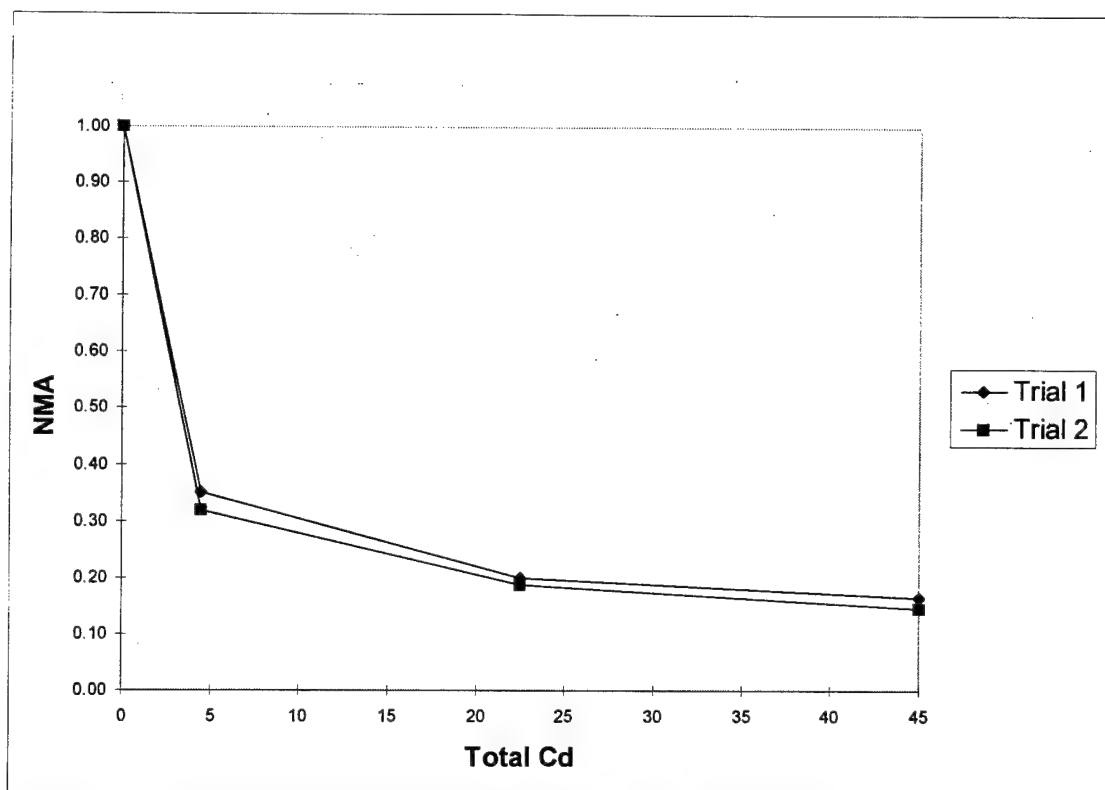


Figure C.7. Total cadmium versus NMA for 31 July experiment.

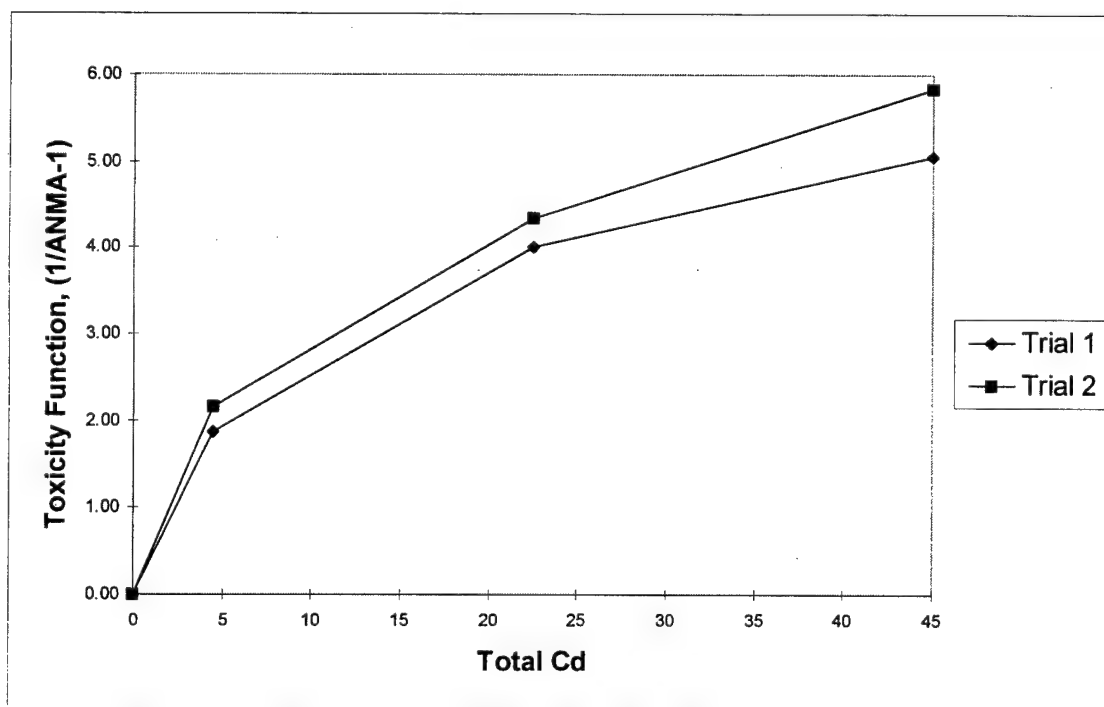


Figure C.8. Total cadmium versus toxicity function for 31 July experiment.

14 Aug Experiment. The 14 Aug experiment consisted of two trials with 6 microcosms per trial. A single draw of inoculum was used to provide the microorganisms for each trial. The trials were performed concurrently using two different DO instruments. The untreated microcosm's DO consumption rate was used to normalize the metabolic activities. The total metal concentration, DO consumption rate, NMA, and toxicity function value for trial one and trial two are summarized in Table C-8 and Table C-9, respectively. The NMA and toxicity function values are plotted as a function of total copper in Figures C-9 and C-10, respectively.

TABLE C.8. TOTAL Cd^{2+} , DO CONSUMPTION RATE, NMA, AND TOXICITY FUNCTION VALUE FOR TRIAL 1 OF THE 14 AUG EXPERIMENT

Bottle #	Total Cd^{2+} (ppm)	DO Consum. Rate (mg/L/min)	NMA	Toxicity Function Value
21	0.00	0.0131	1.00	0.00
91	0.90	0.0121	0.92	0.09
7	2.25	0.0118	0.90	0.11
10	4.50	0.0093	0.71	0.41
12	9.00	0.0089	0.68	0.47
17	0 (blank)	0.0011	0.08	11.25

TABLE C.9. TOTAL Cd^{2+} , DO CONSUMPTION RATE, NMA, AND TOXICITY FUNCTION VALUE FOR TRIAL 2 OF THE 14 AUG EXPERIMENT

Bottle #	Total Cd^{2+} (ppm)	DO Consum. Rate (mg/L/min)	NMA	Toxicity Function Value
16	0.00	0.0097	1.00	0.00
19	0.90	0.0094	0.97	0.04
20	2.25	0.0070	0.72	0.40
15	4.50	0.0072	0.74	0.35
6	9.00	0.0056	0.58	0.73
11	0 (blank)	0.0009	0.09	10.42

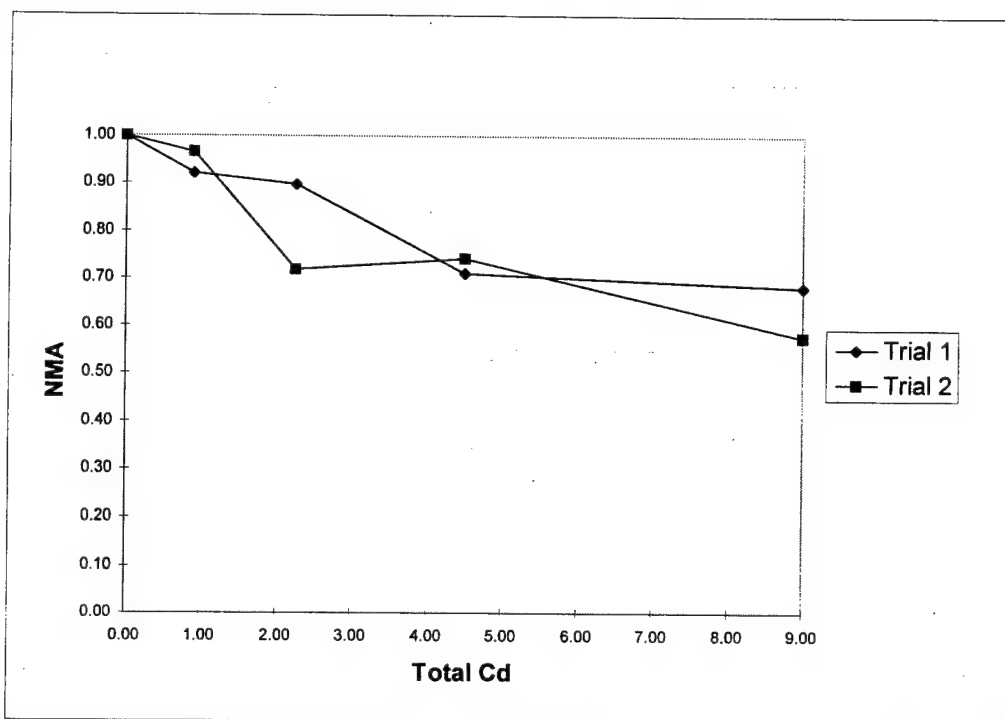


Figure C.9. Total cadmium versus NMA for 14 Aug experiment.

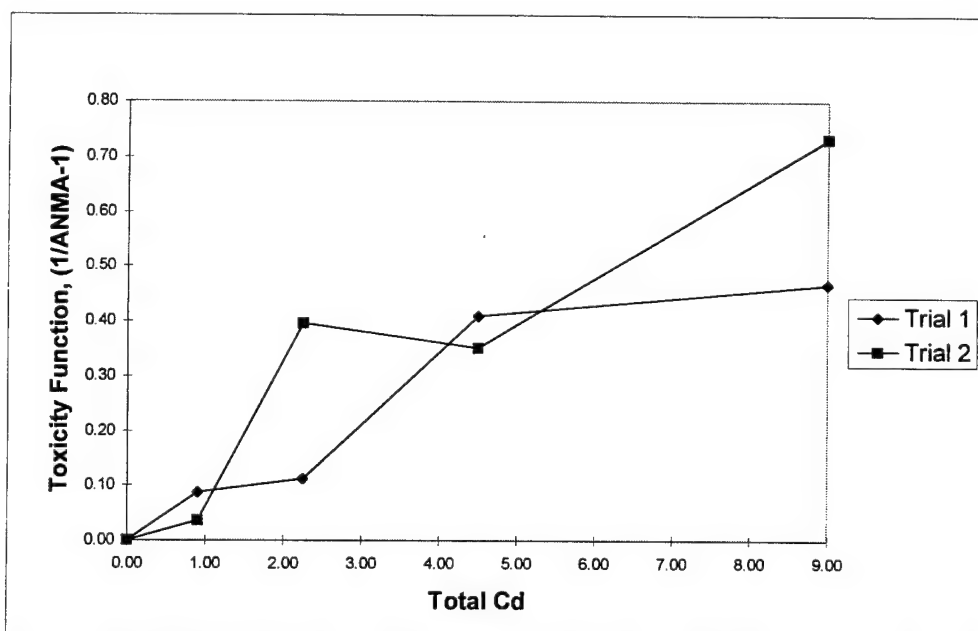


Figure C.10. Total cadmium versus toxicity function for 14 Aug experiment.

20 Aug Experiment. The 20 Aug experiment consisted of three trials with 6 microcosms per trial. A single draw of inoculum was used to provide the microorganisms for each trial. The untreated microcosm's DO consumption rate was used to normalize the metabolic activities. The total metal concentration, DO consumption rate, NMA, and toxicity function value for trial one, two, and three are summarized in Table C-10 and Table C-11, and C-12, respectively. The NMA and toxicity function values are plotted as a function of total copper in Figures C-11 and C-12, respectively.

TABLE C.10. TOTAL Cd^{2+} , DO CONSUMPTION RATE, NMA, AND TOXICITY FUNCTION VALUE FOR TRIAL 1 OF THE 20 AUG EXPERIMENT

Bottle #	Total Cd^{2+} (ppm)	DO Consum. Rate (mg/L/min)	NMA	Toxicity Function Value
91	0.00	0.0110	1.00	0.00
17	0.90	0.0098	0.88	0.13
11	2.25	0.0080	0.72	0.39
14	4.50	0.0049	0.44	1.26
7	9.00	0.0025	0.23	3.41
0	0 (blank)	0.0021	0.19	4.32

TABLE C.11. TOTAL Cd^{2+} , DO CONSUMPTION RATE, NMA, AND TOXICITY FUNCTION VALUE FOR TRIAL 2 OF THE 20 AUG EXPERIMENT

Bottle #	Total Cd^{2+} (ppm)	DO Consum. Rate (mg/L/min)	NMA	Toxicity Function Value
4	0.00	0.0170	1.00	0.00
21	0.90	0.0148	0.87	0.15
22	2.25	0.0126	0.74	0.35
3	4.50	0.0095	0.56	0.79
20	9.00	0.0078	0.46	1.19
1	0 (blank)	0.0013	0.08	12.18

TABLE C.12. TOTAL Cd²⁺, DO CONSUMPTION RATE, NMA, AND TOXICITY FUNCTION VALUE FOR TRIAL 3 OF THE 20 AUG EXPERIMENT

Bottle #	Total Cd ²⁺ (ppm)	DO Consum. Rate (mg/L/min)	NMA	Toxicity Function Value
16	0.00	0.0143	1.00	0.00
15	0.90	0.0119	0.83	0.20
10	2.25	0.0095	0.66	0.52
23	4.50	0.0084	0.59	0.71
51	9.00	0.0059	0.41	1.41
13	0 (blank)	0.0006	0.04	24.57

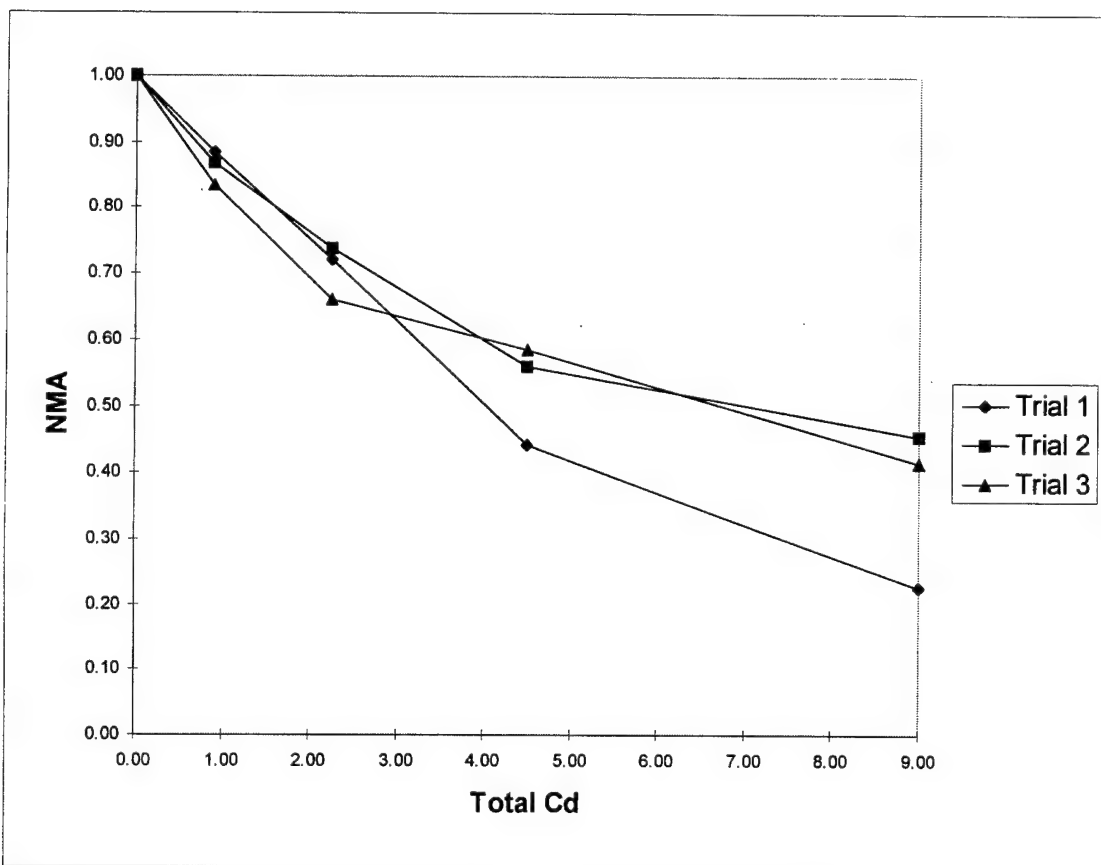


Figure C.11. Total cadmium versus NMA for 20 Aug experiment.

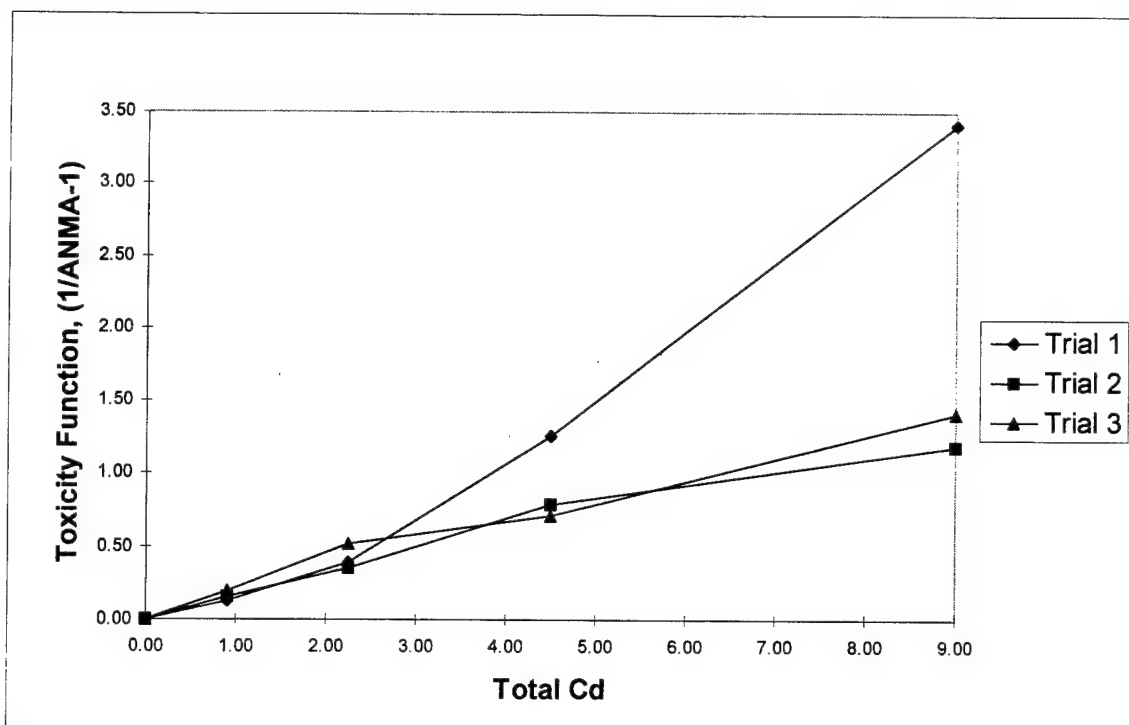


Figure C.12. Total cadmium versus toxicity function for 20 Aug experiment.

12 Sep Experiment. Eighteen microcosms were tested in the 12 Sep experiment in a single trial. The average untreated DO consumption rate was used to normalize the average DO consumption rates per metal treatment. The total metal concentration, DO consumption rate, ANMA, and average toxicity function value for the experiment is summarized in Table C-13. The NMA and toxicity function values are plotted as a function of total copper in Figures C-13 and C-14, respectively.

TABLE C.13. TOTAL Cd²⁺, DO CONSUMPTION RATE, ANMA, AND AVERAGE TOXICITY FUNCTION VALUE FOR 12 SEPT EXPERIMENT

Bottle #	Total Cd ²⁺ (ppm)	DO Consum. Rate (mg/L/min)	Ave DO rate (mg/L/min)	ANMA	Ave Toxicity Function
12	0.00	0.0123	0.010	1.000	0.000
51		0.0048			
60		0.0124			
20	1.00	0.0062	0.009	0.864	0.157
19		0.0096			
21		0.0097			
14	5.00	0.0081	0.008	0.763	0.311
6		0.0081			
3		0.0063			
91	10.00	0.0074	0.006	0.634	0.578
10		0.0057			
23		0.0056			
17	50.00	0.0043	0.005	0.461	1.169
18		0.0045			
7		0.0048			

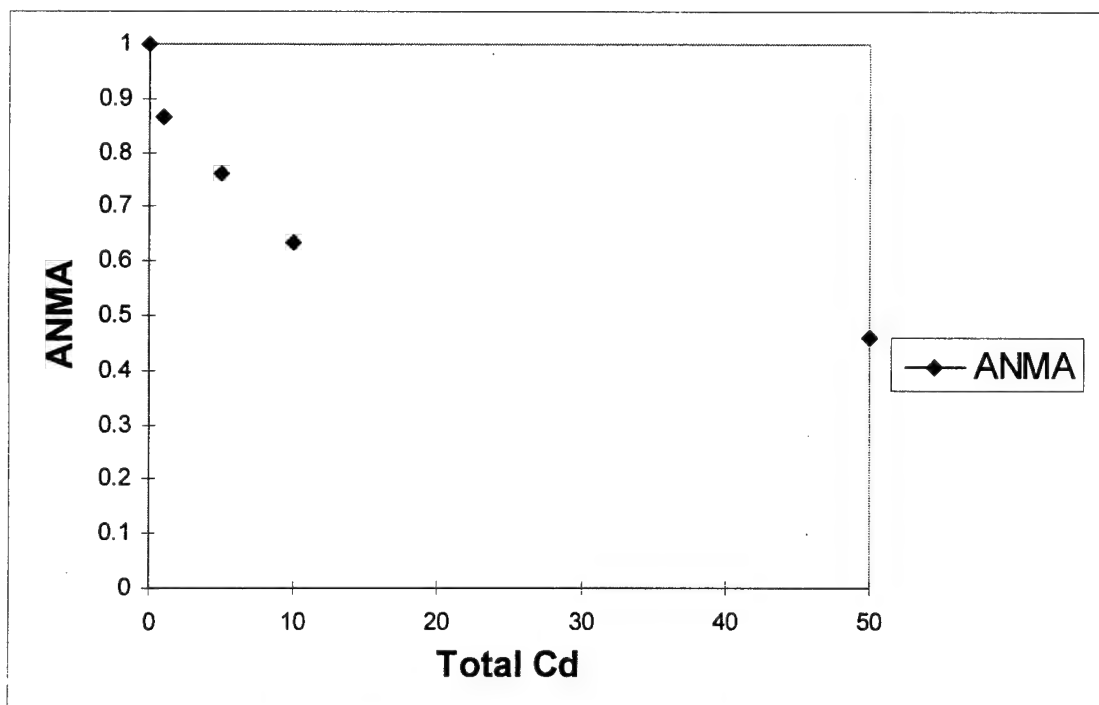


Figure C.13. Total cadmium versus ANMA for 12 Sept experiment.

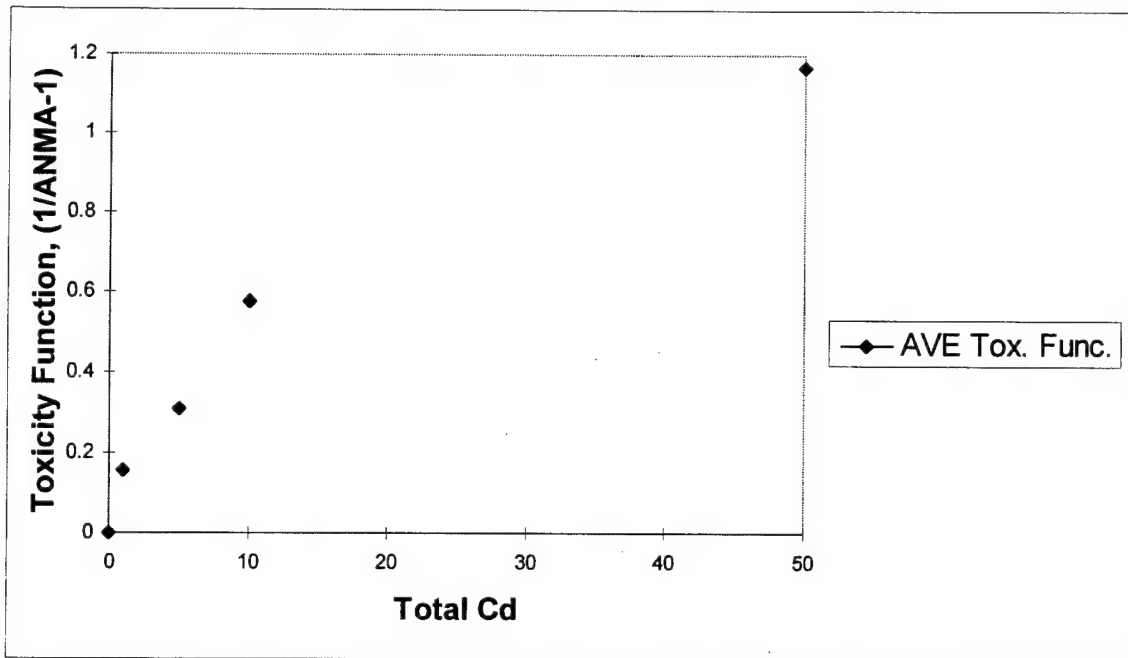


Figure C.14. Total cadmium versus toxicity function for 12 Sept experiment.

Bibliography

1. American Public Health Association, American Water Works Association, and Water Pollution Control Federation. Standard Methods For the examination of Water and Wastewater. Washington, D.C.: American Public Health Association (1981).
2. Beveridge, T. J., and R.J. Doyle. Metal Ions and Bacteria. New York: John Wiley and Sons, Inc., (1989).
3. Bitton, G., K. Jung, and B. Koopman. "Evaluation of a Microplate Assay Specific for Heavy Metal Toxicity," Archives of Environmental Contamination and Toxicology, 27: 25-28 (1994).
4. Beveridge, T. J. *In* International Review of Cytology. Bourne, G.H. and J.F. Danielle (editors). New York: Academic Press 229-241 (1981).
5. Burggraf, L.W., S.D. Hansen, and C.A. Bleckmann. "Metabolic Inhibition by Transition Metal Ions in a Slow-Growing Toluene-Enriched Microbial Population," Environmental Toxicology and Water Quality, 13:31 (1998).
6. Codina, J.C., A. Perez-Gracia, P. Romero, and A. de Vicente. "A Comparison of Microbial Bioassays for the Detection of Metal Toxicity," Archives of Environmental Contamination and Toxicology, 25: 250-254 (1993).
7. Coughlin, P.T., S. Tonsager, and E.J. McGroarty. "Quantitation of Metal Cations Bound to Membranes and Extracted Lipopolysaccharide of *Escherichia coli*," Biochemistry, 22: 2002-2007 (1983).
8. Crist, R.H., K. Oberhoiser, D. Schwartz, J. Marzoff, and D. Ryder. "Interactions of Metals and Protons with Algae," Environmental and Science Technology, 22: 755-760 (1988).
9. Doyle, R.J., T.H. Matthews, and U.S. Streips. "Chemical Basis for Selectivity of Metal Ions by the *Bacillus subtilis* Cell Wall," Journal of Bacteriology, 143: 471-480 (July 1980).
10. Duetz, W.A., C. de Jong, P.A. Williams, and J.G. van Aniel. "Competition in Chemostat Culture Between *Pseudomonas* Strains That Use Different Pathways for the Degradation of Toluene," Applied and Environmental Microbiology, 60: 2858-2863 (Aug. 1994).
11. Fargasova, A. "Toxicity of Metals on *Daphnia magna* and *Tubifex tubifex*," Ecotoxicology and Environmental Safety, 27: 210-213 (1994).

12. Folsom, B. R., N. A. Popescu, and J. M. Wood. "Comparative Study of Aluminum and Copper Transport and Toxicity in an Acid-Tolerant Freshwater Green Alga," Environmental and Science Technology, 20: 616-620 (1986).
13. Goodbody, J. Heavy Metal Toxicity in Bioremediation: Microbial Cultures and Microscopy MS thesis, AFIT/GEEM/ENV. School of Engineering Air Force Institute of Technology, Wright-Patterson AFB OH, December 1997.
14. Gottschalk, G. Bacterial Metabolism. Springer-Verlag, New York, 2ed., 1979
15. Hansen, S.D. Bioremediation Factors Influencing Metal Ion Toxicity in A Toluene-Selected Bacterial Population. MS thesis, AFIT/GEEM/ENV. School of Engineering Air Force Institute of Technology, Wright-Patterson AFB OH, December 1995.
16. Hoyle, B.D. and T.J. Beveridge. "Metal Binding by the Peptidoglycan Sacculus of *Escherichia coli* K-12," Canadian Journal of Microbiology, 30: 204-211 (1984).
17. Inouye, M. Bacterial Outer Membrane Biogenesis and Functions. New York: John Wiley and Sons, Inc. (1979).
18. Morel, F. M. M. Principles of Aquatic Chemistry. New York: John Wiley and Sons, Inc. (1983).
19. Mullen, M.D., D.C. Wolf, F.G. Ferris, T.J. Beveridge, C.A. Fleming, and G.W. Bailey. "Bacterial Sorption of Heavy Metals," Applied Environmental Microbiology, 55: 3143-3149 (1989).
20. Naziruddin, M., C.P.L. Grady Jr., and H.H. Tabak. "Determination of Biodegradation Kinetics of Volatile Organic Compounds Through the Use of Respirometry," Water Environment Research, 67: 151-158 (1995).
21. Plette, A.C.C., M.F. Benedetti, and W.H. Van Riemsdijk. "Competitive Binding of Protons, Calcium, Cadmium, and Zinc to Isolated Cell Walls of a Gram-Positive Soil Bacterium," Environmental Science and Technology, 30: 1902-1910 (1996).
22. Prescott, L. M., J. P. Harley, and D. A. Klein. Microbiology: Dubuque, IA: Wm. C. Brown Publishers (1990).
23. Rothstein, Aser. "A Reappraisal of the Action of Uranyl Ion on Cell Membranes," In Effects of Metals on Cells, Subcellular Elements, and Macromolecules. Ed. J. Maniloff, J.R. Coleman, and M.W. Miller. Springfield, Illinois: Charles C. Thomas Publisher, 1970.

24. Sawyer C.N., P.L. McCarty, and G.F. Parkin. Chemistry for Environmental Engineering. 4th Ed., McGraw-Hill, New York (1994).
25. Wackett, L. P., W. H. Orme-Johnson, and C. T. Walsh. *In* Metal Ions and Bacteria. New York: John Wiley and Sons, Inc., 185 (1989).
26. Walum, E., K. Stenberg, and D. Jenssen. Understanding Cell Toxicology Principles and Practice. New York: Ellis Horwood (1990).

Vita

Capt Patrick J. S. Marbas was born on 5 April 1970 in Honolulu, Hawaii. He graduated from Olympic High School in 1988 and entered undergraduate studies at the University of Portland in Portland, Oregon. He graduated with a Bachelor of Science degree in Civil Engineering in December 1992. He received his commission on 19 December 1992 upon completion of the Reserved Offer Training Corp program.

His first assignment was at Goodfellow AFB where he served as a CE design engineer, and later, the chief of maintenance engineering. In May 1996, he entered the School of Engineering, Air Force Institute of Technology.

Permanent Address: 724 North Avenue N
Portales, NM 88130

REPORT DOCUMENTATION PAGE			Form Approved OMB No. 0704-0188	
Public reporting burden for this collection of information is estimated to average 1 hour per response, including the time for reviewing instructions, searching existing data sources, gathering and maintaining the data needed, and completing and reviewing the collection of information. Send comments regarding this burden estimate or any other aspect of this collection of information, including suggestions for reducing this burden, to Washington Headquarters Services, Directorate for Information Operations and Reports, 1215 Jefferson Davis Highway, Suite 1204, Arlington, VA 22202-4302, and to the Office of Management and Budget, Paperwork Reduction Project (0704-0188), Washington, DC 20503.				
1. AGENCY USE ONLY (Leave blank)		2. REPORT DATE December 1997		3. REPORT TYPE AND DATES COVERED Master's Thesis
4. TITLE AND SUBTITLE Metabolic Inhibition of a Toluene-Enriched Microbial Population Due to Lead (Pb(II)): Verification of a Free Metal Ion Toxicity Model			5. FUNDING NUMBERS	
6. AUTHOR(S) Patrick J. S. Marbas, Capt, USAF				
7. PERFORMING ORGANIZATION NAME(S) AND ADDRESS(ES) Air Force Institute of Technology 2750 P Street WPAFB, OH 45433-7126			8. PERFORMING ORGANIZATION REPORT NUMBER AFIT/GEE/ENV/97D-18	
9. SPONSORING/MONITORING AGENCY NAME(S) AND ADDRESS(ES) Air Force Office of Scientific Research Major Michael Chipley 110 Duncan Ave, Suite B115 Bolling AFB, DC 20332-0001			10. SPONSORING/MONITORING AGENCY REPORT NUMBER	
11. SUPPLEMENTARY NOTES				
12a. DISTRIBUTION AVAILABILITY STATEMENT Approved for public release; distribution unlimited			12b. DISTRIBUTION CODE	
13. ABSTRACT (Maximum 200 words) <p>A dissolved oxygen probe and an ion specific electrode were used to study the lead-induced metabolic inhibition in a toluene-enriched microbial population. Predicted toxicity values were compared to the actual toxicity responses using a free metal ion toxicity model (TM) which linked metabolic inhibition with lead activity. Experimentally derived values for the model parameters (lead activity and a lead distribution coefficient) were used in the TM. It was postulated that cellular metabolism is disrupted by the conformational changes to the cell's plasma membrane produced by lead ion adsorption.</p> <p>The predicted toxicity values were higher than the actual toxicity response. This is expected since the TM did not distinguish between essential and non-essential cellular ligands. Moreover, lead-induced metabolic inhibition appears to be pH dependent as the TM predicted.</p> <p>An adsorption experiment suggested that the microbial mass has two lead binding sites: tightly bound ligands and loosely bound ligands. The tightly bound ligand sites appeared to be saturable. No evidence of saturation was observed in the loosely bound ligand sites. Contrary to expectations, the loosely bound ligand sites appear to be more essential to cellular metabolism than the tightly bound ligand sites.</p>				
14. SUBJECT TERMS Lead Toxicity, Toxicity Model, Metabolic Inhibition, Ion Selective Electrode, Dissolved Oxygen, Microorganisms, Metal Adsorption, Potentiometry, Toluene Degradation, Microbial Population, Metal Ion Toxicity, Heavy Metal Toxicity, Free Ion Toxicity Model			15. NUMBER OF PAGES 89	
			16. PRICE CODE	
17. SECURITY CLASSIFICATION OF REPORT Unclassified		18. SECURITY CLASSIFICATION OF THIS PAGE Unclassified		19. SECURITY CLASSIFICATION OF ABSTRACT Unclassified
				20. LIMITATION OF ABSTRACT UL